

PART I

KINETIC THEORY DESCRIPTION
OF PLANE, COMPRESSIBLE COUETTE FLOW

PART II

KINETIC THEORY DESCRIPTION
OF CONDUCTIVE HEAT TRANSFER
FROM A FINE WIRE

Thesis by

Chung-Yen Liu

In Partial Fulfillment of the Requirements

For the Degree of

Doctor of Philosophy

California Institute of Technology

Pasadena, California

1962

ACKNOWLEDGMENT

The author owes deepest gratitude to Professor Lester Lees, under whose constant guidance and supervision this work was carried out. He also thanks Mrs. G. Van Gieson for typing the manuscript.

PART I

KINETIC THEORY DESCRIPTION
OF PLANE, COMPRESSIBLE COUETTE FLOW

ABSTRACT

By utilizing the two-stream Maxwellian in Maxwell's integral equations of transfer we are able to find a closed-form solution of the problem of compressible plane Couette flow over the whole range of gas density from free molecule flow to atmospheric. The ratio of shear stress to the product of ordinary viscosity and velocity gradient, which is unity for a Newtonian fluid, here depends also on the gas density, the plate temperatures and the plate spacing. For example, this ratio decreases rapidly with increasing plate Mach number when the plate temperatures are fixed. On the other hand, at a fixed Mach number based on the temperature of one plate, this ratio approaches unity as the temperature of the other plate increases. Similar remarks can be made for the ratio of heat flux to the product of ordinary heat conduction coefficient and temperature gradient.

The effect of gas density on the skin friction and heat transfer coefficients is described in terms of a single rarefaction parameter, which amounts to evaluating gas properties at a certain "kinetic temperature" defined in terms of plate Mach number and plate temperature ratio. One interesting result is the effect of plate temperature on velocity "slip". In the Navier-Stokes regime most of the gas follows the hot plate, because the gas viscosity is larger there. As the gas density decreases the situation is reversed, because the velocity slip is larger at the hot plate than at the cold plate. In the limiting case of a highly rarefied gas most of the gas follows the cold plate.

Limitations of the present six-moment approximation at high

plate Mach numbers are discussed and it is concluded that an eight-moment approximation would eliminate these difficulties. The results obtained in this simple geometry suggest certain conclusions about hypersonic flow over solid bodies when the surface temperature is much lower than the kinetic temperature.

TABLE OF CONTENTS

PART	PAGE
Acknowledgments	ii
Abstract	iii
Table of Contents	v
List of Figures	vi
List of Symbols	vii
I. Introduction	1
II. Maxwell's Moment Method for Plane Compressible Couette Flow	6
II. A. Formulation of the Problem	6
II. A. 1. Differential Equations	6
II. A. 2. Boundary Conditions	11
II. B. Low Mach Number Flow with Arbitrary Plate Temperature Ratio	14
II. C. Arbitrary Mach Number and Plate Temperature Ratio	20
II. D. Special Case of Equal Plate Temperatures, But Arbitrary Mach Number	25
III. Discussion and Conclusions	27
III. A. Skin-Friction and Heat Transfer Coefficients	27
III. B. Shear Stress and Normal Heat Flux	28
III. C. Mean Temperature and Mean Velocity Profiles	30
III. D. Comparison of Present Results with Maxwell's Velocity Slip Relation	32
III. E. Limitations of Six-Moment Approximation	34
III. F. Conclusions and Future Work	38
References	40
Appendix -- Plane Compressible Couette Flow According to the Classical Navier-Stokes Equation	42
Figures	44

LIST OF FIGURES

NUMBER		PAGE
1	"Two-Stream Maxwellian"	44
2	Geometrical Configuration of the Problem	44
3	Velocity Profiles for Plane Couette Flow	45
4	Temperature Profiles for Plane Couette Flow	46
5	Skin Friction in Plane Couette Flow	47
6	Heat Transfer in Plane Couette Flow	48
7	Typical Variation of $F(\bar{y})$	49
8	Velocity Profiles for Plane Couette Flow	50
9	Temperature Profiles for Plane Couette Flow	51
10	Velocity Profiles for Plane Couette Flow	52
11	Temperature Profiles for Plane Couette Flow	53
12	Skin Friction Vs. Normalized Rarefaction Parameter	54
13	Departure from Navier-Stokes Relation in Plane Couette Flow, $(Re/M) = 0$	55
14	Departure from Fourier's Relation in Plane Couette Flow, $(Re/M) = 0$	56
15	Departure from Navier-Stokes Relation as a Function of Re/M	57

LIST OF SYMBOLS

a_1, a_2	functions in two-stream Maxwellian for eight-moment approximation
A_2	= 1.3682, value of scattering integral
b	impact parameter, or perpendicular distance from particle "i" to initial trajectory of particle "j"
b_i	integration constant, $i = 1, 2, 3, 4$. (See Appendix.)
\vec{c}	relative particle velocity, $\vec{\xi} - \vec{u}$
\bar{c}	mean molecular speed, $\sqrt{8RT/\pi}$
c_i	component of relative particle velocity in i^{th} direction
c_p, c_v	heat capacity at constant pressure and constant volume, respectively
C_D	skin-friction coefficient, $p_{xy}/(\frac{1}{2}\rho_{II} U^2)$
C_H	Stanton number, $q_y/\rho_{II} c_p U (T_{II} - T_I)$
d	distance between lower and upper plates
f, f_1	velocity distribution functions for "probe" and colliding particles, respectively
f_1, f_2	components of two-stream Maxwellian
f_{max}	local full-range Maxwellian
F	interparticle force, also function defined by Eq. (33)
G	function defined by the relation $\bar{n}_1 \sqrt{T_1} = \bar{n}_2 \sqrt{T_2} = [G]^{-1}$
k	Boltzmann constant
k_c	"classical" thermal conductivity
K	constant in expression for inverse fifth-power force law, $F = (m_1 m_2 K)/r^5$
L	square root of plate temperature ratio, $\sqrt{T_I/T_{II}}$
m	mass of a particle

M	Mach number, $U / \sqrt{\gamma R T_{II}}$
\tilde{M}	"proper" Mach number, $\tilde{M}^2 = U^2 / \gamma R \sqrt{T_I T_{II}}$
n	particle number density, per unit volume
n_1, n_2	number density functions in two-stream Maxwellian
p	$nkT = \rho RT$
P_{ii}	defined by the relation $P_{ii} = -p + p_{ii}$
P_{ij}, P_{ij}	shear stress, $i \neq j$, $P_{ij} = -m \int f c_i c_j d\vec{\xi}$
P_{ii}	normal stress, $P_{ii} = -m \int f c_i^2 d\vec{\xi}$
Pr	Prandtl number, $c_p \mu / k c$
q_y	heat flux in y-direction
Q	arbitrary function of particle velocity
ΔQ	change in Q produced by collisions
r	distance between two particles
\vec{R}	radius vector
Re	Reynolds number, $\rho_{II} U d / \mu_{II}$
R	gas constant, k/m
s_n	non-dimensional relative velocity in the normal direction
t	time
T	absolute temperature, $3/2 n k T = m \int (c^2/2) f d\vec{\xi}$
T_1, T_2	temperature functions in two-stream Maxwellian
\vec{u}	mean velocity vector, $\rho \vec{u} = m \int f \vec{\xi} d\vec{\xi}$
u, v	components of mean velocity parallel to x- and y- axes, respectively
\vec{u}_∞	free stream velocity vector
\vec{u}_1, \vec{u}_2	vector velocity functions in two-stream Maxwellian
u_i	component of mean velocity in i^{th} direction

U	relative plate velocity
V	relative velocity between two interacting particles = $\left \vec{\xi}_1 - \vec{\xi} \right $
x, y	coordinates along and normal to plates
x_i	coordinate in i^{th} direction
a_i	integration constant, $i = 1, 2, 3, 4, 5$
β	quantity defined by the relation $\beta = (8/15) \sqrt{2/\pi\gamma} (Re/M)$
γ	ratio of specific heats, c_p/c_v
ϵ	angle between plane of the orbit and plane containing the original relative velocity and the x-axis in a binary collision
λ	Maxwell mean free path
λ_i	$i = 1, 2, 3$, functions defined by Eqs. (35a) and (37)
Λ	Pohlhausen parameter
μ_c	"classical" viscosity coefficient
$\tilde{\mu}$	viscosity coefficient = $p_{xy} / (du/dy)$
$\vec{\xi}$	vector particle velocity, $\xi^2 = \vec{\xi} ^2$
$d\vec{\xi}$	$d\xi_i d\xi_j d\xi_k$
ξ_j	component of particle velocity in j^{th} direction
ξ_1	velocity of colliding particles
ρ	nm, mass density, $\rho = \int m f d\vec{\xi}$

The subscripts "1" and "2" generally denote the two components of the two-stream Maxwellian, and the subscripts "I" and "II" refer to quantities given at the upper and lower plates respectively. A prime denotes quantities evaluated after a collision, while unprimed quantities refer to conditions before a collision. The subscript "o" denotes free molecular flow conditions, the subscript "w" denotes surface values, the subscript " ∞ " denotes free stream quantities far ahead of a body, and the subscript "n" denotes quantities normal to the surface.

I. INTRODUCTION

In principle, the Maxwell-Boltzmann integro-differential equation for the single particle velocity distribution function is fully capable of describing the flow of a monatomic gas over the whole range of gas densities from "free-molecule" flow to the classical Navier-Stokes regime^{2, 8, 10}. However the formidable difficulties involved in constructing solutions of this equation are too well known to require repetition here⁶. Fortunately, in fluid mechanics one is not particularly interested in the velocity distribution function itself, but in certain lower moments of this function, such as mean velocity, shear stress, etc. Recognizing this fact, Maxwell¹¹ converted the original Maxwell-Boltzmann equation into an integral equation of transfer, or moment equation, for any quantity Q that is a function only of the components of the particle velocity. In the absence of external forces Maxwell's integral equation takes the following form in a rectangular Cartesian coordinate system:*

$$(\partial/\partial t) \left(\int f Q d\vec{\xi} \right) + \sum_i (\partial/\partial x_i) \left(\int f \xi_i Q d\vec{\xi} \right) = \Delta Q, \quad (1)$$

where ΔQ represents the time rate of change of Q produced by particle collisions, and is given by

$$\Delta Q = \iiint (Q' - Q) f f_1 V d\vec{\xi} d\vec{\xi}_1 b db d\epsilon \quad (2)$$

Actually Maxwell employed a special form of the distribution function, but an important advantage of Eq. (1) is just the fact that it permits a large amount of flexibility in the choice of f . The distribution

* Maxwell's integral equation including external forces and coordinate system curvature is given in Reference 10.

function can be expressed in terms of a certain number of arbitrary functions of space and time, selected in such a way that essential physical features of the problem are introduced. Of course the proper number of moments (Q 's) must be taken to insure that a complete set of first-order partial differential equations is obtained for these undetermined functions. As shown by Maxwell¹¹ the ordinary gas dynamic conservation equations are obtained regardless of the choice of f by taking Q to be successively the collisional invariants of mass, momentum, and energy [$Q = m, m\xi_i, m\xi^2/2$], for which $\Delta Q = 0$. The number of additional moments (and arbitrary functions) employed depends on the degree of detail desired, and also on the relative magnitude of these additional moments (Section III. E).

Clearly this procedure amounts to satisfying the Maxwell-Boltzmann equation in a certain average sense, rather than point-by-point, just as one does in the more familiar Karman-Pohlhausen method for boundary layer flows¹⁴ and its extension by Tani¹³. The distribution function employed should be regarded as a suitable weighting function which is not in general an "exact" solution of the original Maxwell-Boltzmann equation. Thus, there is no need to retain the undesirable rigidity inherent in a polynomial of Chapman-Enskog type, as in Grad's method⁵. In fact, Mott-Smith¹² found that a distribution function consisting of the sum of two full-range Maxwellians is quite suitable for a rough description of the structure of a strong, steady, normal shock wave. A careful study of shear flows in rarefied gases and of the difficulties encountered with Grad's thirteen moment approximation¹ shows that the following basic requirements must be satisfied by the distribution function employed in Maxwell's moment method¹⁰:

(1) It must have the "two-sided" character that is an essential feature of highly rarefied gas flows, and especially of non-linear rarefied flows;

(2) It must be capable of providing a smooth transition from rarefied flows to the classical Navier-Stokes regime;

(3) It should lead to the simplest possible set of differential equations and boundary conditions consistent with (1) and (2).

Of course the class of distribution functions satisfying requirements (1) and (2) is very large. In Reference 10, Lees introduced the "two-stream" Maxwellian, which is probably one of the simplest such functions, as a natural generalization of the situation for free-molecule flow. In body coordinates all outwardly directed particle velocity vectors lying within the "cone of influence" (Region 1 in Figure 1) are described by the function $f = f_1$, where

$$f_1 = \frac{n_1(\vec{R}, t)}{[2\pi R T_1(\vec{R}, t)]^{3/2}} \exp \left\{ - \frac{[\vec{w} - \vec{u}_1(\vec{R}, t)]^2}{2 R T_1(\vec{R}, t)} \right\} \quad (3a)$$

In Region 2 (all other \vec{w})

$$f = f_2 = \frac{n_2(\vec{R}, t)}{[2\pi R T_2(\vec{R}, t)]^{3/2}} \exp \left\{ - \frac{[\vec{w} - \vec{u}_2(\vec{R}, t)]^2}{2 R T_2(\vec{R}, t)} \right\} \quad (3b)$$

where $n_1, n_2, T_1, T_2, \vec{u}_1, \vec{u}_2$ are ten initially undetermined functions of \vec{R} and t . In the limiting case of free-molecule flow the distribution function described by Eqs. (3a) and (3b) is an exact solution for completely diffuse reemission, provided that $\vec{u}_2 = \vec{u}_\infty, n_2 = n_\infty, T_2 = T_\infty, \vec{u}_1 = \vec{u}_w, T_1 = T_w$, and n_1 is the function determined by the boundary condition on

the normal velocity at the body surface. In the present method the variation of these ten functions with R and t is a measure of the effect of particle collisions in the gas, as determined by Maxwell's moment equations [Eqs. (1) and (2)]. Thus, one gives up once and for all the search for "higher order" macroscopic equations in terms of the mean quantities, such as the Burnett equations, Grad's equations, etc. Once these ten functions are determined, the mean quantities are obtained by utilizing the distribution function defined by Eqs. (3a) and (3b), as in any true statistical approach.

One important advantage of the two stream Maxwellian is that the surface boundary conditions are easily incorporated into the analysis [Requirement (3) above]. For example, for completely diffuse reemission, the reemitted particles have a Maxwellian velocity distribution corresponding to T_w , by definition, and the mean velocity of the reemitted particles is identical with the local surface velocity. Thus [Eq. (3a)], $\vec{u}_1(\vec{R}, t) = \vec{u}_w$ and $T_1(\vec{R}, t) = T_w$ when $\vec{R} = \vec{R}_w$. When there is no net mass transfer at the surface an additional boundary condition must be satisfied which is similar to the usual free-molecule flow condition, except that now $\vec{u}_2 \neq \vec{u}_\infty$ in general:

$$n_1 \sqrt{R T_1} = n_1 \sqrt{R T_w} = n_2 \sqrt{R T_2} C(-s_{2n}) \quad (4)$$

where

$$C(s_n) = e^{-s_n^2} + \sqrt{\pi} s_n (1 + \operatorname{erf} s_n) \quad (5)$$

Here

$$s_{2n} = \frac{(\vec{u}_{2n} - \vec{u}_{w_n})}{\sqrt{2 R T_2}} \quad ,$$

where u_{2n} and u_{wn} are the normal components of \vec{u}_2 and \vec{u}_w , respectively. In considering the uniform rectilinear motion of a finite body in a fluid of infinite extent the following boundary conditions must also be imposed (in body coordinates):

$$\vec{u}_2 \rightarrow \vec{u}_\infty, \quad T_2 \rightarrow T_\infty, \quad n_2 \rightarrow n_\infty, \quad \text{as } x \rightarrow +\infty.$$

As an illustration the present method was applied in Reference 10 to linearized plane Couette flow and to the linearized form of Rayleigh's problem. But plane, parallel flows at low Mach number with small temperature differences cannot provide a serious test of any method that is supposed to be general. In this paper we apply the present technique to steady, plane compressible Couette flow, in order to study the effects of large temperature differences and dissipation in the simplest possible geometry. In Section II. A. the basic equations and boundary conditions for this problem are formulated. In order to simplify the work the particles are supposed to obey Maxwell's inverse fifth-power law of repulsion, but this restriction is not an essential one. Solutions are obtained first for arbitrary temperature ratio between the two plates, but $M^2 \rightarrow \ll 1$, (Section II. B.), and then similar methods are employed for the case of arbitrary Mach number and temperature ratio (Sections II. C. and II. D.). In Section III we utilize the calculated behavior of the velocity and temperature profiles and other mean quantities in this problem to gain some insight into the effect of Mach number and the ratio of plate temperatures on the nature of the transition from free-molecule flow to the classical Navier-Stokes regime.

II. MAXWELL'S MOMENT METHOD FOR PLANE COMPRESSIBLE COUETTE FLOW

II. A. Formulation of the Problem

II. A. 1. Differential Equations

Maxwell's moment method is applied to the problem of the steady flow generated by the relative shearing motion of two infinite parallel flat plates. The upper plate moves with velocity $+ U/2$ in its own plane at $y = d/2$ and is held at temperature T_I , while the lower plate at $y = -d/2$ moves parallel to the upper plate with velocity $- U/2$, and is kept at temperature T_{II} [Figure 2]. The only independent variable in this problem is the coordinate normal to the plates, y ; thus, Eq. (1) reduces to

$$d/dy \left(\int f \xi_y Q d\vec{\xi} \right) = \Delta Q \quad (6)$$

By taking Q to be the collisional invariants m , $m\xi_x$, $m\xi_y$, and $m\xi^2/2$, successively, four equations are obtained from Eq. (6), corresponding to the ordinary gas dynamic conservation equations. For these moments $\Delta Q = 0$, and

$$\int f \xi_y Q d\vec{\xi} = \text{constant} \quad (7)$$

According to kinetic theory,

$$\rho u_i = \int m f \xi_i d\vec{\xi} \quad (8a)$$

where

$$\rho = \int m f d\vec{\xi} \quad (8b)$$

Thus the first of Eqs. (7) with $Q = m$ is just the ordinary equation of continuity for this problem, namely,

$$\rho v = \text{constant} \quad . \quad (9a)$$

But

$$v(-d/2) = v(d/2) = 0, \text{ so that } v(y) \equiv 0 \quad . \quad (9b)$$

$$\text{By definition } P_{ij} = -m \int f c_i c_j d\vec{\xi} \quad ,$$

where \vec{c} is the intrinsic or relative velocity $\vec{\xi} - \vec{u}$. Here

$$P_{ij} = p_{ij}, \quad i \neq j \quad ,$$

$$P_{ii} = -p + p_{ii}, \quad i = j \quad ,$$

$$\text{where } p = - \sum (P_{ii}/3) = pRT = (2/3) \int m f (c^2/2) d\vec{\xi} \quad .$$

With $Q = m \xi_x$ and $m \xi_y$, one obtains [Eq. (7) and (9b)]

$$P_{xy} = \text{constant} \quad (9c)$$

and

$$P_{yy} = \text{constant, respectively.} \quad (9d)$$

Similarly, by taking $Q = m \xi^2/2$ in Eq. (7), and recognizing that

$\xi_x = c_x + u$, $\xi_y = c_y$, $\xi_z = c_z$ and $v \equiv 0$ in this problem, one finds as expected that

$$q_y - P_{xy} u = \text{constant} \quad (9e)$$

where

$$q_y = m \int f c_y c^2/2 d\vec{\xi} \quad , \text{ by definition.}$$

In this case the "two-stream Maxwellian" [Eqs. (3a) and (3b)]

takes the following form (Figure 2) :

$$\text{For } \xi_y < 0 \quad ,$$

$$f = f_1 = n_1(y) \frac{1}{[2\pi RT_1(y)]^{3/2}} \exp \left\{ - \frac{[\xi_x - u_1(y)]^2 + \xi_y^2 + \xi_z^2}{2RT_1(y)} \right\} \quad . (10a)$$

For $\xi_y > 0$.

$$f = f_2 \quad , \quad (10b)$$

where f_2 is a similar generalized Maxwellian containing the functions $n_2(y)$, $T_2(y)$, $u_2(y)$. Two independent moment equations in addition to the four represented by Eqs. (7) [or Eqs. (9a) - (9e)] are required to determine these six arbitrary functions of y . Of course these additional moments can be chosen quite arbitrarily. Because of our special interest in the shear stress and normal heat flux in this problem we take

$$Q_5 = m \xi_x \xi_y \quad \text{and} \quad Q_6 = m \xi_y (\xi^2/2). \quad [\text{See, however, Section III. E.}]$$

Once the two-stream Maxwellian is selected for f , the collision integral ΔQ [Eq. (2)] can be evaluated for any arbitrary law of force between the particles. For simplicity we utilize Maxwell's inverse fifth-power force law $F = \frac{m_1 m_2 K}{r^5}$. With this choice the relative velocity $V = | \vec{v}_1 - \vec{v} |$ is eliminated from the collision integral, and ΔQ for the lower moments contains the components of the heat flux vector and the shear stress tensor [(7), (10), (11)] . To be specific, for

$Q_5 = m \xi_j \xi_k$, one finds

$$Q_5 = (3/2) A_2 \sqrt{2 m K} \quad n p_{jk} \quad ; \quad (11)$$

while if $Q_6 = m \xi_j (\xi^2/2)$, one has

$$Q_6 = (3/2) A_2 \sqrt{2 m K} \quad n \left[-(2/3) q_j + \sum_k p_{jk} u_k \right] . \quad (12)$$

[Here $A_2 = 1.3682$ is the value of the scattering integral found by Maxwell¹¹]. Both of these results are independent of the choice of f .

Now the ordinary or "classical" coefficient of viscosity for Maxwell particles based on the local full-range Maxwellian is given by the expression

$$\mu_c = \frac{k T}{(3/2) A_2 \sqrt{2 m K}} \quad (13)$$

where k is the Boltzmann constant. Therefore,

$$(3/2) A_2 \sqrt{2 m K} n = (p/\mu_c) \quad * \quad (14)$$

Thus the two moment equations supplementing Eqs. (7) are as follows

[Eqs. (6), (11), and (12)] :

$$(d/dy) \left(\int m f \xi_x \xi_y^2 d\vec{\xi} \right) = (p/\mu_c) p_{xy} \quad (15)$$

$$(d/dy) \left(\int m f \xi_y^2 \xi^2/2 d\vec{\xi} \right) = (p/\mu_c) \left[-(2/3) q_y + p_{xy} u + p_{yy} v \right] \quad (16)$$

If the local full-range Maxwellian

$$f_{\max}(\vec{\xi}, y) = \frac{n}{(2\pi RT)^{3/2}} \exp\left(-\frac{c^2}{2RT}\right)$$

is introduced into the left-hand sides of Eqs. (15) and (16) one obtains the familiar relations

$$\mu_c (du/dy) = p_{xy}$$

$$-(3/2) c_p \mu_c (dT/dy) = -k_c (dT/dy) = q_y$$

In fact this approximation corresponds exactly to the first step of the Chapman-Enskog expansion procedure (see for example Reference 10).

But in general $f \neq f_{\max}$, so that $p_{xy} \neq \mu_c (du/dy)$ and $q_c \neq -k_c (dT/dy)$.

Six equations for the six arbitrary functions of y appearing in the

* The ordinary coefficient of viscosity μ_c is introduced here mainly for convenience. It must be emphasized that $\mu_c \neq p_{jk} / \left(\frac{\partial u_j}{\partial x_k} + \frac{\partial u_k}{\partial x_j} \right)$ except in the limiting case $Re/M \rightarrow \infty$, which corresponds to the classical Navier-Stokes regime (Sections II. B and II. C).

two stream Maxwellian are obtained by substituting this f [Eqs. (3a) and (3b)] into Eqs. (7) and Eqs. (15) and (16). All moments and mean flow quantities are evaluated as follows:

$$\begin{aligned} \langle \phi \rangle = \int \phi f d\vec{\xi} &= \int_{-\infty}^{+\infty} \int_{-\infty}^0 \int_{-\infty}^{+\infty} \phi f_1 d\xi_x d\xi_y d\xi_z \\ &+ \int_{-\infty}^{+\infty} \int_0^{\infty} \int_{-\infty}^{+\infty} \phi f_2 d\xi_x d\xi_y d\xi_z . \end{aligned}$$

For example,

$$\rho(y) = \langle m \rangle = (m/2) [n_1(y) + n_2(y)] = m n(y) \quad (17)$$

$$u(y) = (1/\rho) \langle m \xi_x \rangle = \frac{n_1(y) u_1(y) + n_2(y) u_2(y)}{n_1(y) + n_2(y)} . \quad (18)$$

Since it is more convenient to work with non-dimensional quantities, we select n_{II} , U , T_{II} , d as the characteristic number density, velocity, temperature and length, respectively. A Mach number and Reynolds number are introduced based on these characteristic quantities

$$M = U / \sqrt{\gamma R T_{II}}$$

$$Re = \frac{m n_{II} U d}{(\mu_c)_{II}} ,$$

where $(\mu_c)_{II}$ denotes the ordinary viscosity coefficient evaluated at temperature T_{II} . The parameter Re/M is inversely proportional to the ratio of mean free path, λ_{II} , to the characteristic length d , and this parameter characterizes the density level of the gas. In fact

$$Re/M = \sqrt{\pi \gamma / 2} (d/\lambda_{II}) .$$

Let normalized quantities be denoted by a bar superscript. Then

the non-dimensional governing equations are as follows:

Continuity

$$\bar{n}_1 \sqrt{\bar{T}_1} = \bar{n}_2 \sqrt{\bar{T}_2} \quad (19a)$$

Momentum

$$\bar{n}_1 \sqrt{\bar{T}_1} (\bar{u}_2 - \bar{u}_1) = a_1 \quad (19b)$$

$$\bar{n}_1 \bar{T}_1 + \bar{n}_2 \bar{T}_2 = a_2 \quad (19c)$$

Energy

$$\bar{n}_1 \sqrt{\bar{T}_1} \left[\bar{T}_2 - \bar{T}_1 + (\gamma M^2/4) (\bar{u}_2^2 - \bar{u}_1^2) \right] = a_2 a_3 \quad (19d)$$

Stress

$$(d/d\bar{y})(\bar{n}_1 \bar{u}_1 \bar{T}_1 + \bar{n}_2 \bar{u}_2 \bar{T}_2) + \frac{1}{\gamma 2\pi \gamma} (\text{Re}/M) a_1 (\bar{n}_1 + \bar{n}_2) = 0 \quad (19e)$$

Heat Flux

$$\begin{aligned} & (d/d\bar{y})(\bar{n}_1 \bar{T}_1^2 + \bar{n}_2 \bar{T}_2^2) + (\gamma M^2/5)(d/d\bar{y}) \left[\bar{n}_1 \bar{T}_1 \bar{u}_1^2 + \bar{n}_2 \bar{T}_2 \bar{u}_2^2 \right] \\ & - (2/5) \gamma M^2 \bar{u} (d/d\bar{y}) (\bar{n}_1 \bar{T}_1 \bar{u}_1 + \bar{n}_2 \bar{T}_2 \bar{u}_2) \\ & - (4/15) \sqrt{\gamma/2\pi} (\text{Re}/M) M^2 a_1 (\bar{n}_1 \bar{u}_1 + \bar{n}_2 \bar{u}_2) \\ & + (4/15) \sqrt{2/\pi \gamma} (\text{Re}/M) a_2 a_3 (\bar{n}_1 + \bar{n}_2) = 0 \end{aligned} \quad (19f)$$

where a_1, a_2, a_3 are undetermined integration constants.

II. A. 2. Boundary Conditions

For completely diffuse reemission the boundary conditions are quite simple. (See Introduction.):

At $y = +d/2$ (Figure 2) , $u_1 = +(U/2)$; $T_1 = T_I$.

$$\text{At } y = -d/2, \quad u_2 = -(U/2), \quad T_2 = T_{II}.$$

Also, $v(\pm d/2) = 0$, but $v \equiv 0$ everywhere [Eqs. (9a) and (9b)], so that Eq. (19a) satisfies this boundary condition automatically.

The sixth boundary condition involves a specification of the density level of the gas between the plates, by choosing ρ or n_1 or n_2 at a given point. Since the results evidently do not depend on the position of this reference point we select

$$n_2 = n_{II} \quad \text{at } y = -d/2.$$

In non-dimensional form the boundary conditions are as follows:

$$\left. \begin{aligned} \bar{u}_1 &= \frac{1}{2} \\ \bar{T}_1 &= T_I/T_{II} \end{aligned} \right\} \quad \text{at } \bar{y} = \frac{1}{2} \quad \begin{array}{l} (20a) \\ (20b) \end{array}$$

$$\left. \begin{aligned} \bar{u}_2 &= -\frac{1}{2} \end{aligned} \right\} \quad \text{at } \bar{y} = -\frac{1}{2} \quad (20c)$$

$$\left. \begin{aligned} \bar{T}_2 &= 1 \end{aligned} \right\} \quad \text{at } \bar{y} = -\frac{1}{2} \quad (20d)$$

$$\left. \begin{aligned} \bar{n}_2 &= 1 \end{aligned} \right\} \quad \text{at } \bar{y} = -\frac{1}{2} \quad (20e)$$

Plane compressible Couette flow is completely determined by three independent parameters: (Re/M) (or d/λ_{II}) the rarefaction parameter; M^2 , the dissipation parameter; and the plate temperature ratio T_I/T_{II} appearing explicitly only in the boundary conditions. The governing equations and boundary conditions [Eqs. (19) and (20)] are all regular in the parameters Re/M , T_I/T_{II} , and M^2 for all finite values of these parameters. In particular, in the limiting case $Re/M \rightarrow 0$ all six equations reduce to algebraic equations, and the six unknown functions approach the (constant) values given by free-molecule flow. In the opposite limiting case $Re/M \rightarrow \infty$, clearly α_1 and α_3 are both

$O(M/Re)$ [Eqs. (19d) and (19e)] . Thus the pairs \bar{u}_2 and \bar{u}_1 , \bar{n}_2 , and \bar{n}_1 , and \bar{T}_2 and \bar{T}_1 each differ by a term of order $M/Re \sim \lambda_{II}/d$, which corresponds to the classical Navier-Stokes regime [Sections II. B and II. C] .

In order to bring out the effect of temperature difference between the two plates we study first the simpler case $M^2 \ll 1$, and then generalize the technique for obtaining solutions to the case of arbitrary Mach number. All mean flow quantities are easily evaluated once the six functions $\bar{n}_1(\bar{y}) \dots \bar{u}_2(\bar{y})$ are determined. For convenience the necessary relations are listed here:

$$\frac{P_{xy}(y)}{\rho_{II} \sqrt{\frac{R T_{II}}{2\pi}} U} = \bar{p}_{xy}(\bar{y}) = -\bar{n}_1 \sqrt{\bar{T}_1} (\bar{u}_2 - \bar{u}_1) = -\alpha_1 \quad (21a)$$

$$\frac{P_{xx}(y)}{\rho_{II} k T_{II}} = \gamma M^2 (\bar{\rho} \bar{u}^2) - \frac{1}{2} (\bar{n}_1 \bar{T}_1 + \bar{n}_2 \bar{T}_2) - \gamma M^2 (\bar{n}_1 \bar{u}_1^2 + \bar{n}_2 \bar{u}_2^2) \quad (21b)$$

$$\frac{P_{yy}(y)}{\rho_{II} k T_{II}} = \frac{P_{zz}(y)}{\rho_{II} k T_{II}} = -\frac{1}{2} (\bar{n}_1 \bar{T}_1 + \bar{n}_2 \bar{T}_2) \quad (21c)$$

$$\bar{T}(\bar{y}) = \frac{\bar{n}_1 \bar{T}_1 + \bar{n}_2 \bar{T}_2}{\bar{n}_1 + \bar{n}_2} + (\gamma/3) M^2 \left[\frac{\bar{n}_1 (\bar{u} - \bar{u}_1)^2 + \bar{n}_2 (\bar{u} - \bar{u}_2)^2}{\bar{n}_1 + \bar{n}_2} \right] \quad (21d)$$

$$\frac{P(y)}{\rho_{II} k T_{II}} = \frac{1}{2} (\bar{n}_1 \bar{T}_1 + \bar{n}_2 \bar{T}_2) + (\gamma/6) M^2 \left[\bar{n}_1 (\bar{u} - \bar{u}_1)^2 + \bar{n}_2 (\bar{u} - \bar{u}_2)^2 \right] \quad (21e)$$

$$\frac{q_y}{\rho_{II} k T_{II} \sqrt{(2/\pi) R T_{II}}} = (\gamma M^2/2) \bar{p}_{xy} \bar{u} + \bar{n}_2 \bar{T}_2^{3/2} \left[1 + (\gamma M^2/4) (\bar{u}_2^2/\bar{T}_2) \right] - \bar{n}_1 \bar{T}_1^{3/2} \left[1 + \frac{\gamma M^2}{4} \frac{\bar{u}_1^2}{\bar{T}_1} \right] \quad (21f)$$

The expressions for $\rho(y)$ and $u(y)$ have already been given [Eqs. (17) and (18)] .

According to Eqs. (21b), (21c), and (21e), $P_{yy} \rightarrow P_{xx} \rightarrow -p$ when $M^2 \rightarrow 0$, or when $Re/M \rightarrow \infty$. In general however, $P_{yy} \neq P_{xx} \neq -p$, so that $p_{ii} \neq 0$, in spite of the fact that $\text{div } \vec{u} \equiv 0$. This behavior shows again the inadequacy of any concept relating the stresses to the purely local mean velocity gradients in a rarefied gas flow.

II. B. Low Mach Number Flow with Arbitrary Plate Temperature Ratio

In this case ($M^2 \ll 1$) the basic equations [Eqs. (19)] are considerably simplified:

Continuity

$$\bar{n}_1 \sqrt{\bar{T}_1} = \bar{n}_2 \sqrt{\bar{T}_2} \quad (22a)$$

Momentum

$$\bar{n}_1 \sqrt{\bar{T}_1} (\bar{u}_2 - \bar{u}_1) = a_1 \quad (22b)$$

$$\bar{n}_1 \bar{T}_1 + \bar{n}_2 \bar{T}_2 = a_2 \quad (22c)$$

Energy

$$\bar{n}_1 \sqrt{\bar{T}_1} (\bar{T}_2 - \bar{T}_1) = a_2 a_3 \quad (22d)$$

Stress

$$(d/d\bar{y})(\bar{n}_1 \bar{u}_1 \bar{T}_1 + \bar{n}_2 \bar{u}_2 \bar{T}_2) + \frac{1}{\sqrt{2\pi\gamma}} (Re/M) a_1 (\bar{n}_1 + \bar{n}_2) = 0 \quad (22e)$$

Heat Flux

$$(d/d\bar{y})(\bar{n}_1 \bar{T}_1^2 + \bar{n}_2 \bar{T}_2^2) + (4/15) \sqrt{(2/\pi\gamma)} \text{Re}/M) a_2 a_3 (\bar{n}_1 + \bar{n}_2) = 0 \quad (22f)$$

Of course the boundary conditions [Eqs. (20)] are unchanged.

As expected, the small Mach number simplification leads to a split in the system of equations; namely, Eqs. (22 a, c, d, f) govern the four functions \bar{n}_1 , \bar{n}_2 , \bar{T}_1 , and \bar{T}_2 , while Eqs. (22 b, e) describe the behavior of \bar{u}_1 and \bar{u}_2 . This independence of thermodynamic variables and dynamic variables is a basic feature of low Mach number flow¹⁰.

The heat flux, temperature and density profiles so obtained are clearly valid for the problem of convective heat transfer between two stationary plates.

The three algebraic equations for the four functions \bar{n}_1 , \bar{n}_2 , \bar{T}_1 , and \bar{T}_2 [Eqs. (22a), (22c), and (22d)] permit these variables to be eliminated in favor of a single function $G(\bar{y})$; then Eq. (22f) furnishes an ordinary first-order non-linear equation for $G(\bar{y})$. It turns out to be most convenient to take $\bar{n}_1 \sqrt{\bar{T}_1} = \bar{n}_2 \sqrt{\bar{T}_2} = G(\bar{y})^{-1}$. Then Eq. (22c) is reduced to

$$\sqrt{\bar{T}_1} + \sqrt{\bar{T}_2} = a_2 G \quad (23a)$$

while Eq. (22d) becomes

$$\bar{T}_2 - \bar{T}_1 = a_2 a_3 G \quad (23b)$$

From Eqs. (23a) and (23b) one finds

$$\bar{T}_1(\bar{y}) = (1/4) (a_2 G - a_3)^2 \quad (24a)$$

$$\bar{T}_2(\bar{y}) = (1/4) (a_2 G + a_3)^2 \quad (24b)$$

so that

$$\bar{n}_1(\bar{y}) = \frac{2}{G(a_2 G - a_3)} \quad (24c)$$

$$\bar{n}_2(\bar{y}) = \frac{2}{G(a_2 G + a_3)} \quad (24d)$$

After substitution, Eq. (22f) becomes

$$(a_2^2 G^2 - a_3^2) (d/d\bar{y})(a_2^2 G^2) + (64/15) \sqrt{(2/\pi\gamma)} (Re/M) a_2 a_3 = 0. \quad (25a)$$

Integration of this equation yields

$$G(\bar{y}) = \left[(a_3/a_2)^2 \pm (2/a_2)(a_4 - \frac{32}{15} \sqrt{\frac{2}{\pi\gamma}} \frac{a_3}{a_2} \frac{Re}{M} \bar{y})^{\frac{1}{3}} \right]^{\frac{1}{2}}, \quad (25b)$$

where a_4 is the new integration constant. The plus sign in $G(\bar{y})$ is taken owing to the fact that

$$a_2^2 G^2 - a_3^2 = (2a_2/\bar{n}),$$

and

$$a_2 > 0, \quad \bar{n} > 0 \text{ always.}$$

By using Eqs. (24), one finds that the boundary conditions

(Eqs. 20 b, d, and e) lead to the following conditions on $G(\bar{y})$:

$$G = \frac{2L + a_3}{a_2} \quad \text{at} \quad \bar{y} = \frac{1}{2} \quad (26a)$$

$$G = 1 \quad \left. \vphantom{G = 1} \right\} \quad \text{at} \quad \bar{y} = -\frac{1}{2} \quad (26b)$$

$$a_2 + a_3 = 2 \quad \left. \vphantom{a_2 + a_3 = 2} \right\} \quad (26c)$$

[Here $L = \sqrt{(T_I/T_{II})}$]. These three conditions are sufficient for the evaluation of a_2 , a_3 , and a_4 ; the results are

$$a_2 = \frac{\left[(1 + \beta)(L^4 + 2L^3 + \beta) + L^2 \right]^{\frac{1}{2}} - (L^3 + 2L^2 - \beta - 1)}{(1 + \beta - L^2)} \quad (27a)$$

$$a_3 = 2 - a_2 = \frac{-\left[(1 + \beta)(L^4 + 2L^3 + \beta) + L^2\right]^{\frac{1}{2}} + (L^3 + \beta + 1)}{(1 + \beta - L^2)} \quad (27b)$$

$$a_4 = 1 - 2(1 + \beta)(a_3/a_2) + (a_3/a_2)^2, \quad (27c)$$

in which the abbreviation $\beta = (8/15) \sqrt{2/\pi\gamma} (Re/M)$ is employed.

Once $G(\bar{y})$ is known, \bar{n}_1 , \bar{n}_2 , \bar{T}_1 , \bar{T}_2 are completely determined, and so are the average density ρ , temperature T , pressure p and the heat flux q_y . We obtain explicit solutions for these quantities, as follows:

$$\rho/\rho_{II} = \left(a_4 - 4\beta \frac{a_3}{a_2} \frac{y}{d}\right)^{-\frac{1}{2}} \quad (28a)$$

$$T/T_{II} = (a_2/2) \left(a_4 - 4\beta \frac{a_3}{a_2} \frac{y}{d}\right)^{\frac{1}{2}} \quad (28b)$$

$$p/p_{II} = (a_2/2) \quad (28c)$$

$$\frac{q_y}{\frac{k}{c_{II}} \frac{T_{II}}{d}} = (4/15) \sqrt{(2/\pi\gamma)} a_2 a_3 (Re/M), \quad (28d)$$

where the subscript II denotes quantities evaluated at T_{II} , ρ_{II} .

By introducing the Stanton number

$$C_H = \frac{q_y}{\rho_{II} c_{pII} U (T_{II} - T_I)}$$

and using Eq. (28d), we obtain

$$C_H M = (4/15) \sqrt{(2/\pi\gamma)} \frac{a_2 a_3}{Pr (1 - L^2)}. \quad (29)$$

Once the solutions for \bar{n}_1 , \bar{n}_2 , \bar{T}_1 , and \bar{T}_2 are obtained one can solve for \bar{u}_1 and \bar{u}_2 from Eqs. (22b) and (22e). But one is interested in the average velocity \bar{u} rather than \bar{u}_1 or \bar{u}_2 . According to Eq. (24)

$$\bar{n}_1 \bar{u}_1 \bar{T}_1 + \bar{n}_2 \bar{u}_2 \bar{T}_2 = (\alpha_2/2) (\bar{u}_1 + \bar{u}_2) + \frac{\alpha_3 \alpha_1}{2}$$

while

$$\bar{u}(\bar{y}) = \frac{\bar{n}_1 \bar{u}_1 + \bar{n}_2 \bar{u}_2}{\bar{n}_1 + \bar{n}_2} = \frac{\bar{u}_1 + \bar{u}_2}{2} - \frac{\alpha_3 \alpha_1}{2 \alpha_2}$$

Therefore,

$$d/d\bar{y} (\bar{n}_1 \bar{u}_1 \bar{T}_1 + \bar{n}_2 \bar{u}_2 \bar{T}_2) = \alpha_2 (d\bar{u}/d\bar{y}) \quad , \quad * \quad (30)$$

and Eq. (22e) is readily integrated to give

$$\bar{u} = (15/16) (\alpha_1/\alpha_3) (\alpha_4 - 4\beta \frac{\alpha_3}{\alpha_2} \bar{y})^{\frac{1}{2}} + \alpha_5 \quad (31)$$

where α_1 and α_5 are undetermined integration constants. The boundary conditions for \bar{u}_1 and \bar{u}_2 [Eqs. (20a, c)] can also be converted into two boundary conditions for \bar{u} :

$$\bar{u} = \frac{1}{2} + L (\alpha_1/\alpha_2) \quad \text{at } \bar{y} = +\frac{1}{2}$$

$$\bar{u} = -\frac{1}{2} - (\alpha_1/2) \left(1 + \frac{\alpha_3}{\alpha_2}\right) = -\frac{1}{2} - (\alpha_1/\alpha_2) \quad \text{at } \bar{y} = -\frac{1}{2} ,$$

with α_2 , α_3 , and α_4 given by Eqs. (27).

These two conditions lead to the evaluation of α_1 and α_5 in terms of the known quantities α_2 , α_3 , and α_4 .

$$\alpha_1 = \frac{1}{(15/16)(1/\alpha_3) \left[(\alpha_4 - 2\beta \frac{\alpha_3}{\alpha_2})^{\frac{1}{2}} - (\alpha_4 + 2\beta \frac{\alpha_3}{\alpha_2})^{\frac{1}{2}} \right] - \frac{1+L}{\alpha_2}}$$

$$\alpha_5 = -\frac{1}{2} \cdot \frac{(15/16)(1/\alpha_3) \left[(\alpha_4 - 2\beta \frac{\alpha_3}{\alpha_2})^{\frac{1}{2}} + (\alpha_4 + 2\beta \frac{\alpha_3}{\alpha_2})^{\frac{1}{2}} \right] + \frac{1-L}{\alpha_2}}{(15/16)(1/\alpha_3) \left[(\alpha_4 - 2\beta \frac{\alpha_3}{\alpha_2})^{\frac{1}{2}} - (\alpha_4 + 2\beta \frac{\alpha_3}{\alpha_2})^{\frac{1}{2}} \right] - \frac{1+L}{\alpha_2}}$$

* This result means that $p_{xy} = \mu_c (du/dy)$ in the limiting case $M^2 \ll 1$ regardless of the plate temperature ratio.

Therefore,

$$u/U = \frac{(15/16)(1/a_3)}{(15/16)(1/a_3) \left[(a_4 - 2\beta \frac{a_3}{a_2})^{\frac{1}{2}} - (a_4 + 2\beta \frac{a_3}{a_2})^{\frac{1}{2}} \right] - \frac{1+L}{a_2}} \times \left\{ (a_4 - 4\beta \frac{a_3}{a_2} \frac{y}{d})^{\frac{1}{2}} - \frac{1}{2} \left[(a_4 - 2\beta \frac{a_3}{a_2})^{\frac{1}{2}} + (a_4 + 2\beta \frac{a_3}{a_2})^{\frac{1}{2}} \right] - \frac{1-L}{2a_2} \right\} \quad (32)$$

By employing Eq. (21a), we can express the shearing stress as

$$\frac{P_{xy}}{\rho_{II} \sqrt{\gamma R T_{II}} U} = - \frac{a_1}{\sqrt{2\pi\gamma}}$$

where $a_1 < 0$.

Define the skin friction coefficient C_D

$$C_D = \frac{P_{xy}}{\frac{1}{2} \rho_{II} U^2}$$

then

$$C_D M = - (C_D M)_0 a_1$$

where $(C_D M)_0 =$ the value of $C_D M$ for free molecular flow ($Re/M = 0$)
 $= \sqrt{2/\pi\gamma}$.

In this limiting case of low Mach number flow $P_{yy} \approx -p$ and $p_{yy} \approx 0$ [Eqs. (21c, e)] so that both P_{yy} and p are constant across the flow, as shown by Eq. (28c). Also the energy equation [Eq. (9e)] states that $q_y =$ constant in the absence of dissipation. When in addition $L^2 = (T_I/T_{II}) \rightarrow 1$, then $a_3 = 0$ ($\frac{T_I - T_{II}}{T_I}$), as shown by Eq. (27b)

and all of these results [Eqs. (28a), (28b), (29), and (31)] reduce to the solutions found previously in Reference 10.

As a numerical example we take $T_Y/T_{II} = 4$; the velocity and temperature profiles for this case are shown in Figures 3 and 4. In Figures 5 and 6 the normalized skin-friction and heat transfer coefficients are plotted against Re/M . These results are discussed in Section III.

II. C. Arbitrary Mach Number and Plate Temperature Ratio

When the Mach number and plate temperature ratio are both arbitrary the velocity and temperature fields are closely coupled. In that case the four algebraic conservation relations [Eqs. (19a) - (19d)] allow us to replace the six unknown functions by two independent functions $F(\bar{y})$ and $G(\bar{y}) = (\bar{n}_1 \sqrt{T_1})^{-1} = (\bar{n}_2 \sqrt{T_2})^{-1}$, and Eqs. (19e) and (19f) furnish two simultaneous, first-order, non-linear ordinary differential equations for F and G .

In the expressions for \bar{n}_1 , \bar{T}_1 , \bar{n}_2 , \bar{T}_2 given in Section II. B the constant a_3 is replaced by the function $F(\bar{y})$. Thus, Eqs. (19a) and (19c) are automatically satisfied by taking

$$\bar{n}_1(\bar{y}) = \frac{2}{G(a_2 G - F)} \quad (33a)$$

$$\bar{n}_2(\bar{y}) = \frac{2}{G(a_2 G + F)} \quad (33b)$$

$$\bar{T}_1(\bar{y}) = (1/4)(a_2 G - F)^2 \quad (33c)$$

$$\bar{T}_2(\bar{y}) = (1/4)(a_2 G + F)^2 \quad (33d)$$

and Eqs. (19b) and (19d) yield

$$\bar{u}_1(\bar{y}) = \frac{1}{2} \left[\frac{4}{\gamma M^2} \cdot \frac{a_2}{a_1} (a_3 - F) - a_1 G \right] \quad (33e)$$

$$\bar{u}_2(\bar{y}) = \frac{1}{2} \left[\frac{4}{\gamma M^2} \cdot \frac{a_2}{a_1} (a_3 - F) + a_1 G \right] \quad (33f)$$

After substitution, Eqs. (19e) and (19f) become two integrable equations governing $G(\bar{y})$ and $F(\bar{y})$, as follows:

$$(a_2^2 G^2 - F^2) (dF/d\bar{y}) - \frac{8}{\gamma 2\pi \gamma} (\text{Re}/M) \frac{a_1}{\left(\frac{4}{\gamma M^2} \frac{a_2}{a_1} - \frac{a_1}{a_2} \right)} = 0 \quad (34)$$

$$G (dG/d\bar{y}) + \lambda_1 F (dF/d\bar{y}) = 0 \quad (35)$$

where

$$\lambda_1 = \lambda_1(a_1, a_2, \gamma M^2) = (1/3) \cdot \frac{21 + \gamma M^2 \left(\frac{a_1}{a_2} \right)^2 + \frac{32}{\gamma M^2} \left(\frac{a_2}{a_1} \right)^2}{\gamma M^2 a_1^2 + 5 a_2^2} \quad (35a)$$

Eq. (35) immediately yields the relation

$$G^2 + \lambda_1 F^2 = a_5 \quad (36)$$

By employing this expression, Eq. (34) can also be integrated. Thus

$$\lambda_3 F^3 - \lambda_2 a_5 F + \frac{8}{\gamma 2\pi \gamma} \cdot (\text{Re}/M) \cdot (a_1/a_2) \bar{y} + a_4 = 0 \quad (37)$$

where a_4, a_5 are two new integration constants, and

$$\lambda_2 = \lambda_2(a_1, a_2, \gamma M^2) = a_2 \left(\frac{4}{\gamma M^2} \cdot \frac{a_2}{a_1} - \frac{a_1}{a_2} \right)$$

$$\lambda_3 = \lambda_3(a_1, a_2, \gamma M^2) = (1/3) \left(a_2 \lambda_1 + \frac{1}{a_2} \right) \left(\frac{4}{\gamma M^2} \frac{a_2}{a_1} - \frac{a_1}{a_2} \right)$$

When the five boundary conditions [Eq. (20)] are converted into

conditions on $G(\bar{y})$ and $F(\bar{y})$ by employing Eqs. (33), one obtains

$$\text{at } \bar{y} = -\frac{1}{2} \left\{ \begin{array}{l} G = 1 \\ F = 2 - a_2 \\ (a_2/a_1)(a_3 - F) + \frac{\gamma M^2}{4} a_1 G + \frac{\gamma M^2}{4} = 0 \end{array} \right. \quad \begin{array}{l} (38a) \\ (38b) \\ (38c) \end{array}$$

$$\text{at } \bar{y} = +\frac{1}{2} \left\{ \begin{array}{l} G = -\frac{\frac{\gamma M^2}{4} a_1 - 2 L a_2 - a_2 a_3}{(\gamma M^2/4) a_1^2 + a_2^2} \\ F = -\frac{(\gamma M^2/2) L a_1^2 + (\gamma M^2/4) a_1 a_2 - a_2^2 a_3}{(\gamma M^2/4) a_1^2 + a_2^2} \end{array} \right. \quad \begin{array}{l} (38d) \\ (38e) \end{array}$$

By substituting these conditions into Eqs. (36) and (37) one gets a system of five algebraic equations governing the five a 's:

$$\left(\frac{\frac{\gamma M^2}{4} a_1 - 2 L a_2 - a_2 a_3}{(\gamma M^2/4) a_1^2 + a_2^2} \right)^2 + \lambda_1 \left[\left(\frac{\frac{\gamma M^2}{4} L a_1^2 + \frac{\gamma M^2}{4} a_1 a_2 - a_2^2 a_3}{(\gamma M^2/4) a_1^2 + a_2^2} \right)^2 - (2 - a_2)^2 \right] - 1 = 0 \quad (39a)$$

$$\lambda_3 \left[\left(\frac{\frac{\gamma M^2}{2} L a_1 + \frac{\gamma M^2}{4} a_1 a_2 - a_2^2 a_3}{(\gamma M^2/4) a_1^2 + a_2^2} \right)^3 + (2 - a_2)^3 \right] - \lambda_2 \left[1 + \lambda_2 (2 - a_2)^2 \right] \quad (39b)$$

$$x \left[\left(\frac{\frac{\gamma M^2}{2} L a_1 + \frac{\gamma M^2}{4} a_1 a_2 - a_2^2 a_3}{(\gamma M^2/4) a_1^2 + a_2^2} \right) + (2 - a) \right] - \frac{8}{\gamma 2\pi\gamma} \frac{\text{Re } a_1}{M a_2} = 0$$

$$a_3 = 2 - a_2 - (\gamma M^2/4) (a_1/a_2)(1 + a_1) \quad (39c)$$

$$a_4 = (\lambda_1 \lambda_2 - \lambda_3)(2 - a_2)^3 + \lambda_2 (2 - a_2) + (4/\sqrt{2\pi\gamma}) (\text{Re}/M)(a_1/a_2) \quad (39d)$$

$$a_5 = 1 + \lambda_1 (2 - a_2)^2 \quad (39e)$$

Solving numerically for the a 's is not so tedious as it seems. The first two equations, in which the value of a_3 is given by Eq. (39c), can be solved simultaneously for a_1 and a_2 by means of trial and error. The fact that $(-a_1)$ always varies monotonically between unity and zero as Re/M increases simplifies the iteration procedure considerably. By consulting the $C_D M / (C_D M)_0$ diagram, one can make a fairly good first estimate of a_1 , then one can solve for a_2 from Eq. (39a), and substitute these values of a_1 and a_2 into Eqs. (39b) to check if the Re/M so obtained deviates from the given value. This procedure converges very rapidly to the final result. As soon as a_1 , a_2 are known, the other three constants are readily determined from Eqs. (39c, d, and e).

All mean quantities of interest are expressed in terms of F , G , and the five a 's as follows:

$$u/U = (2/\gamma M^2) \left[(a_3 a_2 / a_1) - \left(\frac{a_2}{a_1} + \frac{\gamma M^2}{4} \frac{a_1}{a_2} \right) F \right] \quad (40a)$$

$$T/T_H = 1/4 \left[1 + (\gamma M^2/3) (a_1/a_2)^2 \right] (a_2^2 G^2 - F^2) \quad (40b)$$

$$p/p_H = \frac{2a_2}{a_2^2 G^2 - F^2} \quad (40c)$$

$$\frac{P_{xy}}{p_H \gamma \gamma R T_H U} = - (a_1 / \sqrt{2\pi\gamma}) \quad (40d)$$

$$\frac{a_y}{(k_{cH} T_H / a)} = (4/15) \sqrt{(2/\pi\gamma)} (\text{Re}/M) a_1 \left(\frac{a_2}{a_1} + \frac{\gamma M^2}{4} \frac{a_1}{a_2} F \right). \quad (40e)$$

Hence,

$$C_{D M}/(C_{D M})_0 = -a_1 \text{ where } (C_{D M})_0 = \sqrt{(2/\pi\gamma)} \quad (40f)$$

and

$$C_{H M} = (4/15) \sqrt{(2/\pi\gamma)} \frac{a_1}{\text{Pr} (1 - L^2)} \left(\frac{a_2}{a_1} + \frac{\gamma M^2}{4} \frac{a_1}{a_2} F \right). \quad (40g)$$

In practice, for a particular \bar{y} , more than one value of F is obtained, because Eq. (37) is a third order algebraic equation always having three real roots. A typical variation of $F(\bar{y})$ is sketched in Figure 7. Now $F(\bar{y})$ is a continuous function of \bar{y} in the gas, so that only one of the three possible branches is physically acceptable. When $L^2 = 1$, the velocity profile is always anti-symmetrical about the mid-plane, so that $F(\bar{y})$ is also anti-symmetrical [Eq. (40a)]. Thus, only the intermediate heavily-lined branch 2 is physically realistic in this case. When $L^2 > 1$ the behavior of $F(\bar{y})$ is more complicated. According to Eq. (34) for $(dF/d\bar{y})$, when $\text{Re}/M \rightarrow \infty$, $F(\bar{y}) \rightarrow \text{constant}$. As Re/M decreases the curve of F vs. \bar{y} gradually rotates in the counterclockwise direction at first, and the pivot point moves smoothly along the F -axis in one direction. At some intermediate value of Re/M the curve of F vs. \bar{y} reverses its direction of rotation and finally reaches a horizontal position in the limit $\text{Re}/M \rightarrow 0$. Evidently only the heavily-lined branch is physically realistic for any arbitrary values of L^2 , M^2 , and Re/M . [See Section III.E.]

As a numerical illustration we take $M = 3$, $L^2 = T_{II}/T_I = 4$. The skin-friction and heat transfer coefficients are shown as functions of Re/M in Figures 5 and 6, and the velocity and temperature profiles are plotted in Figures 8 and 9. These results are discussed in Section III.

II. D. Special Case of Equal Plate Temperatures, But Arbitrary Mach Number

Although this special case is included in the general analysis given in Section II. C, there are certain important simplifications. When both plates have the same temperature, then obviously \bar{u}_1 , \bar{u}_2 , and \bar{u} are all anti-symmetrical, while \bar{T}_1 , \bar{T}_2 , and \bar{T} (or \bar{n}) must be symmetrical with respect to $\bar{y} = 0$, i. e.,

$$\bar{u}_1(\bar{y}) = -\bar{u}_2(-\bar{y}) \quad \text{and} \quad \bar{T}_1(\bar{y}) = \bar{T}_2(-\bar{y}) \quad .$$

From Eqs. (33a) and (40a), one sees that

$$F(\bar{y}) = -F(-\bar{y}) \quad (41a)$$

$$G(\bar{y}) = G(-\bar{y}) \quad . \quad (41b)$$

Therefore, $F(0) = 0$, and from Eq. (37), we have $\alpha_4 = 0$. At $\bar{y} = 0$, one can conclude from Eqs. (41b), (33e), and (33f) that

$$\alpha_3 = 0 \quad ,$$

since α_1 and α_2 remain finite for all possible values of M and Re/M .

The non-trivial α 's are then governed by Eqs. (39c, d, and e)

$$\alpha_2(2 - \alpha_2) - (\gamma M^2/4)\alpha_1(1 + \alpha_1) = 0 \quad (42a)$$

$$(\lambda_1\lambda_2 - \lambda_3)(2 - \alpha_2)^3 + \lambda_2(2 - \alpha_2) + \frac{4}{\gamma 2\pi\gamma}(\text{Re}/M)(\alpha_1/\alpha_2) = 0 \quad (42b)$$

$$\alpha_5 = 1 + \lambda_1(2 - \alpha_2)^2 \quad (42c)$$

So one can easily express α_2 in terms of α_1 by means of Eq. (42a).

Selecting the positive root,

$$\alpha_2 = 1 + \sqrt{1 - (\gamma M^2/4)\alpha_1(1 + \alpha_1)} \quad .$$

By substituting this expression for α_2 into Eq. (42b), one solves for α_1 , and then one obtains α_5 from Eq. (42c).

The variation of skin-friction coefficient with the rarefaction parameter Re/M for the case $M = 3$, $T_I/T_{II} = 1$ is shown in Figure 5, and the velocity and temperature profiles are plotted in Figures 10 and 11.

III. DISCUSSION AND CONCLUSIONS

III. A. Skin-Friction and Heat Transfer Coefficients

As expected from the structure of the basic differential equations [Eq. (19)] the variation of the skin friction and heat transfer coefficients with Re/M is smooth and continuous over the whole range (Figures 5 and 6). For all values of Mach number and plate temperature ratio $C_D M$ approaches the value given by the solution of the Navier-Stokes equations as $Re/M \rightarrow \infty$ (Appendix), and $C_D M$ approaches the free molecule flow value of $\sqrt{(\pi\gamma/2)}$ as $Re/M \rightarrow 0$. According to Eq. (A-9)

$$(C_{D M})_{\text{Navier Stokes}} = \frac{2}{(Re/M)} \cdot \left\{ \frac{1}{2} \left[1 + (T_I/T_{II}) + \left(\frac{\gamma-1}{6} \right) Pr M^2 \right] \right\} \quad (A-9)$$

This behavior suggests that the rarefaction parameter should be renormalized by replacing Re/M , based on physical quantities evaluated at T_{II} , ρ_{II} , with a new parameter $(Re/M)^*$, where

$$(Re/M)^* = (Re/M) \cdot \frac{2}{1 + (T_I/T_{II}) + \left(\frac{\gamma-1}{6} \right) Pr M^2}$$

This procedure amounts to evaluating the "proper" mean free path at a density corresponding to a certain "kinetic temperature", i. e.,

$$(\lambda/d)^* = (\lambda_{II}/d) \cdot (T_K/T_{II})$$

where T_K/T_{II} is given by the bracket in Eq. (A-9). Evidently $(\lambda/d)^* \gg (\lambda_{II}/d)$ for high values of M^2 and/or T_I/T_{II} .

In Figure 12 the drag coefficient is replotted in terms of this new rarefaction parameter $(Re/M)^*$. In these coordinates all the curves deviate only slightly from the "basic" curve corresponding to $M^2 = 0$,

$T_I/T_{II} = 1$. Appreciable deviations ($\cong 10$ per cent) from the classical Navier-Stokes solution occur even at values of Re/M as high as 30, or $(\lambda/d)^* = 1/20$. The approach to free-molecule flow is also quite slow, because the solutions are simple algebraic functions of Re/M . On the other hand, the major portion of the transition from the classical Navier-Stokes regime to the highly rarefied regime occurs over an interval of less than a decade in Re/M or gas density $\left[3 < (Re/M)^* < 30, \text{ or } \frac{1}{2} < (\lambda/d)^* < 1/20 \right]$. This behavior must be closely connected with the "cascading" effect of particle collisions in the gas. When a particle suffers only one or two collisions in passing from one plate to the other the effect on the particle velocity distribution is small. But when 5 - 10 collisions occur, especially with particles emitted from the opposite plate, the effect is cumulative, and almost all the particles quickly forget their original place of birth.

Since the Mach number appears in the definition of "kinetic temperature" only as the factor $\left[\frac{\gamma-1}{6} \right] Pr M^2 = (2/27) M^2$ for a monatomic gas, the drag coefficient is rather insensitive to Mach number for $M < 1.5$. This conclusion agrees with the experimental results of Bowyer and Talbot³, Kuhlthau⁹, and Chiang⁴ for cylindrical Couette flow with small ratio of annulus width to cylinder radius.

III. B. Shear Stress and Normal Heat Flux

By utilizing Eq. (21a), one finds that

$$\frac{P_{xy}}{\mu_c (du/dy)} = - (Re/M) \frac{a_1}{\gamma 2\pi \gamma} \left(\frac{1}{n} \frac{d\bar{u}}{dy} \right)^{-1} \quad (43)$$

But according to Eq. (40a),

$$(\overline{du}/\overline{dy}) = -\frac{1}{2} \left[\frac{4}{\gamma M^2} \frac{a_2}{a_1} + \frac{a_1}{a_2} \right] \frac{dF}{dy},$$

so that the ratio $\frac{P_{xy}}{\mu_c (\overline{du}/\overline{dy})}$ is constant across the flow [Eq. (43)], and is given by

$$\frac{P_{xy}}{\mu_c (\overline{du}/\overline{dy})} = (\tilde{\mu}/\mu_c) = \frac{1}{\left[1 + \frac{\gamma M^2}{3} (a_1/a_2)^2 \right]} \cdot \frac{\left[\frac{4}{\gamma M^2} (a_2/a_1) - (a_1/a_2) \right]}{\left[\frac{4}{\gamma M^2} (a_2/a_1) + (a_1/a_2) \right]}. \quad (44)$$

Clearly $\tilde{\mu} \rightarrow \mu_c$ when $M^2 \rightarrow 0$, or when $Re/M \gg 1$, for any values of M^2 and T_I/T_{II} . On the other hand at any finite fixed values of T_I/T_{II} and Re/M the ratio $\tilde{\mu}/\mu_c$ decreases rapidly with increasing plate Mach number. This behavior is connected with the fact that the (non-dimensional) shear stress is not much affected by plate velocity, but the gas temperature is everywhere large in a rarefied gas at high plate Mach number. In Figure 13 this behavior is shown schematically for the limiting case $Re/M = 0$. In Figure 15 the variation of $\tilde{\mu}/\mu_c$ with Re/M is illustrated for two values of T_I/T_{II} at $M = 3$. Again one sees that the transition from the classical Navier-Stokes regime to the almost free molecule flow regime occurs over about one decade in the rarefaction parameter.

We observe that $\tilde{\mu}/\mu_c \rightarrow 1$ when $T_I/T_{II} \gg 1$ (Figure 13). In this case the condition of zero normal velocity [Eq. (19a)] shows that $n_{II}/n_I = \sqrt{T_I/T_{II}} \gg 1$ when $Re/M = 0$, and the mean temperature in the gas approaches the geometric mean value $\sqrt{T_I T_{II}}$, regardless of the Mach number [Eq. (21d)]. Thus the "proper" Mach number is based on this mean temperature, or

$$\tilde{M}^2 = M^2 \cdot \sqrt{T_{II}/T_I} \rightarrow 0 \quad \text{when} \quad T_I/T_{II} > 1,$$

and it is not surprising that $p_{xy} \rightarrow \mu_c (du/dy)$ in this limiting case.

In fact this argument is valid for all values of Re/M and M^2 . To prove this conclusion formally, one observes that

$$\frac{P_{yy}}{n_{II} k T_{II}} = -(\alpha_2/2) = -\frac{1}{2} (\bar{n}_1 \bar{T}_1 + \bar{n}_2 \bar{T}_2) \approx -\frac{1}{2} \bar{n}_2 \bar{T}_2 \sqrt{T_I/T_{II}},$$

when $T_I/T_{II} > 1$, so that $\alpha_2 \gg 1$. Then Eq. (44) shows that

$$\mu_c \rightarrow \mu_c.$$

Similar remarks apply to the ratio of normal heat flux q_y to $-k_c (dT/dy)$. One finds that

$$\frac{q_y}{-k_c (dT/dy)} = \frac{(2/15)\gamma M^2 \left[\left(\frac{4}{\gamma M^2} (\alpha_2/a_1) + (\alpha_1/a_2) \right) \left(\frac{4}{\gamma M^2} (\alpha_2/a_1) - (\alpha_1/a_2) \right) \right]}{\left[1 + \frac{\gamma M^2}{3} (\alpha_1/a_2)^2 \right] \cdot \left[1 + \alpha_2^2 \lambda_1 \right]}.$$

The variation of this ratio with the parameters T_I/T_{II} and M^2 in the limiting case $Re/M \rightarrow 0$ is shown in Figure 14.

III. C. Mean Temperature and Mean Velocity Profiles

When $M^2 \ll 1$ the mean gas temperature approaches the geometric mean $\sqrt{T_I T_{II}}$ in the limit $Re/M \rightarrow 0$, as expected from the statistical weighting of the two Maxwellian streams. For arbitrary Mach numbers the gas temperature in this limiting case is equal to the geometric mean, plus a "kinetic" term [Eq. (21d) and Figure 9]. The temperature profiles pass smoothly from this free-molecule flow behavior to the behavior predicted by the Navier-Stokes-Fourier relations as Re/M increases.

The behavior of the mean velocity profiles is more interesting. By starting with Eq. (21a) for the shear stress, and introducing the boundary conditions [Eq. (20)], one can derive a very simple relation for the ratio of the velocity slip at the two plates. Thus,

$$\text{at } y = +d/2, \quad \bar{n}_1 \sqrt{\bar{T}_1} \left(\frac{1}{2} - \bar{u}_2 \right) = -\alpha_1 \quad (45a)$$

$$\text{at } y = -d/2, \quad \left(\frac{1}{2} + \bar{u}_1 \right) = -\alpha_1 \quad (45b)$$

By utilizing the expression for mean velocity Eq. (18) at $y = \pm d/2$, the quantities $\bar{u}_2 (+d/2)$ and $\bar{u}_1 (-d/2)$ are eliminated in favor of \bar{u} , and Eqs. (45a) and (45b) become

$$\left(\bar{n}_1 / \bar{n}_2 \right) \bar{n} \sqrt{\bar{T}_1} \left[\frac{1}{2} - \bar{u}(d/2) \right] = -\alpha_1 \quad (45c)$$

$$\left(\bar{n} / \bar{n}_1 \right) \left[\bar{u}(-d/2) + \frac{1}{2} \right] = -\alpha_1 \quad (45d)$$

But Eqs. (19a) and (19c) yield the relation

$$\bar{n} \sqrt{\bar{T}_1 \bar{T}_2} = \text{constant} = \alpha_2 \quad (45e)$$

By utilizing this last relation, Eq. (19a), and the boundary conditions on \bar{T}_1 and \bar{T}_2 one obtains

$$\frac{\frac{1}{2} - \bar{u}(+d/2)}{\bar{u}(-d/2) + \frac{1}{2}} = \sqrt{\bar{T}_I / \bar{T}_{II}} \quad (46)$$

independently of Re/M or M^2 .

In the Navier-Stokes regime most of the gas follows the hot plate (Figures 3 and 8) because $\mu_c \sim T$, and the stopping power of the hot plate is larger. However, the situation is reversed as the gas density decreases, because according to Eq. (46) the velocity "slip" at the hot plate is larger than at the cold plate. Finally, in the limit $Re/M \rightarrow 0$, most of the gas follows the cold plate.

When $T_I/T_{II} \gg 1$, the velocity slip at the cold plate is small, because the number density of particles emitted from the cold plate is much larger than the number density emitted from the hot plate. In this case $p_{xy} \rightarrow \mu_c (du/dy)$ (Section III. B), yet the flow bears no resemblance to the predictions of the classical Navier-Stokes equations with no slip. Especially in the highly rarefied flow regime the mean velocity is determined by the statistical weighting of the influence of the two plates.

III. D. Comparison of Present Results with Maxwell's Velocity Slip Relation

When the gas is not too rarefied Maxwell suggested that the Newtonian relation $p_{xy} = \mu_c (du/dy)$ might hold in the main body of the gas, up to a distance of the order of one local mean free path from a solid surface. By considering the balance of tangential momentum at the surface itself, Maxwell found that

$$u_{\text{gas}} - u_{\text{wall}} \approx \left(\frac{2 \mu_c}{\rho \tilde{c}} \frac{du}{dy} \right)_{\text{wall}} ,$$

for completely diffuse reemission. According to kinetic theory,

$$\mu_c = (a/2) \rho \tilde{c} \lambda , \text{ where } \tilde{c} = \sqrt{(8RT/\pi)} , \text{ and } a \text{ is a numerical factor}$$

of order unity, so that $u_g - u_w \approx a \left(\lambda \frac{du}{dy} \right)_w$. It is interesting to

compare this simple and widely-used suggestion with the results obtained from the present approximate solution of the Maxwell-Boltzmann equation.

When $M^2 \ll 1$, $p_{xy} \rightarrow \mu_c (du/dy)$ everywhere, according to the present solution (Sections II. B and III. B). At the upper plate

[Eqs. (21a), (45c), and (45e)] ,

$$p_{xy} (+d/2) = \left(\rho_{II} \sqrt{\frac{R T_{II}}{2\pi}} U \right) \left[\frac{a_2}{\sqrt{T_I/T_{II}}} \left(\frac{1}{2} - \bar{u} \right) \right] = \left(\mu_c \frac{du}{dy} \right)_{y=+d/2}$$

But $(a_2/2) = \rho T / \rho_{II} T_{II}$ [Eq. (28c)]; therefore ,

$$(U/2) - u (+d/2) = \frac{2\mu_c}{\rho \tilde{c}} \sqrt{T_I/T} \left(\frac{du}{dy} \right)_{y=+d/2} = a \lambda \sqrt{T_I/T} \left(\frac{du}{dy} \right)_{y=+d/2} ,$$

where $(\rho \tilde{c})$ and μ_c , and λ are evaluated at the gas temperature (or the gas density), and not the surface temperature.

One sees that even for $M^2 \ll 1$ the Maxwell velocity slip relation is strictly correct only when the gas temperature and the surface temperature are nearly equal, i. e., when $(T_I - T_{II})/T_I \ll 1$ (Reference 10), or when $Re/M \gg 1$. But

$$\sqrt{T_I/T} \approx 1 + \frac{1}{2} \left(\frac{\Delta T}{T_I - T_{II}} \right) \left(\frac{T_I - T_{II}}{T_I} \right) + \dots ,$$

where $\Delta T = T_I - T(d/2)$. Now, $\Delta T / (T_I - T_{II}) \sim 0.10$ when $(Re/M)^* = 30$, so that the Maxwell velocity slip relation is in error by 5 per cent when $\sqrt{T_I/T_{II}} = 2$ and $(Re/M)^* = 30$, or $(\lambda/d)^* = 1/20$. Thus the usual velocity slip relation is quite useful in the near-Navier-Stokes regime, as Maxwell suggested.

For arbitrary Mach number $p_{xy} \neq \mu_c (du/dy)$, and $(a_2/2) \neq \rho T / \rho_{II} T_{II}$. In that case the velocity slip can be expressed as follows:

$$(U/2) - u (+d/2) = a \left[\lambda \frac{\delta}{\sqrt{T_2/T}} \left(\frac{du}{dy} \right) \right]_{y=+d/2} ,$$

where

$$\delta = \frac{P_{xy}}{\mu_c (du/dy)} .$$

By utilizing Eq. (44), Section III. B, one can show that for $Re/M \gg 1$,

$$\delta = 1 - \beta_1 (Re/m)^{-2} + \dots ;$$

also, $T_2/T = 1 + \beta_2 (Re/M)^{-1}$ where β_1 and β_2 are constants.

Once again the Maxwell velocity slip relation is found to be correct to first order $\left[(Re/M)^{-1} \right]$ for large Re/M . The departure from the Navier-Stokes relation is of second order. We conclude that Maxwell's suggestion is a good first-approximation for arbitrary Mach number and plate temperature ratio in the near-Navier-Stokes regime. One could not expect it to hold for the transitional or highly rarefied flow regimes.

III. E. Limitations of the Six-Moment Approximation

Our original choice of six Maxwell moments (Section II. A) is expected to furnish a good first approximation for plane Couette flow when $M = 0(1)$. But at high plate Mach numbers ($M^2 \gg 1$) p_{xx} and p_{yy} are of the same order as q_y in a rarefied gas [Eqs. (21b), (21c), (21e), and (21f)], and the six-moment approximation is inadequate.

As an indication of the limitations of this approximation, consider the differential equation for $(dF/d\bar{y})$ [Eq. (34)] :

$$dF/d\bar{y} = - \frac{\delta}{\gamma 2\pi\gamma} \frac{\alpha_1}{(\alpha_2^2 G^2 - F^2)} \left[\left(- \frac{4}{M^2} \frac{\alpha_2}{\alpha_1} + \frac{\alpha_1}{\alpha_2} \right)^{-1} \right]. \quad (47)$$

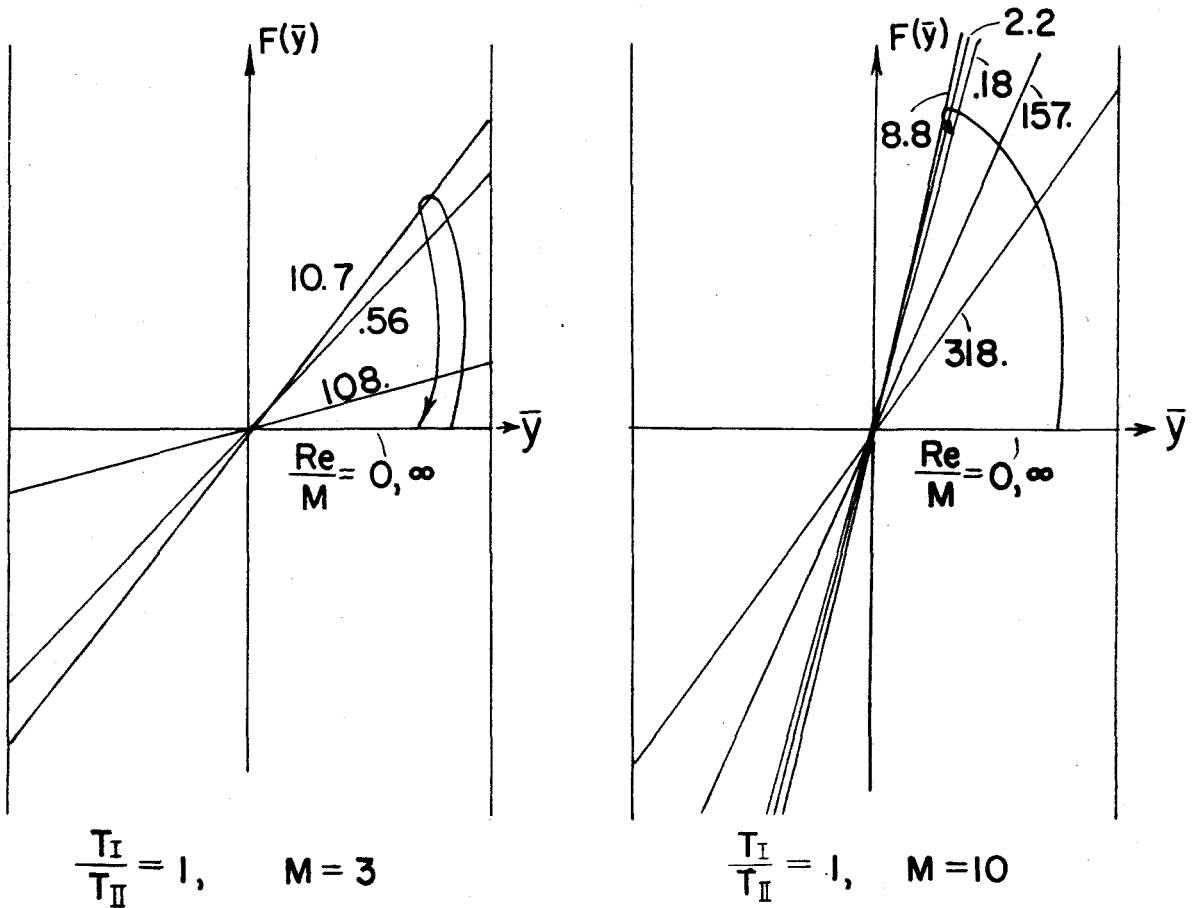
When $Re/M \gg 1$, $\alpha_2 \rightarrow 2$ and $\alpha_1 = 0 \left[(Re/M)^{-1} \right]$, so the quantity in brackets is positive and $0 \left[(Re/M)^{-1} \right]$. On the other hand when $Re/M \rightarrow 0$, $\alpha_2 = \bar{n}_1 \bar{T}_1 + \bar{n}_2 \bar{T}_2 \rightarrow (1 + \sqrt{T_I/T_{II}})$, and $\alpha_1 \rightarrow -1$,

so the bracket $\rightarrow (1 + L) \left[\frac{4}{\gamma M^2} (1 + L)^2 - 1 \right]^{-1}$, where $L = \sqrt{T_I/T_{II}}$.

So long as $M^2 < (4/\gamma)(1 + L)^2$ this bracket is positive when $Re/M = 0$, and remains positive for all values of Re/M . However, when $M^2 > (4/\gamma)(1 + L)^2$ the bracket is negative in the limit $Re/M \rightarrow 0$, and therefore must have changed sign for some intermediate value of Re/M . Such behavior is physically unrealistic, and some difficulties are to be expected with the six-moment approximation. (For $\gamma = 5/3$ and $L = 1$, the "critical" Mach number is 3.1.)

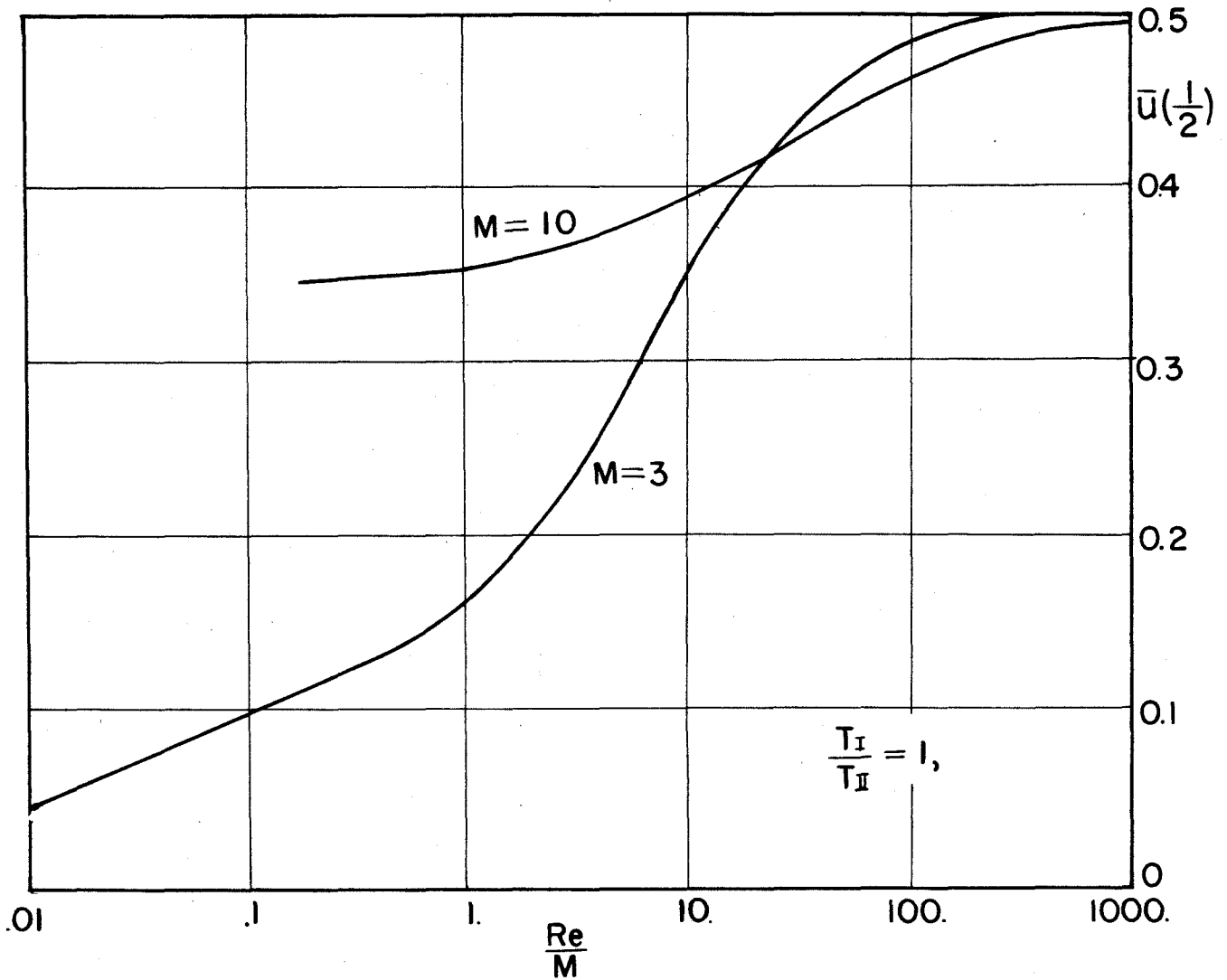
Without going into details we indicate the actual behavior of the curve of $F(\bar{y})$ vs. \bar{y} and the behavior of $\bar{u} + \frac{1}{2}$ for values of M^2 smaller and larger than $(4/\gamma)(1 + L)^2$. As specific examples, we selected $L = 1$ and $M = 3$ and 10. When $M^2 < (4/\gamma)(1 + L)^2$ the curve of $F(\bar{y})$ behaves in the manner described in Section II. C, and shown in the accompanying Sketch A. The value of $\bar{u} + \frac{1}{2}$ decreases smoothly as Re/M decreases, and the point of inflection shown in Sketch B occurs at a value of Re/M very close to the point at which the curve of $F(\bar{y})$ has its maximum inclination. However, for $M = 10$ the curve of $F(\bar{y})$ rotates counter clockwise to a certain maximum angle as Re/M decreases, but is unable to negotiate the return journey to the horizontal position. In fact for values of Re/M less than a certain critical value no real solutions could be found (Sketch A and B).

The situation is somewhat analogous to the difficulty encountered with the Karman-Pohlhausen method¹⁴ when a quartic is employed to approximate the mean velocity profile across the laminar boundary layer. For positive streamwise pressure gradients it is well-known that flow separation occurs at $\Lambda = -12$, where Λ is the Pohlhausen

SKETCH A -- BEHAVIOR OF $F(\bar{y})$

parameter. But there is also a difficulty at $\Delta = +12$, where none is expected on physical grounds. As shown by Tani¹³ the best way to avoid (or postpone) such singularities is to take an additional moment. In our case the importance of the moments associated with p_{xx} and p_{yy} at high Mach numbers dictates a similar procedure.

A rough calculation replacing $Q_5 = m \sum_x \sum_y$ by $Q = m \sum_x^2$



SKETCH B -- BEHAVIOR OF $\bar{u}(\pm \frac{1}{2})$

(corresponding to p_{xx}) already shows that the difficulty illustrated by Eq. (47) disappears. Of course this choice of moments is poor when $M = 0$ (1). Clearly the proper course is to employ an eight-moment approximation, in which the four moments in addition to the collisional invariants are as follows:

$$\begin{aligned}
 Q_5 &= m \sum_x \sum_y \\
 Q_6 &= m \sum_y (\sum_x^2 / 2) \\
 Q_7 &= m \sum_x^2 \\
 Q_8 &= m \sum_y^2 .
 \end{aligned}$$

For this calculation we select a modified two stream Maxwellian of the following form:

$$\begin{aligned}
 \sum_y < 0, \quad f = f_1 \left[1 + a_1(\bar{y}) \sum_x \sum_y \right] \\
 \sum_y > 0, \quad f = f_2 \left[1 + a_2(\bar{y}) \sum_x \sum_y \right] .
 \end{aligned}$$

where f_1 and f_2 are given by Eqs. (10a) and (10b), and $a_1(\bar{y})$, $a_2(\bar{y})$ are two additional functions of \bar{y} . The boundary conditions [Section II. A. 2] lead to the conditions given by Eq. (20), plus $a_1(+\frac{1}{2}) = 0$ and $a_2(-\frac{1}{2}) = 0$. An eight-moment approximation yields four algebraic and four first-order non-linear differential equations for the eight unknown functions $n_1(\bar{y}) \dots u_2(\bar{y})$, $a_1(\bar{y})$, $a_2(\bar{y})$. Thus the problem is completely formulated, and is currently being investigated.

III. F. Conclusions and Future Work

By employing the simple two-stream Maxwellian in Maxwell's moment equations one obtains considerable insight into the nature of the transition from highly rarefied flows to the classical Navier-Stokes regime. The results obtained for plane, compressible Couette flow suggest certain conclusions about hypersonic flow. For a blunt-nosed body with surface temperature much less than the kinetic temperature the tangential velocity slip is expected to be very small near the nose, even in free-molecule flow. In spite of this fact the classical Navier-Stokes relations are not likely to provide a correct description of the

flow field when $\lambda^*/R_0 > 1/20$ (approximately), where λ^* is the mean free path evaluated just behind the bow shock, and R_0 is nose radius. On the other hand the transition from the near-Navier-Stokes regime to nearly-free molecule flow occurs over a range of gas density of about one decade. Similar conclusions apply to those portions of slender bodies where the normal component of flight velocity is large compared with the thermal velocity corresponding to the surface temperature.

There are important differences between the present results and those obtained by the ad hoc procedure of utilizing the Navier-Stokes equations plus Maxwell's velocity slip relation (Section III. D). In spite of this fact, the values of skin-friction and heat transfer coefficients obtained by such an ad hoc procedure are not far wrong. As pointed out by Dr. H. Grad, plane Couette flow is probably still too simple a geometry to show any critical features of these gross macroscopic quantities. For this reason we are studying the problem of heat conduction between two concentric cylinders, where the ad hoc procedure is grossly inaccurate¹.

Another important example of non-linear flow is the steady, plane shock wave. This problem deserves to be investigated in order to learn about molecular effects in longitudinal flows without shear. Eventually one should have a much clearer understanding of the limitations and advantages of Maxwell's moment method.

REFERENCES

1. Ai, D. K.: Cylindrical Couette Flow in a Rarefied Gas According to Grad's Equations. GALCIT Hypersonic Research Project, Memorandum No. 56, July 15, 1960.
2. Born, M. and H. S. Green: A General Kinetic Theory of Liquids. I. pp. 1-10; III. pp. 27-46; notes, pp. 95-98; Cambridge University Press, 1949.
3. Bowyer, J. M. and L. Talbot: Near Free-Molecule Couette Flow Between Concentric Cylinders. University of California, Institute of Engineering Research, Report HE-150-139, July 10, 1956.
4. Chiang, S. F.: Drag on a Rotating Cylinder at Low Pressures. University of California, Institute of Engineering Research, Report HE-150-100, May 19, 1952.
5. Grad, H.: On the Kinetic Theory of Rarefied Gases. Communications on Pure and Applied Mathematics, Vol. 4, No. 4, pp. 331-407, December, 1949.
6. Grad, H.: Principles of the Kinetic Theory of Gases. (Thermodynamics of Gases), Handbuch der Physik, Vol. 12, pp. 205-294, Springer-Verlag, Berlin, 1958.
7. Jeans, J. H.: The Dynamical Theory of Gases. (4th Edition), pp. 213-217, Dover Publications, New York, N. Y., 1954.
8. Kirkwood, J. G.: The Statistical Mechanical Theory of Transport Processes. I. General Theory. The Journal of Chemical Physics, Vol. 14, No. 3, pp. 180-201, March, 1946. Errata, Vol. 14, No. 5, p. 347, May, 1946. II. Transport in Gases. Vol. 15, No. 1, pp. 72-76, January, 1947. Errata, Vol. 15, No. 3, p. 155, March, 1947.
9. Kuhlthau, A. R.: The Application of High Rotational Speed Techniques to Low Density Gas Dynamics. Proceedings of the Third Midwestern Conference on Fluid Mechanics, pp. 495-514, University of Minnesota, 1953.
10. Lees, L.: A Kinetic Theory Description of Rarefied Gas Flows. GALCIT Hypersonic Research Project, Memorandum No. 51, December 15, 1959.
11. Maxwell, J. C.: On the Dynamical Theory of Gases. Philosophical Transactions of the Royal Society, Vol. 157, p. 49, 1867. Also in Scientific Papers, Vol. 2, pp. 26-78, Dover Publications, New York, N. Y. .

12. Mott-Smith, H. M. : The Solution of the Boltzmann Equation for a Shock Wave. *Physical Review*, Vol. 82, No. 6, pp. 885-892, June, 1951.
13. Tani, I. : On the Approximate Solution of the Laminar Boundary Layer Equations. *Journal of the Aeronautical Sciences*, Vol. 21, No. 7, pp. 487-495, p. 504, July, 1954.
14. von Karman, Th. : Uber Laminar und Turbulence Reibung. *Zeit. f. angew. Math. u. Mech.*, Vol. 1, pp. 233-252, 1921. See also, Pohlhausen, K. : Zur Naherungsweise Integration der Differentialgleichung der Laminaren Grenzschicht. *Zeit. f. angew. Math. u. Mech.*, Vol. 1, pp. 252-268, 1921.

APPENDIX

PLANE COMPRESSIBLE COUETTE FLOW
ACCORDING TO THE CLASSICAL NAVIER-STOKES EQUATIONS

The classical Navier-Stokes solution is given here for reference. In obtaining the solution, the medium is assumed to be a perfect gas, and the viscosity coefficient μ_c is directly proportional to the absolute temperature, just as for Maxwell molecules. Also, the Prandtl number is constant.

Clearly, the continuity equation $(d/dy)(\rho v) = 0$, together with the requirement that v vanishes at the plate surfaces leads immediately to

$$v \equiv 0 \quad (A-1)$$

Thus the conservation equations are as follows:

Momentum

$$(d/dy) \left(\mu_c \frac{du}{dy} \right) = 0 \quad (A-2)$$

$$(dp/dy) = 0 \quad (A-3)$$

Energy

$$(d/dy) \left[\frac{k_c}{c_p} \frac{d}{dy} (c_p T) \right] + \mu_c (du/dy)^2 = 0$$

In addition, we have $p = \rho RT$. The corresponding boundary conditions are as follows:

$$y = - (d/2), \quad u = - (U/2), \quad T = T_{II}; \quad y = + (d/2), \quad u = + (U/2), \quad T = T_I. \quad (A-5)$$

Integration of Eqs. (A-2) and (A-4) yields the following momentum and energy integrals:

$$\mu_c (du/dy) = b_1 \quad (\text{A-6})$$

$$c_p T + (\text{Pr}/2) u^2 - (b_2/b_1) u = b_3 \quad (\text{A-7})$$

with the undetermined constants b_1 , b_2 , b_3 ,

Let $(\mu_c)_{II}$ denote the viscosity coefficient evaluated at temperature T_{II} . Then by integrating Eq. (A-6) once again, we have

$$\int \mu_c / (\mu_c)_{II} du = \frac{b_1 y + b_4}{(\mu_c)_{II}} \quad .$$

But $\mu_c / (\mu_c)_{II} = T/T_{II}$, and by using Eq. (A-7) and integrating, we finally obtain

$$1/(c_p T_{II}) \left[b_3 u + (b_2/2b_1) u^2 - (\text{Pr}/b) u^3 \right] = \frac{b_1}{(\mu_c)_{II}} y + \frac{b_4}{(\mu_c)_{II}} \quad (\text{A-8})$$

where b_4 is another integration constant. The four b's appearing in Eqs. (A-7) and (A-8) are determined by the four boundary conditions [Eqs. (A-5)]. The final results expressed in terms of non-dimensional quantities are

$$C_D = (P_{xy}) / (\frac{1}{2} \rho_{II} U^2) = (1/\text{Re}) \left[1 + (T_I/T_{II}) + \frac{\gamma-1}{6} \text{Pr} M^2 \right] \quad (\text{A-9})$$

$$C_H = \frac{1}{2} \left[\frac{1}{\text{Pr} \text{Re}} - \frac{\gamma-1}{2} \frac{T_{II}}{T_{II}-T_I} \frac{M^2}{\text{Re}} \right] \left[1 + \frac{T_I}{T_{II}} + \frac{\gamma-1}{6} \text{Pr} M^2 \right]. \quad (\text{A-10})$$

The velocity and temperature profiles are given by the relations

$$\begin{aligned} & \left[1 + (T_I/T_{II}) + \frac{\gamma-1}{4} \text{Pr} M^2 \right] (u/U) - \left(1 - \frac{T_I}{T_{II}} \right) (u/U)^2 - \frac{\gamma-1}{3} \text{Pr} M^2 (u/U)^3 \\ & = \left[1 + (T_I/T_{II}) + \frac{\gamma-1}{6} \text{Pr} M^2 \right] \bar{y} - 1/4 \left(1 - \frac{T_I}{T_{II}} \right) \end{aligned} \quad (\text{A-11})$$

$$\frac{T}{T_{II}} + \frac{\gamma-1}{2} \text{Pr} M^2 (u/U)^2 + \left(1 - \frac{T_I}{T_{II}} \right) \frac{u}{U} = \frac{1}{2} \left(1 + \frac{T_I}{T_{II}} \right) + \frac{\gamma-1}{8} \text{Pr} M^2 \quad (\text{A-12})$$

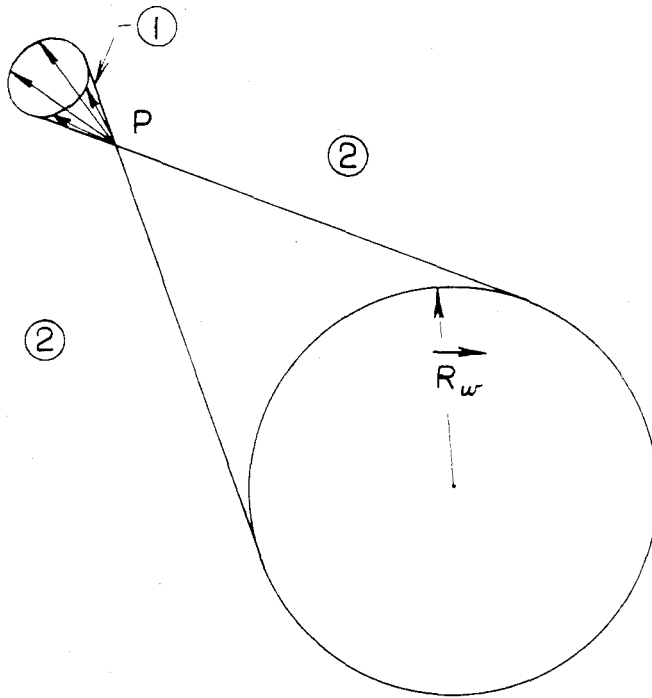


FIG. 1

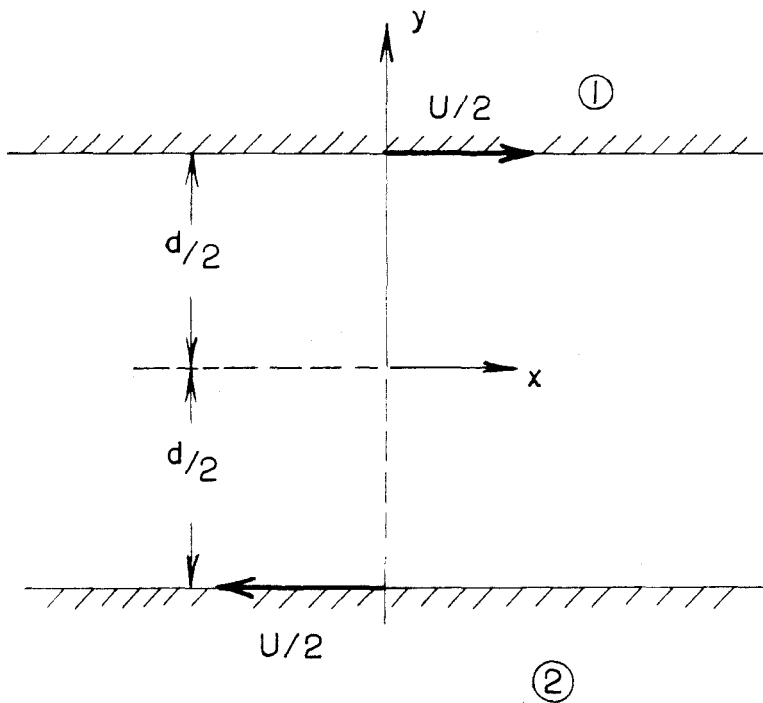


FIG. 2

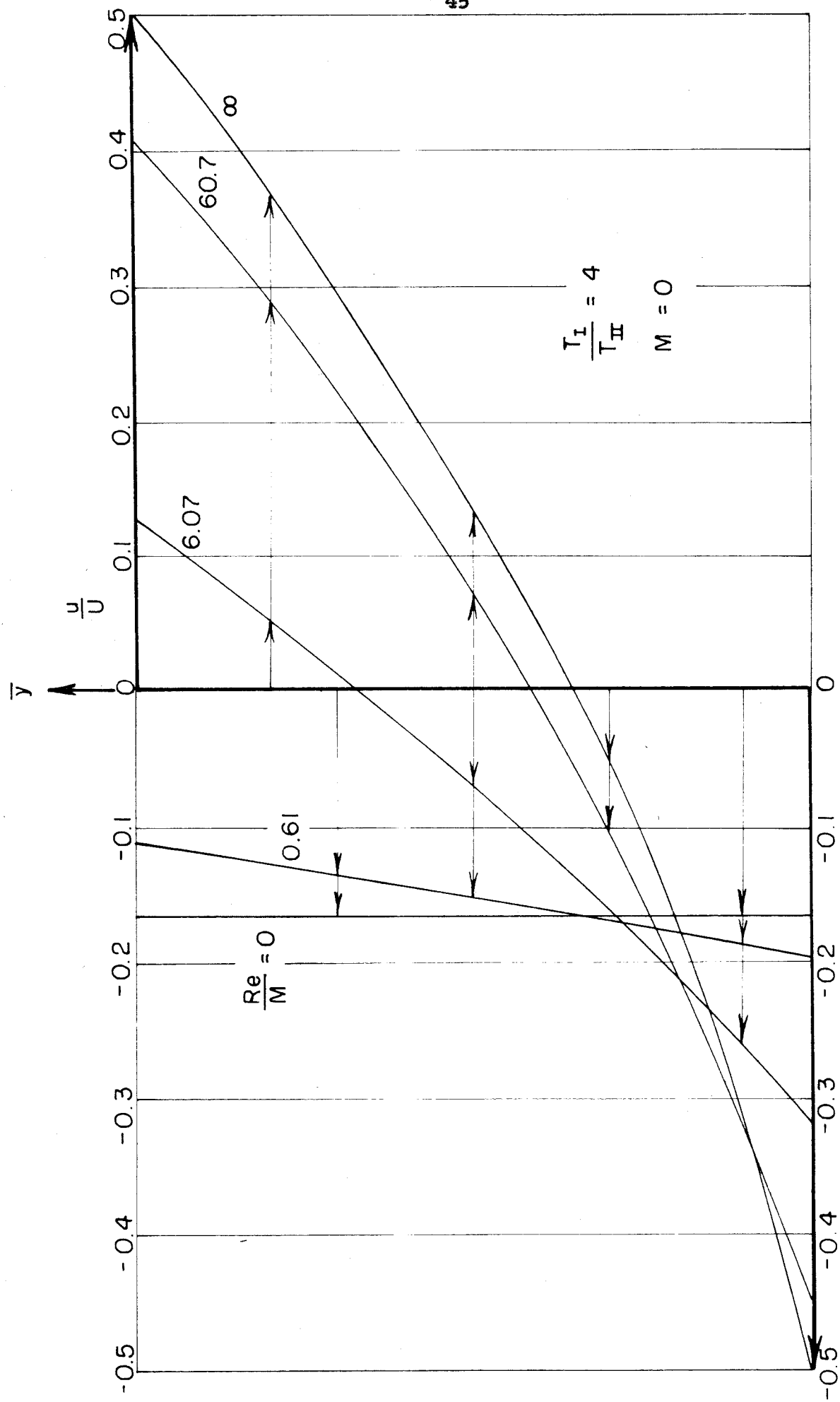


FIG. 3 - VELOCITY PROFILES FOR PLANE COUETTE FLOW

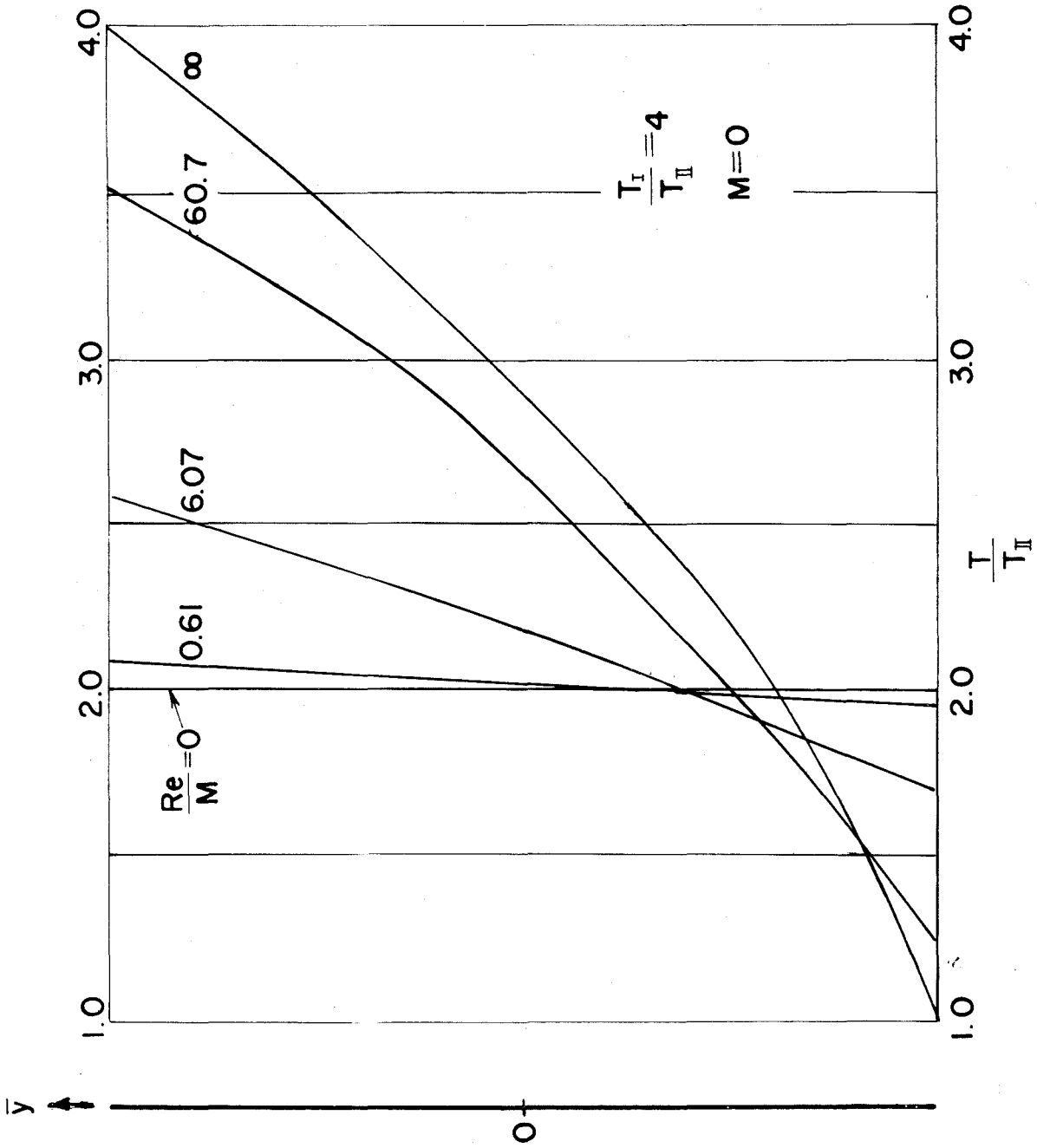


FIG. 4 TEMPERATURE PROFILES FOR PLANE COUETTE FLOW

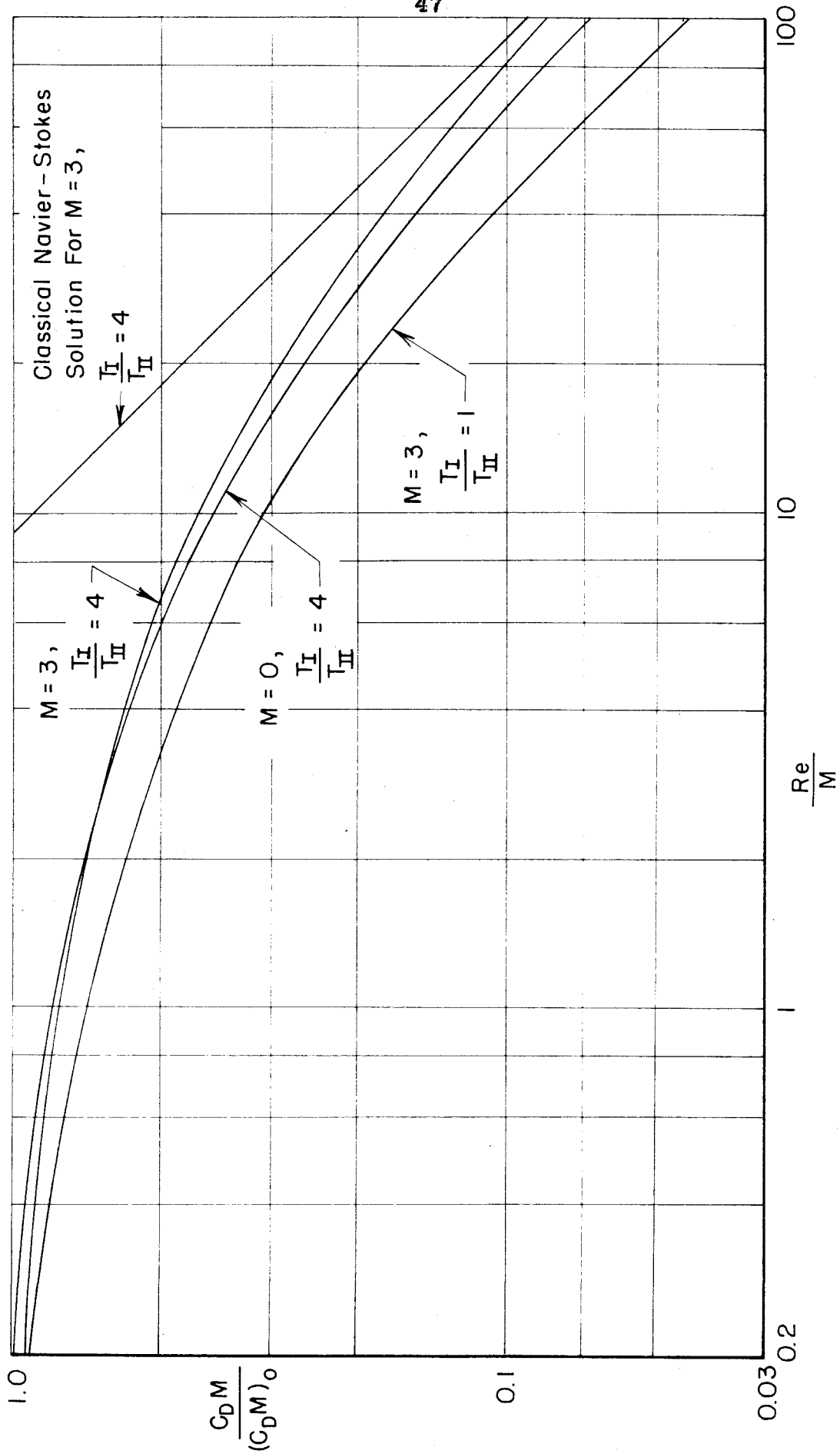
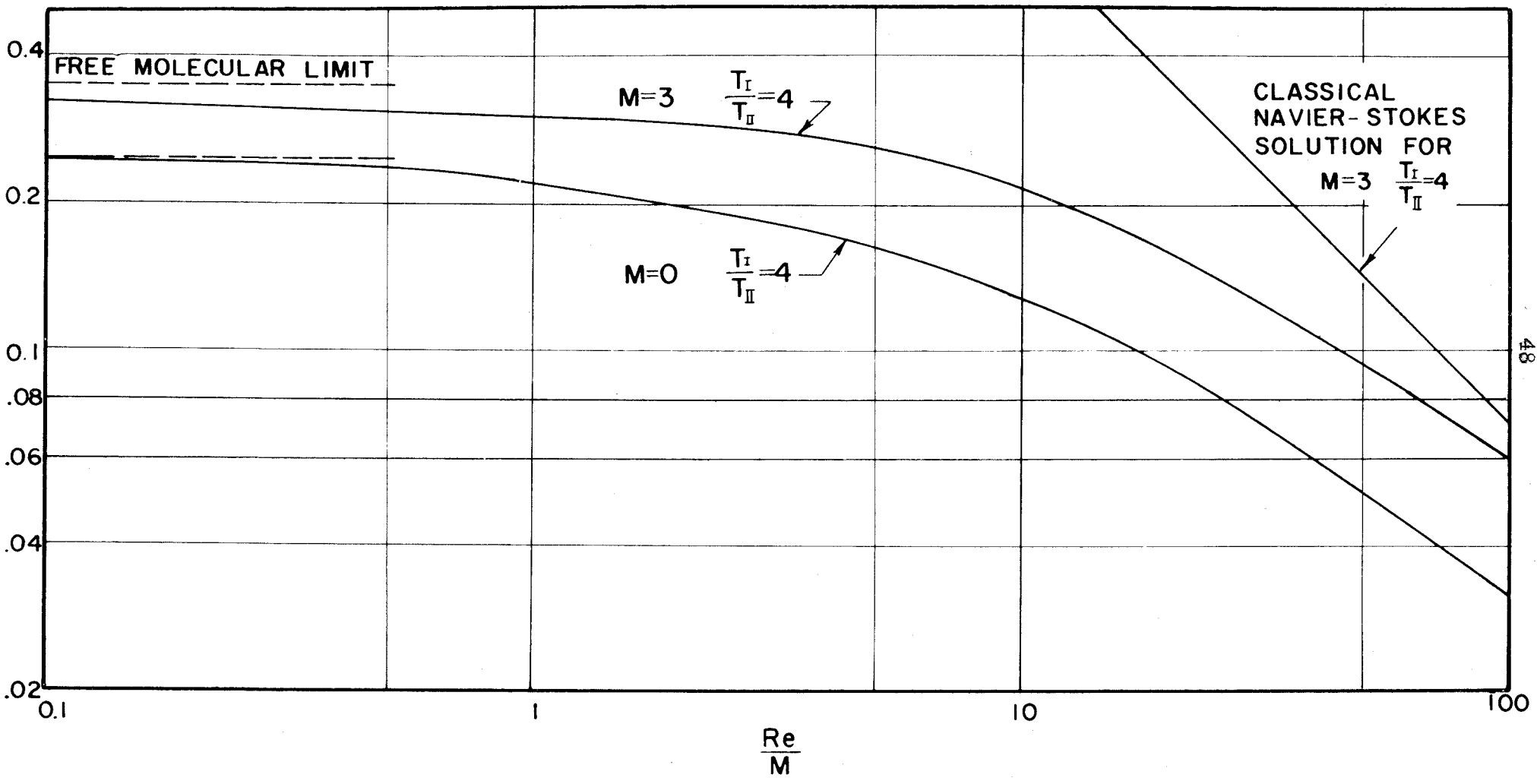


FIG. 5 - SKIN FRICTION IN PLANE COUETTE FLOW

$C_H M$



48

FIG. 6 HEAT TRANSFER IN PLANE COUETTE FLOW

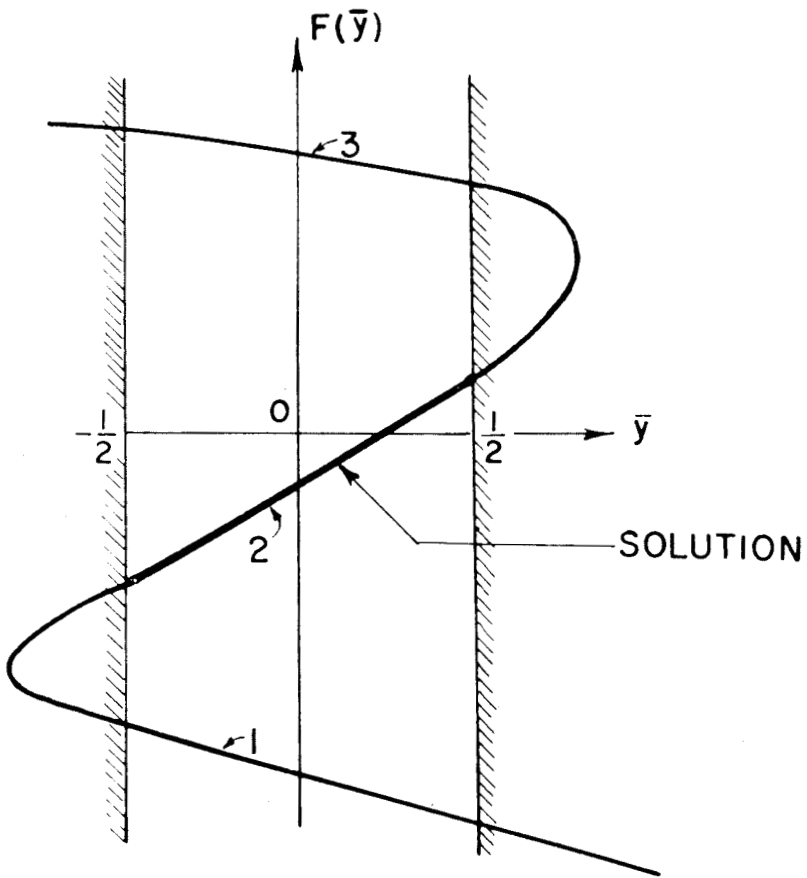


FIG. 7 TYPICAL VARIATION OF $F(\bar{y})$

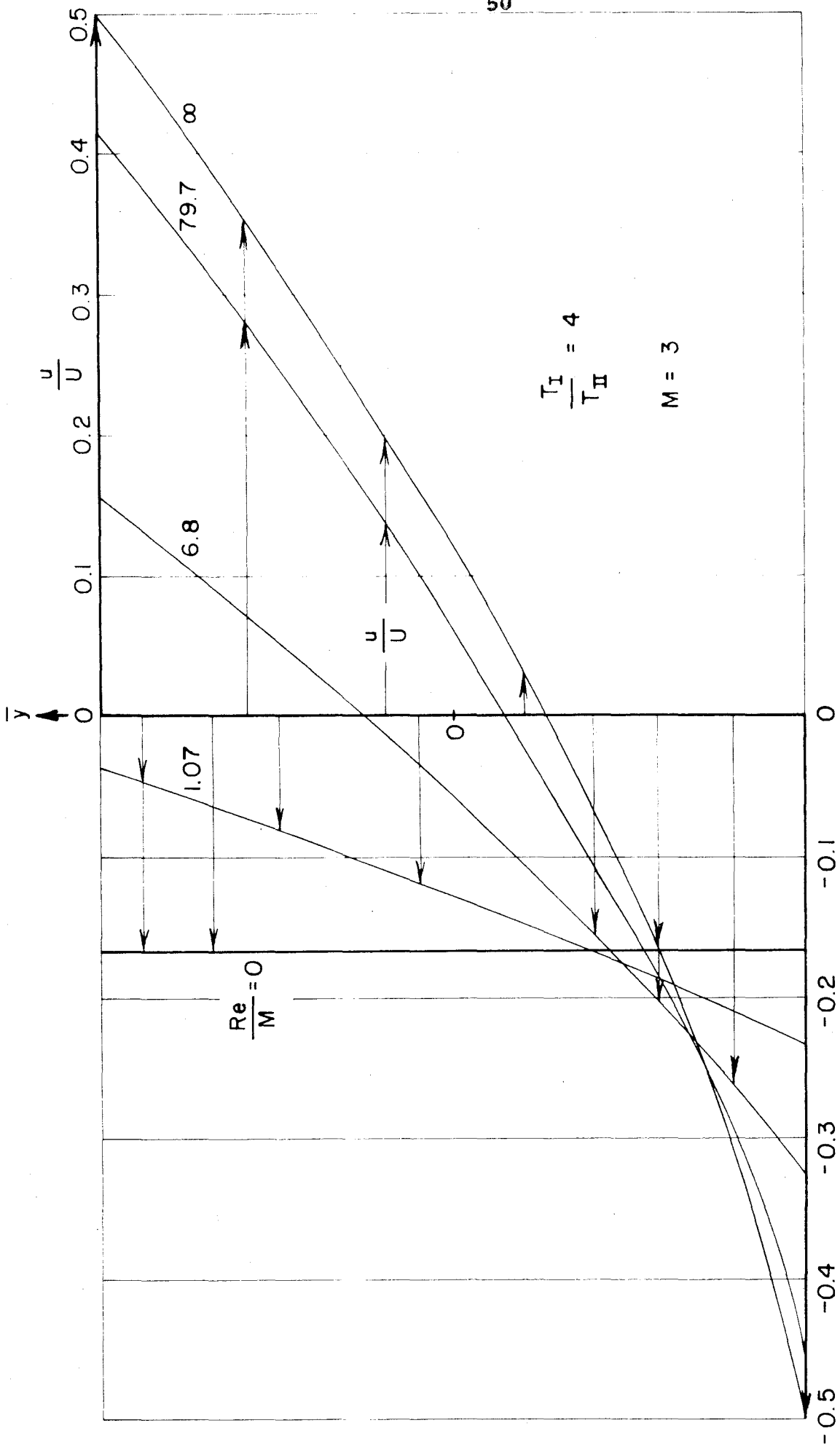


FIG. 8 - VELOCITY PROFILES FOR PLANE COUETTE FLOW

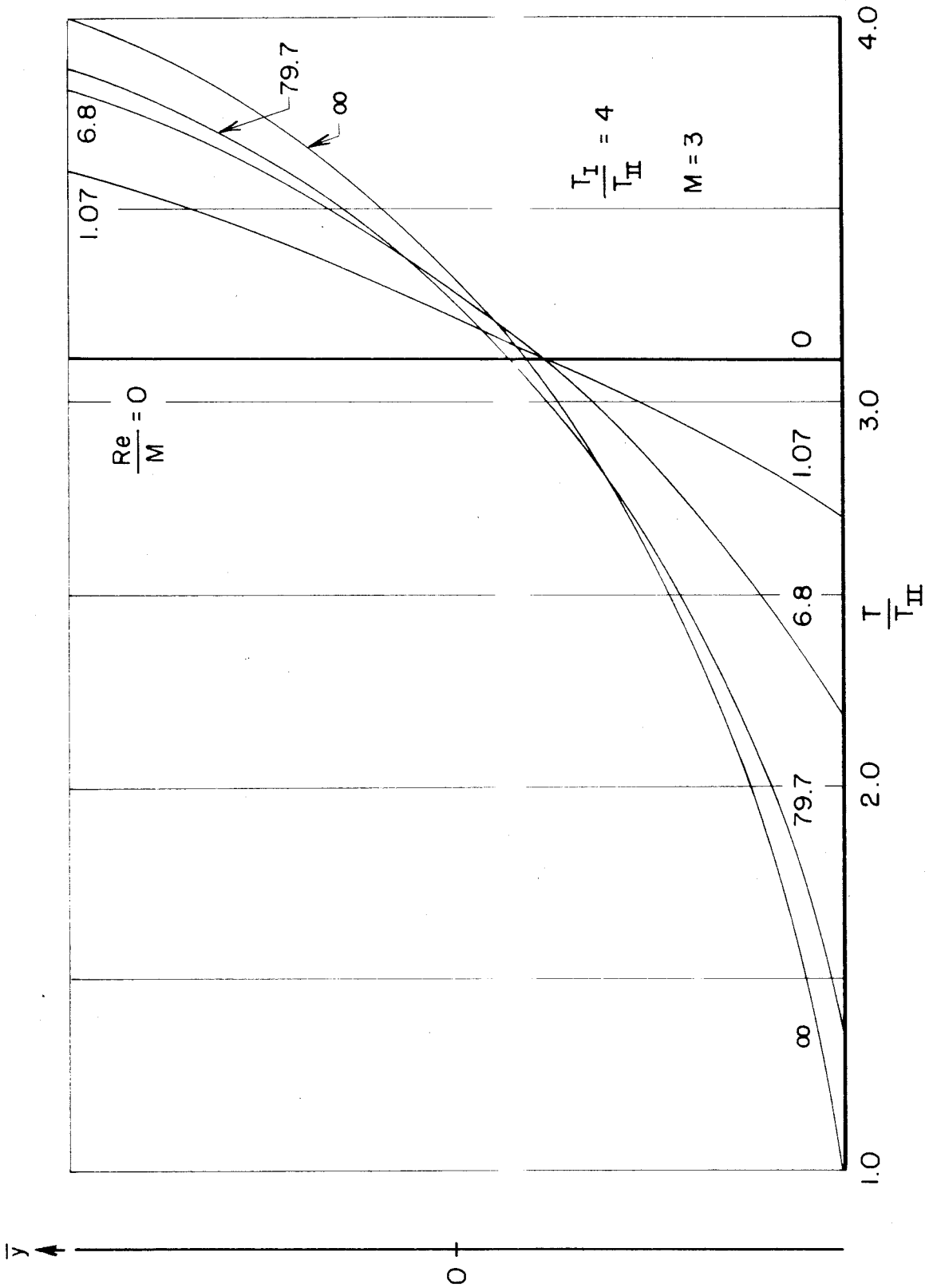


FIG. 9 - TEMPERATURE PROFILES FOR PLANE COUETTE FLOW

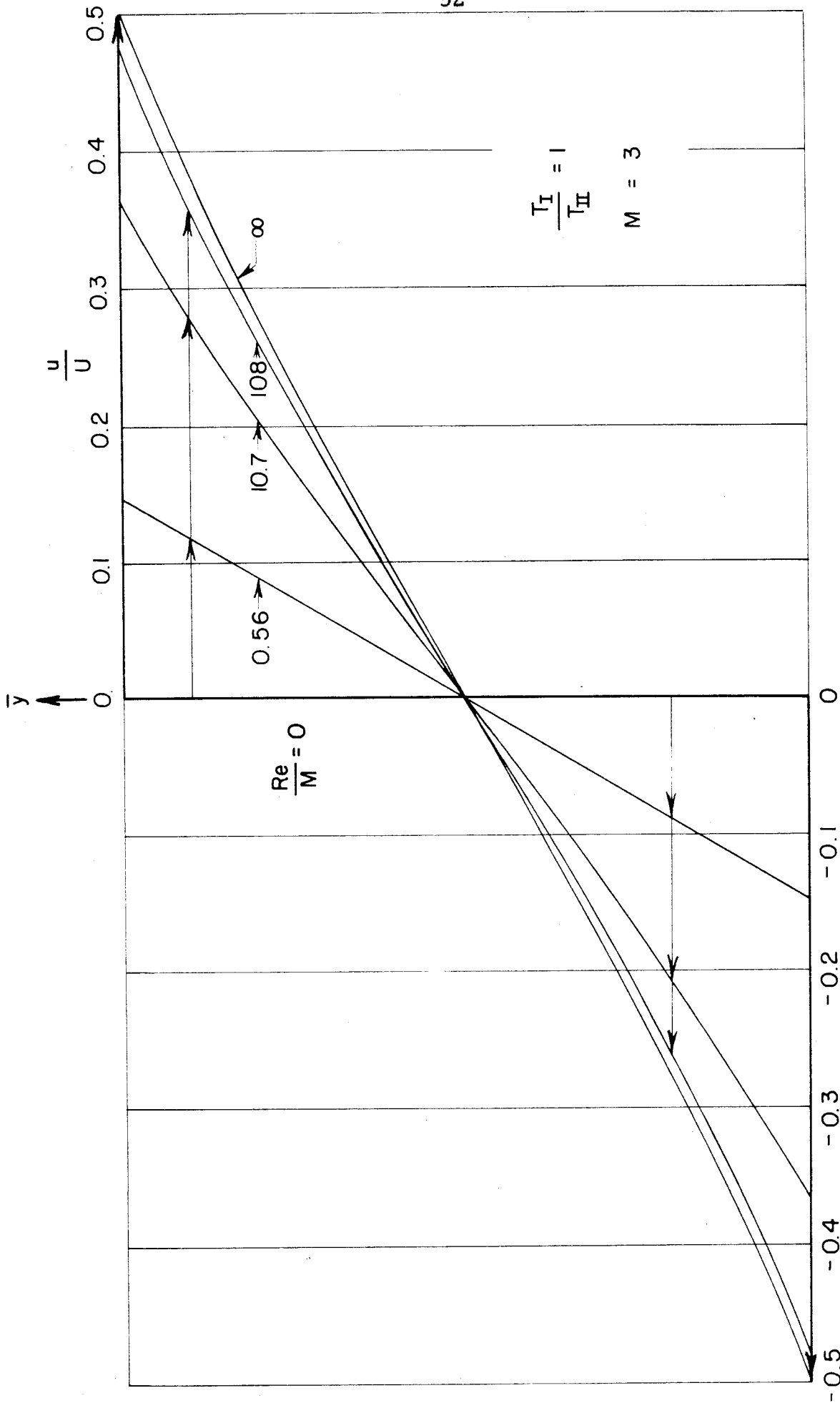


FIG.10- VELOCITY PROFILES FOR PLANE COUETTE FLOW

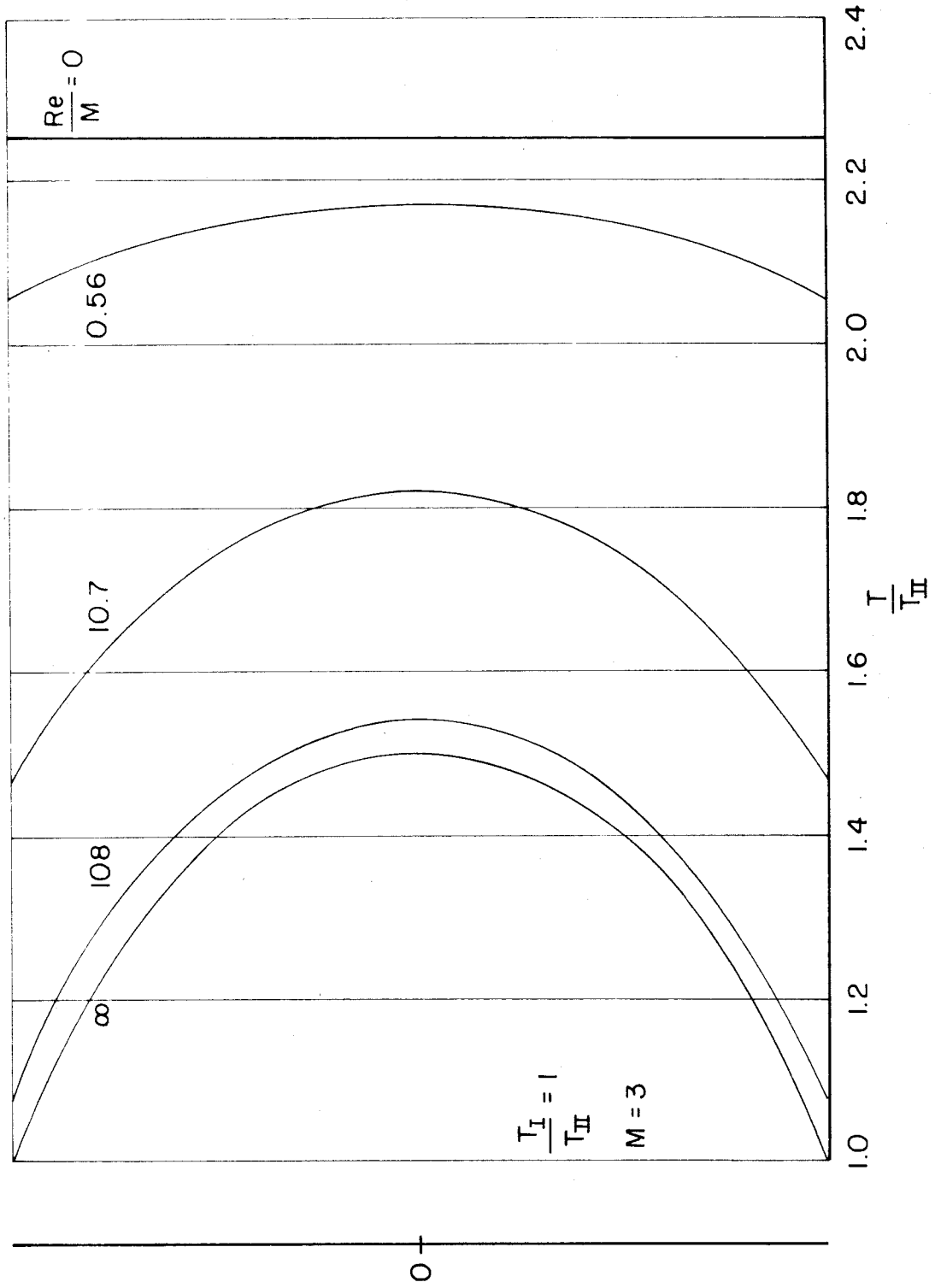
\bar{y} 

FIG. II - TEMPERATURE PROFILES FOR PLANE COUETTE FLOW

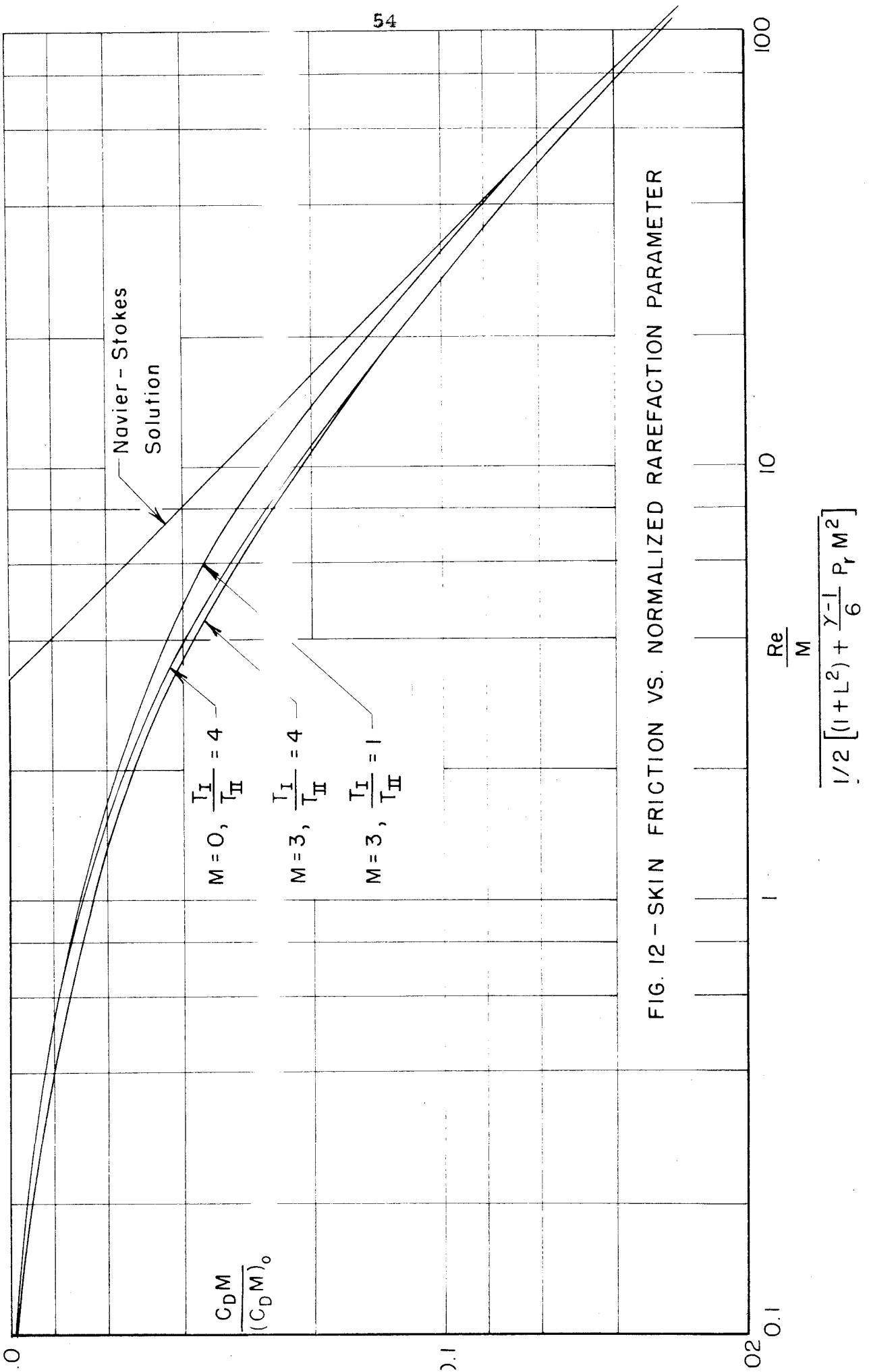


FIG. 12 - SKIN FRICTION VS. NORMALIZED RAREFACTION PARAMETER

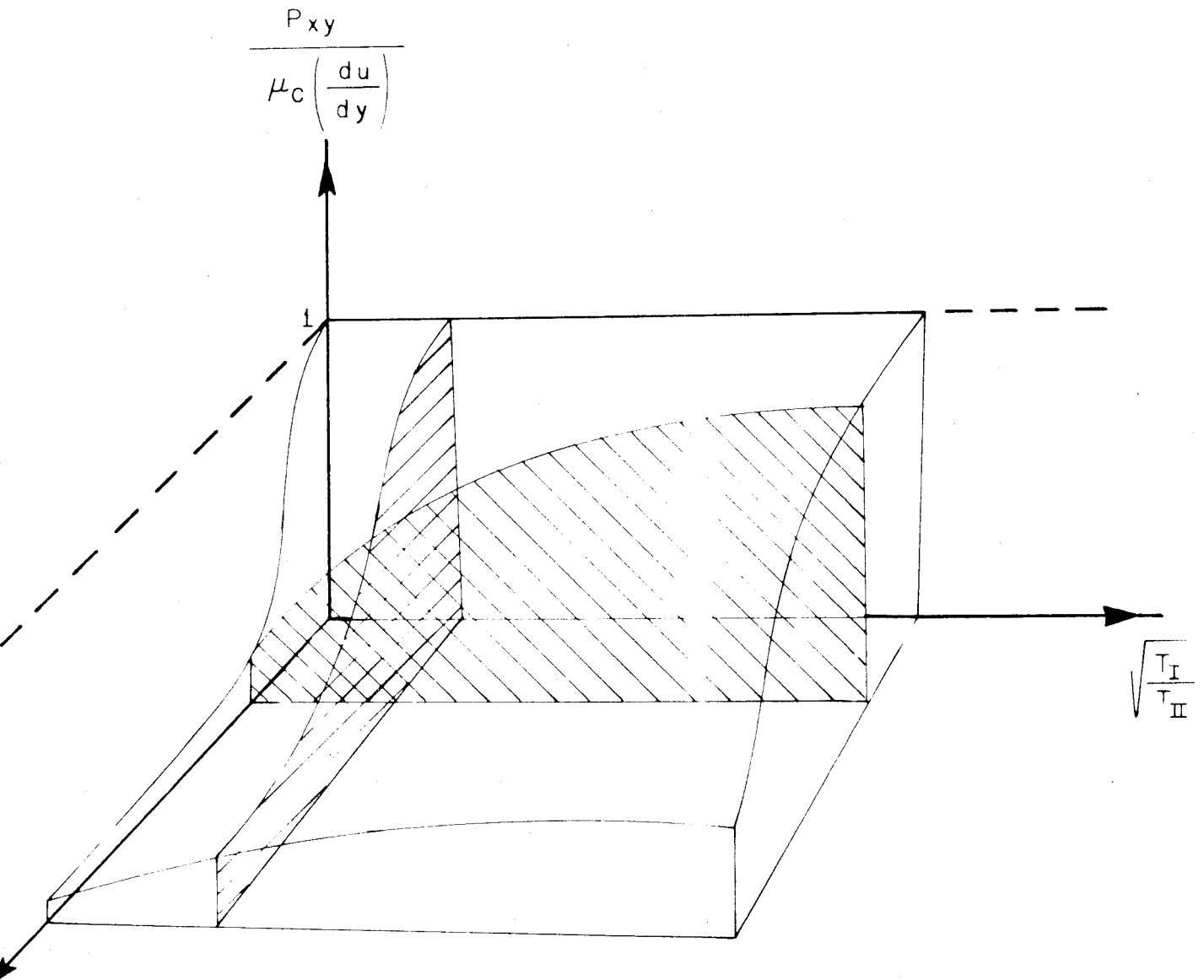


FIG.13—DEPARTURE FROM NAVIER-STOKES RELATION IN
PLANE COUETTE FLOW. $\frac{Re}{M} = 0$

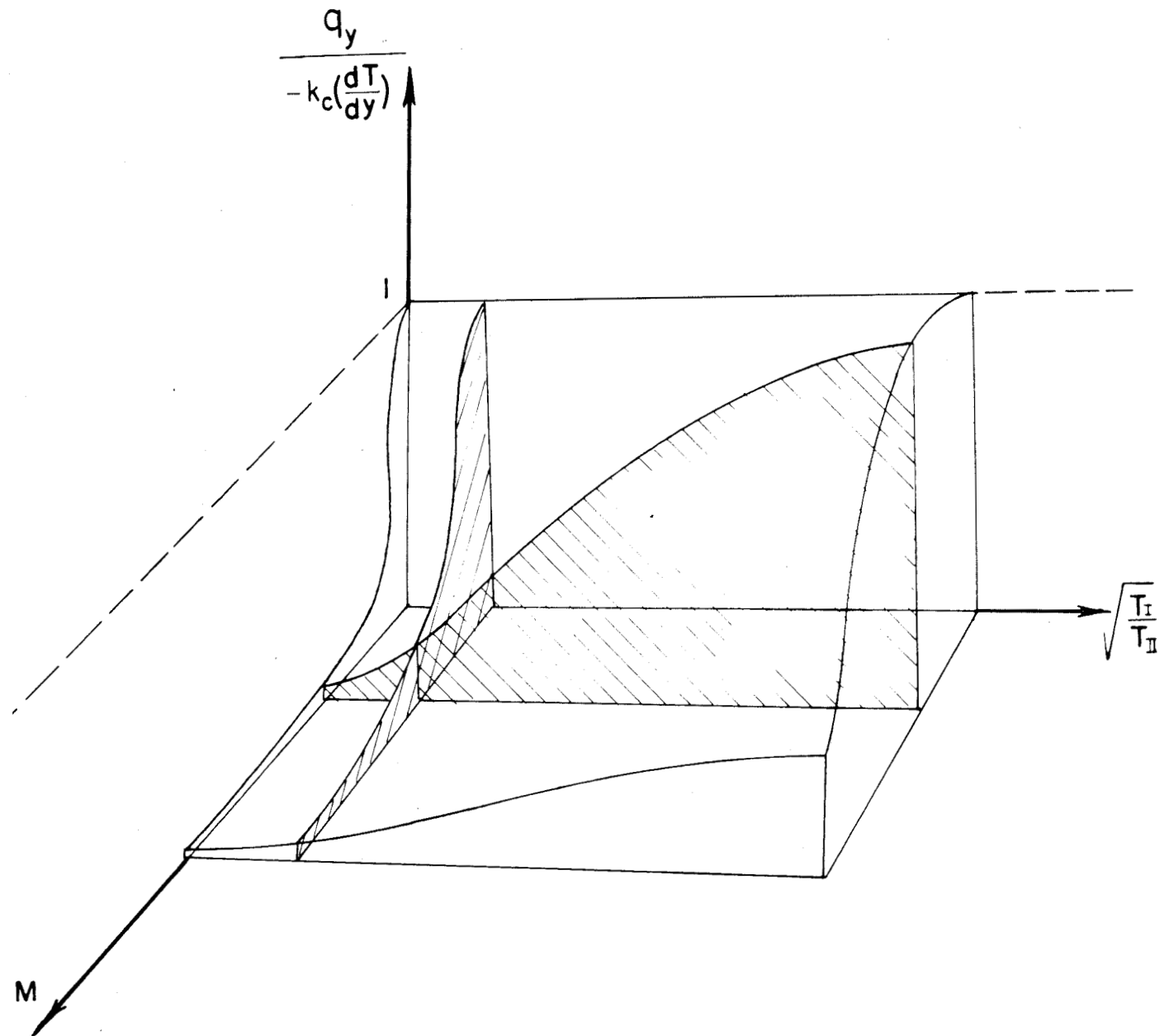


FIG. 14 - DEPARTURE FROM FOURIER'S RELATION IN PLANE
 COUETTE FLOW. $\frac{Re}{M} = 0$

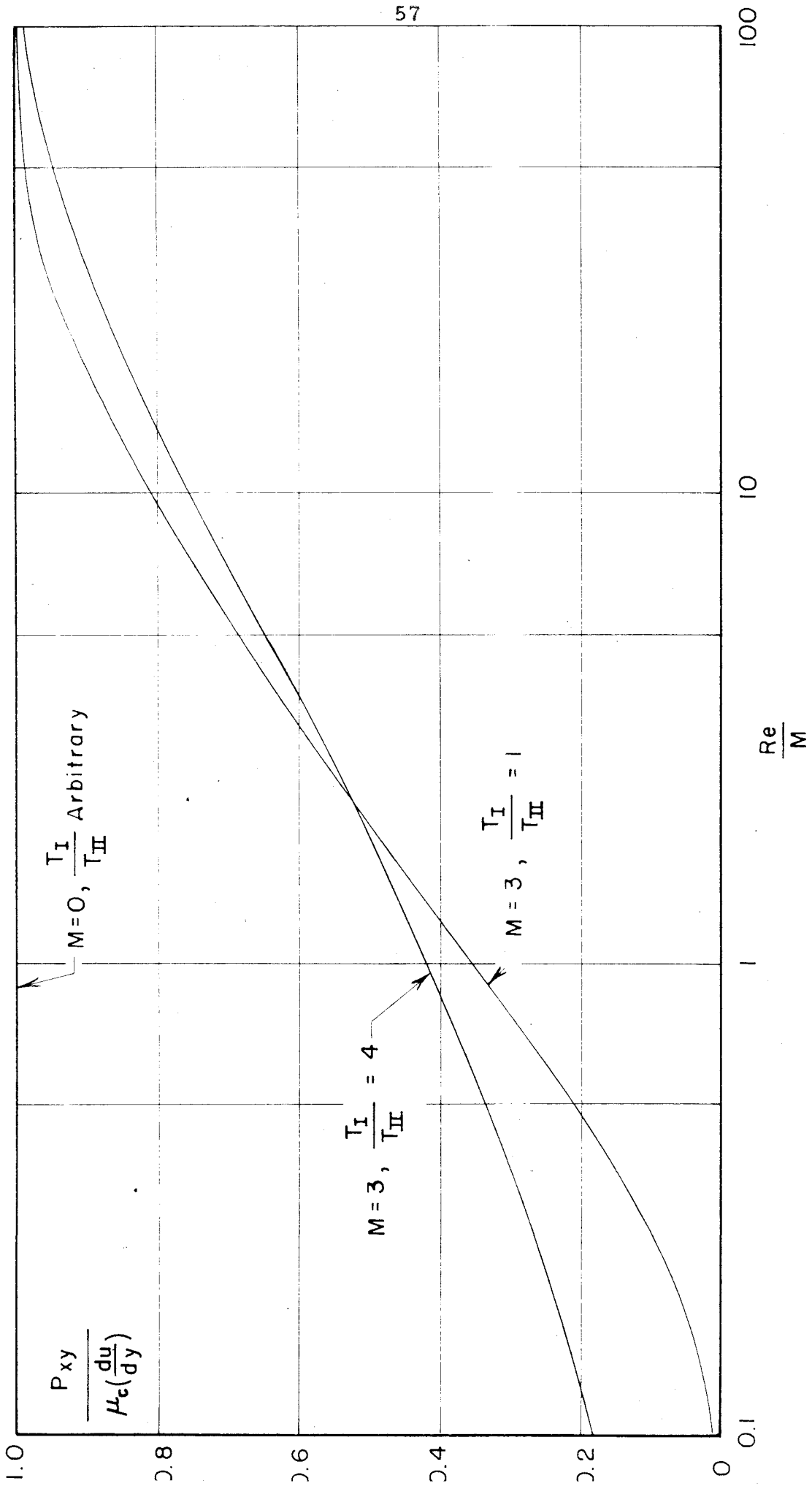


FIG. 15 - DEPARTURE FROM NAVIER - STOKES RELATION AS A FUNCTION OF $\frac{Re}{M}$

PART II

KINETIC THEORY DESCRIPTION
OF CONDUCTIVE HEAT TRANSFER
FROM A FINE WIRE

ABSTRACT

The Maxwell moment method utilizing the two-sided Maxwellian distribution function is applied to the problem of conductive heat transfer between two concentric cylinders at rest. Analytical solutions are obtained for small temperature differences between the cylinders. The predicted heat transfer agrees very well with experiments performed by Bomelburg, Schäfer-Rating and Eucken. Comparison with results given by the Grad's thirteen moment equations, and with those given by Fourier's "law" plus Maxwell-Smoluchowski temperature-jump boundary condition shows that the two-sided character in the distribution function is a crucial factor in problems involving surface curvature.

TABLE OF CONTENTS

PART	PAGE
Abstract	59
Table of Contents	60
List of Figures	61
List of Symbols	62
I. Description of the Problem	65
II. Formulation of the Problem According to the Maxwell Moment Method	70
II. A. Distribution Function and Mean Quantities	70
II. B. Differential Equations	72
II. C. Boundary Conditions	75
II. D. Differential Equations and Boundary Conditions in Non-Dimensional Form	76
III. Solutions for Small Temperature Differences Between Cylinders	79
IV. Discussion	84
IV. A. Heat Transfer and Comparison with Experiment	84
IV. B. Temperature Distribution	88
IV. C. "Free Molecular" Criterion	91
IV. D. Fourier-Maxwell-Smoluchowski Formulation	93
References	96
Figures	98

LIST OF FIGURES

NUMBER		PAGE
1	Variation of Heat Transfer with Gas Pressure	98
2	Configuration in Cylindrical Coordinates	99
3	Comparison with Experiment (Ref. 17)	100
4	Comparison with Experiment (Ref. 2)	101
5	Temperature Distribution Between Two Cylinders	102
6	Temperature Distribution for Various Values of $2R_1/\lambda_1$	103
7	Thickness of Knudsen Layer	104
8	Classification of Density Regimes	105
9	Departure from Fourier's Relation	106

LIST OF SYMBOLS

a	thermal accommodation coefficient
A_2	= 1.3682, value of scattering integral
b	impact parameter
B	integration constant
\bar{c}	mean thermal velocity, $\sqrt{8kT/\pi m}$
f	velocity distribution function
f_0	local full-range Maxwellian
f_1, f_2	components of two-stream Maxwellian
F	interparticle force
G	function defined by the relation $\bar{n}_1 \bar{T}_1 + \bar{n}_2 \bar{T}_2$
k	Boltzmann constant
k_c	"classical" thermal conductivity
K	quantity used in Welander's work (see Section I), also function defined by the relation $\bar{n}_1 \bar{T}_1 - \bar{n}_2 \bar{T}_2$
\tilde{K}	constant in expression for inverse fifth-power force law, $F = (m_1 m_2 \tilde{K})/r^5$
l	length of heated wire
m	mass of a particle
m_1, m_2	mass of two interacting particles
n_1, n_2	number density functions in two-stream Maxwellian
N_1, N_2	perturbations of n_1, n_2 over unity
p	nkT , hydrostatic pressure
$P_{RR}, P_{\theta\theta}, P_{zz}$	normal stresses in R, θ , Z directions
q_R	radial heat transfer rate
Q	arbitrary function of particle velocity, also total heat transfer from heated wire
ΔQ	change in Q produced by collisions

r	distance between two particles
R	radial distance
\bar{R}_l	non-dimensional radial distance of Knudsen layer from center of heated wire
R_1, R_2	radii of inner and outer cylinders
$\Delta R_1, \Delta R_2$	free molecular heat transfer regions near R_1 and R_2
t_1, t_2	perturbations of T_1, T_2 over unity
T	absolute temperature
T_1, T_2	temperature functions in two-stream Maxwellian
T_I, T_{II}	absolute temperatures of inner and outer cylinders
u_R	mean radial velocity
V	relative velocity between two interacting particles
z	axial distance
α	wedge angle, $\cos^{-1}(R_1/R)$
β	integration constant
δ	parameter defined by Eq. (17)
δ'	parameter defined by Eq. (23)
Δ	non-dimensional radial distance of Knudsen layer from surface of heated wire
ε	angle between plane of the orbit and plane containing the original relative velocity and the x-axis in a binary collision (see Reference 13)
ϵ	$(T_I - T_{II})/T_I$
θ	circular angle in cylindrical coordinates
λ	Maxwell mean free path
Λ	correction factor used in Dickins' work (see Section I)
μ_c	"classical" viscosity coefficient

- \vec{v} vector particle velocity
- $d\vec{\xi}_i d\vec{\xi}_j d\vec{\xi}_k$
- \vec{v}_p planar velocity vector, $\xi_p = \sqrt{\xi_R^2 + \xi_\theta^2}$
- ξ_R, ξ_θ, ξ_z velocity components of particle velocity in R, θ , Z directions
- ρ mean mass density
- ϕ angle between particle planar velocity \vec{v}_p and radius vector \vec{R}

The subscripts "I" and "II" refer to quantities given at the inner and outer cylinders, respectively. The subscript " ∞ " denotes quantities evaluated at the continuum limit. The bar (—) superscript refers to non-dimensional quantities.

I. DESCRIPTION OF THE PROBLEM

The present problem deals with the conductive heat transfer from a metallic wire to a monatomic gas at rest. A fine wire is placed coaxially in a large cylindrical bell jar and is electrically heated. The wire temperature is known from its electrical resistance, while the heat input is found by measuring the current. At normal gas density, heat conduction from the wire is clearly independent of the gas pressure; while at very low gas density the heat loss is proportional to gas pressure. When the gas density is in the transition range, the relation between heat conduction and pressure is not as simple, but the two limiting regimes are joined smoothly (Figure 1). This simple device has long been used by many investigators^{1, 2, 3, 4, 6} to determine the thermal conductivity of gases and to study the phenomena of temperature jump and energy accommodation at the wire surface. Some authors have also approached the problem analytically, but they are all forced to introduce certain ad hoc assumptions, which restrict their results to small values of the ratio of the mean free path to the wire radius.

It is easy to see that this type of instrument enjoys the privilege of simplicity. Up until very recently experiments with such a heated wire furnished one of the few sets of data for the full range of gas densities from the free molecular regime to the continuum regime. Moreover, the present problem is fundamentally important because it contains the effect of both convex and concave surfaces. The effects of curvature on heat transfer and temperature distribution in rarefied gases have never been thoroughly investigated. Along with plane Couette flow and shock wave structure, this problem has received a good deal of attention in rarefied gas dynamics. Weber¹ and

Schafer-Rating, and Eucken² sub-divide the annulus into three parts:

two free molecular heat transfer regions near the solid surfaces

$R_1 < R < R_1 + \Delta R_1$, $R_2 - \Delta R_2 < R < R_2$ (R_1 , R_2 are the wire and

bell jar radii respectively); and a region between $R_1 + \Delta R_1$ and $R_2 - \Delta R_2$

where continuum heat conduction is assumed. The arbitrary quantities

ΔR_1 and ΔR_2 are functions of the mean free path λ , and in Weber's

case they are taken simply equal to $(15/8) \lambda$. In Schafer-Rating and

Eucken's calculation $\Delta R_1/\lambda$ and $\Delta R_2/\lambda$ are functions of

λ/R_1 and λ/R_2 , respectively. In their studies, the implication

that λ is small in comparison with R_1 and R_2 has been made. The

choice of ΔR_1 and ΔR_2 is clearly related to the temperature jump

boundary condition proposed by Smoluchowski (see Section IV. 4)⁵.

He suggested that for a small degree of rarefaction, the difference

between the gas temperature and wall temperature at the solid surface

is equal to $-(15/8) \lambda (dT/dn)_{\text{wall}}$, where $(dT/dn)_{\text{wall}}$ is the gas

temperature gradient normal to the wall. Application of Smoluchowski's

relation to the present problem is discussed in Section IV. 4.

Gregory³ and his followers have investigated this "hot-wire" method over the period of a decade. Their primary goal is accurate determination of the gaseous thermal conductivity as a function of temperature. Early developments were more along technical lines than analytical, like keeping the wire temperature constant under different conditions, elimination of convective losses, etc. In computation, they merely used the usual Fourier result that the total heat transfer Q is $2\pi k_c \ell (T_I - T_{II}) / \ln (R_2/R_1)$, in which k_c is the "classical"

thermal conductivity of the gas*, ℓ the length of the wire, and T_I and T_{II} are the temperatures of the wire and the bell jar, respectively. They allow k_c to decrease if the pressure decreases appreciably below atmospheric³; however, their original focal point is the temperature dependence but not the pressure effect.

Later, Dickins⁴ adopted Gregory's apparatus to determine accommodation coefficients. ** He corrected the heat transfer Q at low pressures by an amount Λ/R_1 , so that

$$Q = \frac{2 \pi k_c \ell (T_I - T_{II})}{\ln(R_2/R_1) + (\Lambda/R_1)}$$

in which $\Lambda = (15/8) \lambda (2-a)/a$ and a is Knudsen's accommodation coefficient. As determined by Dickins' experiment "a" is about 0.9 for most gases except helium and hydrogen. The correction Λ is easily seen to be based on Smoluchowski's relation⁵.

Two years later, Gregory⁶ generalized the same relation for polyatomic gases, but Λ then included a numerical factor which accounts for intermolecular forces and has to be determined by experimental data on viscosity and specific heat. At the same time,

* It should be noted that the Fourier relation $q = -k_c \nabla T$ holds only at normal densities; thus the "classical" thermal conductivity k_c introduced here is merely for convenience. (See Section IV. 4.)

** The thermal accommodation coefficient "a" advanced by Knudsen²⁶ is defined as

$$a = \frac{E_g - E_r}{E_g - E_w}$$

E_g = energy transported to surface by incident molecules in equilibrium at the gas temperature

E_r = actual energy carried away by molecules leaving the surface

E_w = energy of re-emitted molecules in equilibrium at the wall temperature

microscopic studies have also been made by Zener⁷ and Devonshire⁸ on the general aspect of solid-gas interchange of energy. They require experimental determination of certain constants related to intermolecular forces.

Welander in 1954⁹ worked the problem anew but used a different constant for Λ , in which the factor $\frac{2-a}{a}$ is replaced by $\frac{2-Ka}{a}$.*

The quantity K is found to be 0.827 by solving the "Krooked" Boltzmann equation^{10**}, in which the collision integral is taken to be

$(3/15)(\bar{c}/\lambda)(f - f_0)$, where f is the unknown velocity distribution function, f_0 is the local Maxwellian, and \bar{c} the mean thermal velocity

$\bar{c} = \sqrt{\frac{8kT}{m\pi}}$. Welander attempted to extend the validity of the

$\frac{2-Ka}{a}$ expression to the free molecular regime by allowing K to be a function of gas density. Under the assumption that $|(dT/dR)_{\text{wall}}(\lambda/T)|$ is small in comparison with unity and that the distribution function differs slightly from the local Maxwellian, he obtained an integral equation governing the K-function, but he did not solve that equation. Instead he estimated K from experimental data given by Schafer-Rating and Eucken², and found that K varied between 0.1 and 0.6. The fact that K depends only on pressure is rather obvious; yet Welander's result demonstrates very little beyond this point.

Though it might be difficult to record all the investigations of this "simple" problem since the first use of the apparatus by Schleiermacher¹¹ for determination of gaseous conductivity in 1888, yet it is

* Welander also used a different numerical factor $75\pi/128$ instead of $15/8$; however, the quantitative difference is negligible.

^{27**} Welander's paper is published at the same time as Krook's work.

clear that a thorough theoretical investigation of the problem is long overdue.

II. FORMULATION OF THE PROBLEM ACCORDING TO THE MAXWELL MOMENT METHOD

II. A. Distribution Function and Mean Quantities

We consider a wire of radius R_1 placed at the center of a concentric cylinder of radius R_2 , with $R_2 > R_1$ (Figure 2). The wire is heated to a temperature T_I , while the outer cylinder is kept at temperature T_{II} . The annular region ($R_1 < R < R_2$) is filled with monatomic gas at an arbitrary density level, which is characterized by the mean free path λ evaluated at a convenient reference point (say $R = R_1$). If the wire is sufficiently long, end effects are negligible; thus the problem is axially symmetric and two-dimensional.

In compliance with the requirements given by Lees¹³ (see also introduction, Part I of this thesis), the simplest distribution function having a "two-sided" character and capable of giving a smooth transition between the highly rarefied gas regime and the continuum limit consists of two Maxwellians, each containing several parametric functions. All outwardly directed molecules with planar velocity vector $\vec{\xi}_p$ ($\xi_p = \sqrt{\xi_R^2 + \xi_\theta^2}$, $\phi = \tan^{-1}(\xi_R/\xi_\theta)$) lying inside the wedge of influence (region I in Figure 2) are characterized by one Maxwellian f_1 , where

$$f = f_1 \quad \text{for} \quad \alpha < \phi < \pi - \alpha$$

in which

$$\alpha = \cos^{-1}(R_1/R) \quad .$$

Then, all molecules with planar velocity $\vec{\xi}_p$ lying outside of region I are characterized by f_2 , i. e.,

$$f = f_2 \quad \text{for} \quad \pi - \alpha < \phi < 2\pi + \alpha \quad .$$

The requirement that f should be discontinuous on the sides of the "wedge of influence" is the most basic feature in the present scheme; its importance will be seen shortly.

In order to satisfy at least the three conservation equations and the heat flux equation, one finds that four parametric functions specifying f_1 and f_2 are the absolute minimum. Thus we prescribe that

$$f_1 = n_1 \left(\frac{m}{2\pi k T_1} \right)^{3/2} \exp \left[-\frac{m}{2k T_1} (\xi_p^2 + \xi_z^2) \right]$$

likewise,

$$f_2 = n_2 \left(\frac{m}{2\pi k T_2} \right)^{3/2} \exp \left[-\frac{m}{2k T_2} (\xi_p^2 + \xi_z^2) \right]$$

where $n_1(R)$, $T_1(R)$, $n_2(R)$, $T_2(R)$ are the four unknown functions of radial distance. Here the n 's have the dimension of a number density, while the T 's have the dimension of a temperature, and it must be stressed that each individual function has no explicit physical significance in general.

Knowing the distribution function f , one can evaluate all mean quantities $\langle \tilde{\phi} \rangle$ by averaging over all velocity space,

$$\langle \tilde{\phi} \rangle = \int \tilde{\phi} f d\vec{\xi} = \int_{\alpha}^{\pi-\alpha} \int_0^{\infty} \int_{-\infty}^{+\infty} \tilde{\phi} f_1 d\xi_z d\xi_p d\phi + \int_{\pi-\alpha}^{2\pi+\alpha} \int_0^{\infty} \int_{-\infty}^{+\infty} \tilde{\phi} f_2 d\xi_z d\xi_p d\phi$$

For example, the mean density is

$$\rho = \rho(R) = \int m f d\vec{\xi} = \frac{m}{2\pi} \left[n_1 (\pi - 2\alpha) + n_2 (\pi + 2\alpha) \right] \quad (1)$$

and the mean temperature is

$$T = T(R) = \frac{n_1 T_1 (\pi - 2\alpha) + n_2 T_2 (\pi + 2\alpha)}{n_1 (\pi - 2\alpha) + n_2 (\pi + 2\alpha)} \quad (2)$$

Notice that the angular dependence appears directly, while T_1 , T_2 , n_1 , n_2 will bring in a purely radial dependence. Expressions for radial velocity u_R , hydrostatic pressure p , and radial heat transfer q_R are listed below for later usage:

$$u_R = \sqrt{\frac{2\pi k}{m}} \cdot \cos \alpha \cdot \frac{n_1 \sqrt{T_1} - n_2 \sqrt{T_2}}{n_1 (\pi - 2\alpha) + n_2 (\pi + 2\alpha)} \quad (3)$$

$$p = \frac{k}{2\pi} [n_1 T_1 (\pi - 2\alpha) + n_2 T_2 (\pi + 2\alpha)] = -\frac{P_{RR} + P_{\theta\theta} + P_{zz}}{3} \quad (4a)$$

$$\left. \begin{aligned} P_{RR} &= -\langle p \xi_R^2 \rangle = -\frac{k}{2\pi} [n_1 T_1 (\pi - 2\alpha + \sin 2\alpha) + n_2 T_2 (\pi + 2\alpha - \sin 2\alpha)] \\ P_{\theta\theta} &= -\langle p \xi_\theta^2 \rangle = -\frac{k}{2\pi} [n_1 T_1 (\pi - 2\alpha - \sin 2\alpha) + n_2 T_2 (\pi + 2\alpha + \sin 2\alpha)] \\ P_{zz} &= -\langle p \xi_z^2 \rangle = -\frac{k}{2\pi} [n_1 T_1 (\pi - 2\alpha) + n_2 T_2 (\pi + 2\alpha)] \end{aligned} \right\} \quad (4b)$$

$$q_R = \sqrt{\frac{2}{\pi m}} \cdot \cos \alpha [n_1 (k T_1)^{3/2} - n_2 (k T_2)^{3/2}] \quad (5)$$

It should be pointed out here that the normal stresses in different directions are generally not the same; namely, $P_{RR} \neq P_{\theta\theta} \neq -p$.

II B. Differential Equations

In cylindrical coordinates the Maxwell integral equation of transfer is as follows¹³:

$$\frac{1}{R} \frac{\partial}{\partial R} \left[R \int f \xi_R Q d\vec{\xi} \right] + \frac{1}{R} \frac{\partial}{\partial \theta} \int f \xi_\theta Q d\vec{\xi} + \frac{\partial}{\partial z} \int f \xi_z Q d\vec{\xi} +$$

$$- \int \frac{f}{R} \left(\xi_\theta^2 \frac{\partial Q}{\partial \xi_R} - \xi_\theta \xi_R \frac{\partial Q}{\partial \xi_\theta} \right) d\vec{\xi} = \Delta Q \quad (6)$$

where

$$Q = Q(\xi_R, \xi_\theta, \xi_z) = Q(\xi_p, \phi, \xi_z)$$

$$\Delta Q = \iiint (Q' - Q) f f_1 V d\vec{\xi} d\vec{\xi}_1 b db d\epsilon \quad *$$

Because of two-dimensionality and axial-symmetry, Eq. (6) further reduces to

$$\frac{1}{R} \frac{d}{dR} \left[R \int f \xi_R Q d\vec{\xi} \right] - \int \frac{f}{R} \left(\xi_\theta^2 \frac{\partial Q}{\partial \xi_R} - \xi_\theta \xi_R \frac{\partial Q}{\partial \xi_\theta} \right) d\vec{\xi} = \Delta Q, \quad (7)$$

Setting $Q = m$, $m \xi_R$, $m \xi^2/2$, respectively, we find $\Delta Q = 0$ because the mass, momentum, and energy are invariant during collisions, and we obtain the ordinary continuity, radial momentum, and energy equations. Since we are primarily interested in radial heat transfer, we take $Q_4 = m \xi_R \xi^2/2$, which yields the heat flux equation in which the collision integral ΔQ , for simplicity, is evaluated with Maxwell's inverse fifth power force law $F = \frac{m_1 m_2 \tilde{K}}{r^5}$, and is found to be proportional to the heat flux q_R ¹³. The four differential equations governing the four unknown functions are as follows:

* See Introduction in Part I of thesis; also Reference 13.

Continuity

$$[\dot{Q} = m] , \quad n_1 \sqrt{T_1} = n_2 \sqrt{T_2} \quad (8a)$$

R-Momentum

$$[\dot{Q} = m \xi_R],$$

$$(\sin 2\alpha - 2\alpha) \frac{d}{dR} (n_1 T_1 - n_2 T_2) + \pi \frac{d}{dR} (n_1 T_1 + n_2 T_2) = 0, \quad (8b)$$

Energy

$$[\dot{Q} = \frac{m}{2} \xi^2],$$

$$\cos. \alpha (n_1 T_1^{3/2} - n_2 T_2^{3/2}) = B/R \quad (8c)$$

Heat Flux

$$[\dot{Q} = \frac{m}{2} \xi_R \xi^2],$$

$$\begin{aligned} (\sin 2\alpha - 2\alpha) \frac{d}{dR} (n_1 T_1^2 - n_2 T_2^2) + \pi \frac{d}{dR} (n_1 T_1^2 + n_2 T_2^2) \\ = -\frac{4}{5} m A_2 \sqrt{\frac{\tilde{K}}{k\pi}} \cdot \frac{B}{R} [n_1 (\pi - 2\alpha) + n_2 (\pi + 2\alpha)] \end{aligned} \quad (8d)$$

In Eq. (8c), B is an undetermined integration constant; in Eq. (8d), $A_2 \equiv 1.3682$ is the value of the scattering integral for Maxwell molecules¹⁴, and k is the Boltzmann constant. A_2 and \tilde{K} are related to the "classical" coefficient of viscosity by the expression

$$\mu_c = \frac{kT}{(3/2) A_2 \sqrt{2m\tilde{K}}} \quad *$$

Since $P_{RR} \neq P_{\theta\theta} \neq -p$ the momentum equation, Eq. (8b) does not imply $(dp/dR) = 0$. This observation is important, because a pressure gradient exists owing to heat conduction but not because of fluid flow.

Also, the heat flux equation, Eq. (8d), relating q_R to two higher

$$\text{moments: } \int m \xi_p^2 \sin^2 \phi (\xi_p^2 + \xi_z^2) d\vec{\xi} \text{ and } \int m \xi_p^2 \cos^2 \phi (\xi_p^2 + \xi_z^2) d\vec{\xi}$$

bears no resemblance to Fourier's "law" in general; in fact Eq. (8d)

reduces to $q_R = -k_c (dT/dR)$ only if the local full-range Maxwellian

is introduced into the left-hand side. In other words, Eq. (8d) would

give Fourier's "law" to the first order if the Chapman-Enskog expansion procedure is employed¹³.

II. C. Boundary Conditions

For completely diffusive reemission, the boundary conditions are very simple¹³, namely

$$T_1 = T_I \quad \text{at} \quad R = R_1 \quad (\text{Figure 2}) \quad (9a)$$

$$T_2 = T_{II} \quad \text{at} \quad R = R_2 \quad (9b)$$

One additional condition is to specify the density level at a convenient point. We may set

$$n_1 = n_I \quad \text{at} \quad R = R_1 \quad (9c)$$

* As it has been mentioned in Reference 15,

$$\mu_c \neq P_{jk} / \left(\frac{\partial u_j}{\partial x_k} + \frac{\partial u_k}{\partial x_j} \right) \text{ except in the Navier-Stokes regime.}$$

Also it should be pointed out that the Prandtl number for Maxwell molecules is equal to 2/3.

The fourth condition is the vanishing of mean radial velocity

$u_R = 0$ at $R = R_1$ and $R = R_2$. From the expression for u_R [Eq. (3)] and the continuity equation [Eq. (8a)], we conclude immediately that $u_R \equiv 0$ everywhere in the annulus, or

$$n_1 \sqrt{T_1} = n_2 \sqrt{T_2} \quad (9d)$$

These four boundary conditions are sufficient for the four equations [Eqs. (8)].

II. D. Differential Equations and Boundary Conditions in Non-Dimensional Form

In order to bring out all pertinent parameters governing the problem, we normalize Eqs. (8) and (9) by choosing n_I , T_I , R_I as the characteristic number density, temperature, and length, respectively. We also utilize the fact that the Maxwell mean free path evaluated at condition I is

$$\lambda_I = \frac{1}{3A_2 \rho_I} \sqrt{\frac{\pi k T_I}{\tilde{\kappa}}}$$

Denoting all normalized quantities by a bar superscript, like

$$\bar{n}_i = \frac{n_i}{n_I}, \quad \bar{T} = \frac{T}{T_I}, \quad \dots$$

and so on, Eqs. (8) in non-dimensional form are as follows:

Continuity

$$\bar{n}_1 \sqrt{\bar{T}_1} = \bar{n}_2 \sqrt{\bar{T}_2} \quad (10a)$$

R-Momentum

$$(\sin 2\alpha - 2\alpha) \frac{d}{dR} (\bar{n}_1 \bar{T}_1 - \bar{n}_2 \bar{T}_2) + \pi \frac{d}{dR} (\bar{n}_1 \bar{T}_1 + \bar{n}_2 \bar{T}_2) = 0 \quad (10b)$$

Energy

$$(\bar{n}_1 \bar{T}_1^{3/2} - \bar{n}_2 \bar{T}_2^{3/2}) = \beta \quad (10c)$$

Heat Flux

$$\begin{aligned} (\sin. 2\alpha - 2\alpha) \frac{d}{d\bar{R}} (\bar{n}_1 \bar{T}_1^2 - \bar{n}_2 \bar{T}_2^2) + \pi \frac{d}{d\bar{R}} (\bar{n}_1 \bar{T}_1^2 + \bar{n}_2 \bar{T}_2^2) \\ + \frac{4}{15} \frac{R_1}{\lambda_I} \frac{\beta}{\bar{R}} [\bar{n}_1 (\pi - 2\alpha) + \bar{n}_2 (\pi + 2\alpha)] = 0 \end{aligned} \quad (10d)$$

in which β is the integration constant.

The normalized boundary conditions corresponding to Eqs. (9) are at $\bar{R} = 1$,

$$\bar{T}_1 = 1 \quad (11a)$$

$$\bar{n}_1 = 1 \quad (11c)$$

At $\bar{R} = (R_2/R_1)$,

$$\bar{T}_2 = (T_{II}/T_I) \quad (11b)$$

There are three parameters governing this problem: the rarefaction parameter λ_I/R_1 of Eq. (10d); the temperature ratio T_{II}/T_I appearing in the boundary condition; and the radius ratio R_2/R_1 describing the geometrical configuration. One can readily see that Eqs. (10) would all become algebraic at the free molecular limit, namely, $(\lambda_I/R_1) \rightarrow \infty$; thus, $\bar{n}_1, \dots, \bar{T}_2$ would all have the constant values prescribed by the boundary conditions. Then the distribution function f would not only be discontinuous in velocity space, but also independent of space coordinates. Nevertheless, mean quantities [see Eqs. (1-5)] would still depend on R even in free molecular flow. It has been mentioned previously that the set of equations, Eqs. (10), reduce to the usual

Fourier formulation if an expansion in λ_I/R_1 is employed. Of course the complete solutions to these equations will demonstrate these limiting characteristics.

III. SOLUTIONS FOR

SMALL TEMPERATURE DIFFERENCES BETWEEN CYLINDERS

In general, one can utilize Eqs. (10a), (10c) to express \bar{n}_1 , \bar{n}_2 , \bar{T}_1 , \bar{T}_2 in favor of two unknown functions; as in Reference 15; then one has to integrate Eqs. (10b, 10d) numerically for these two functions. For example, if we designate

$$\bar{n}_1 \bar{T}_1 + \bar{n}_2 \bar{T}_2 = G(\bar{R})$$

$$\bar{n}_1 \bar{T}_1 - \bar{n}_2 \bar{T}_2 = K(\bar{R})$$

then by using Eqs. (10a), (10c), we can express all four unknown functions by these two new functions G and K as

$$\begin{aligned} \bar{n}_1 &= \frac{2}{\beta^2} \cdot \frac{KG}{\left(\frac{1}{K} + \frac{1}{G}\right)} & \bar{n}_2 &= \frac{2}{\beta^2} \cdot \frac{KG}{\left(\frac{1}{K} - \frac{1}{G}\right)} \\ \bar{T}_1 &= \frac{\beta^2}{4} \cdot \left(\frac{1}{K} + \frac{1}{G}\right)^2 & \bar{T}_2 &= \frac{\beta^2}{4} \cdot \left(\frac{1}{K} - \frac{1}{G}\right)^2 \end{aligned}$$

Substituting into Eqs. (10b) (10d), we obtain two governing equations

$$\frac{dG}{d\bar{R}} = \frac{2\alpha - \sin 2\alpha}{\pi} \cdot \frac{dK}{d\bar{R}} = f_n(K, \bar{R})$$

$$\frac{dK}{d\bar{R}} = \frac{\left(\frac{32}{15} \cdot \frac{1}{\beta^3} \cdot \frac{R_1}{\lambda_I}\right) \cdot \left(\frac{\pi G - 2\alpha G}{\frac{1}{K^2} - \frac{1}{G^2}}\right) \cdot \frac{1}{\bar{R}}}{2(2\alpha - \sin 2\alpha) \left(\frac{1}{G^2} - \frac{1}{K^2}\right) + \pi \frac{G}{K^2} - \frac{K}{G^3} \cdot \frac{(\sin 2\alpha - 2\alpha)^2}{\pi}} = f_n(K, G, \bar{R})$$

Boundary conditions can be converted easily into conditions for G and K. As in all two-point boundary value problems, to start integration at one point one must make a guess on some undetermined constants, then adjust the guessed values until the boundary conditions at the other point

are satisfied. For the present case, once the value of β is assumed, G and K at $\bar{R} = 1$ are known, integration can then be started from $\bar{R} = 1$ towards $\bar{R} = R_2/R_1$. The correct value of β would be the one that leads to the correct \bar{T}_2 value (i. e., $\bar{T}_2 = T_{II}/T_I$) at $\bar{R} = R_2/R_1$. In actual computation, interpolation would be more practical than the iteration scheme; namely, for a given R_1/λ_I , one may work with a spectrum of β 's which lead to a spectrum of corresponding \bar{T}_{II} 's. Then for a prescribed \bar{T}_{II} , the corresponding β value at that particular density level can be found by interpolation.

By examining the situation more closely, one finds that the linear problem is in fact the most important. In all experiments previously performed, the wire is only slightly heated and its temperature never exceeds the temperature of the bell jar by more than 15 per cent. With large temperature difference pure conduction would be quite difficult to achieve. Thus, Eqs. (10) are linearized in order to acquire analytical solutions, to compare with experiments, and to study particularly the effect of surface curvature.

When the temperature ratio T_{II}/T_I departs little from unity, the four functions $\bar{n}_1, \bar{n}_2, \bar{T}_1, \bar{T}_2$ also depart from unity by an amount small compared with one. Symbolically, if

$$T_{II}/T_I = 1 - \epsilon \quad \text{where } \epsilon \ll 1,$$

then

$$\begin{aligned} \bar{n}_1 &= 1 + N_1, & \bar{n}_2 &= 1 + N_2 \\ \bar{T}_1 &= 1 + t_1, & \bar{T}_2 &= 1 + t_2 \end{aligned} \quad (12)$$

in which $N_1, N_2, t_1, t_2 \ll 1$.

Such limiting process implies that each of the distribution functions

f_1 and f_2 are slightly perturbed over a constant Maxwellian, but the distribution is still discontinuous on the surface of the wedge of influence (Figure 2). This procedure is intrinsically different from perturbation over a full-range local Maxwellian which usually is space dependent; the latter procedure follows practically the same line as the Chapman-Enskog scheme. Thus it should not be surprising to learn that the results so obtained would be useful only when the gas is slightly rarefied. In other words, the present linearization implies no restriction on the value of the rarefaction parameter. The scheme does imply that N_1 , N_2 , t_1 , t_2 are of the same order of magnitude.

Introducing Eqs. (12) in Eqs. (10), one readily finds the set of governing equations for quantities N_1 , N_2 , t_1 , t_2 .

$$N_1 + \frac{1}{2}t_1 = N_2 + \frac{1}{2}t_2 \quad (13a)$$

$$(\sin 2\alpha - 2\alpha) \frac{d}{dR} (N_1 + t_1 - N_2 - t_2) + \pi \frac{d}{dR} (N_1 + t_1 + N_2 + t_2) = 0 \quad (13b)$$

$$(N_1 - N_2) + \frac{3}{2}(t_1 - t_2) = \beta \quad (13c)$$

By using Eqs. (13a) and (13c), one obtains

$$t_1 - t_2 = \beta \quad (13c')$$

and

$$N_2 - N_1 = \beta/2 \quad (13a')$$

Eq. (13b) then yields

$$N_1 + t_1 + N_2 + t_2 = \text{constant}$$

or

$$N_1 + t_1 = \text{constant} \quad (13b')$$

$$\frac{Q}{Q_\infty} = \frac{q_R}{q_{R_\infty}} = \frac{\beta}{\beta_\infty} = \frac{1}{1 + \frac{1}{\frac{4}{15} \frac{R_1}{\lambda_I} \ln \frac{R_2}{R_1}}} \quad (16)$$

Inserting the results of N_1 , N_2 , t_1 , t_2 into Eq. (2), we obtain the temperature distribution

$$\bar{T} = 1 - \epsilon \frac{\pi \left(1 + \frac{8}{15} \frac{R_1}{\lambda_I} \ln \frac{R}{R_1} \right) + 2 \cos^{-1} \left(\frac{R_1}{R} \right)}{2\pi \left(1 + \frac{4}{15} \frac{R_1}{\lambda_I} \ln \frac{R_2}{R_1} \right)} + O(\epsilon^2)$$

or

$$\frac{1 - \bar{T}}{1 - \bar{T}_I} = \delta \left[\frac{1}{2} + \frac{1}{\pi} \cos^{-1} \left(\frac{R_1}{R} \right) \right] + (1 - \delta) \frac{\ln \left(\frac{R}{R_1} \right)}{\ln \left(\frac{R_2}{R_1} \right)} \quad (17)$$

with

$$\delta = \left[1 + \frac{4}{15} \left(\frac{R_1}{\lambda_I} \right) \ln \left(\frac{R_2}{R_1} \right) \right]^{-1}$$

Other mean quantities can be immediately written down from Eqs. (1, 3, 4, 5, and 15) in a similar fashion. Results will be discussed in Section IV.

IV. DISCUSSION

IV. A. Heat Transfer and Comparison with Experiment

Knudsen's formula for heat loss from a surface of temperature T_I to a stream of incident molecules of temperature T_{II} at low pressure²¹ has been generally accepted as a good one:

$$q_R \Big|_{\text{at surface}} = \sqrt{\frac{2k}{\pi m}} \frac{pa}{\sqrt{T_I}} (T_I - T_{II}) \quad (18)$$

where a is Knudsen's thermal accommodation coefficient, which in the present study has been taken to be unity. Studies on accommodation coefficients, though quantitatively inconclusive, leave no doubt about the validity of Eq. (18). Dickins⁴ observed the linear dependency of thermal conductivity on pressure below 5 cm Hg. Mann²² also confirmed that " a " is independent of pressure within 2~3 per cent accuracy up to 330 microns for an instrument with $R_2/R_1 = 1250$. Of course direct measurements on heat loss support this fact quantitatively (Section I).

Owing to its "two-sided" character the present formulation naturally brings out Eq. (18) as a limit for $R_1/\lambda_I \rightarrow 0$, as can be seen from Eqs. (5) and (15):

$$\begin{aligned} q_R \Big|_{\substack{\bar{R}=0 \\ p \rightarrow 0}} &= \sqrt{\frac{2}{\pi}} \rho_I (RT_I)^{3/2} \beta = \lim_{\substack{R_1 \\ \lambda_I} \rightarrow 0} \sqrt{\frac{2}{\pi}} p_I \left(\frac{k}{m} T_I\right)^{1/2} \frac{\epsilon}{1 + \frac{4}{15} \frac{R_1}{\lambda_I} \ln \frac{R_2}{R_1}} \\ &= \sqrt{\frac{2k}{\pi m}} \frac{p_I}{\sqrt{T_I}} (T_I - T_{II}) + O(p_I^2) \end{aligned}$$

Here it shows clearly that if $p_I << \frac{1}{30} \sqrt{\frac{m}{2\pi k T_I}} \frac{R_1}{\mu_I} \ln \frac{R_2}{R_1}$,

Knudsen's formula is quite applicable.

On the other hand, Eqs. (5) and (15) readily yield the Fourier result

$$q_R = \frac{k_c (T_I - T_{II})}{R \ln \left(\frac{R_2}{R_1} \right)}$$

as soon as we set $(R_1/\lambda_I) \rightarrow \infty$ and utilize the relation $k_c = \frac{15}{4} \mu_c \frac{k}{m}$ for a monatomic gas.

Calculation of heat loss over the whole range of densities has also been done by Ai using Grad's thirteen moment equations²³. Ai obtains the Fourier heat conduction relation over the whole range of densities and gives the result

$$\frac{Q}{Q_\infty} = \frac{1}{1 + \frac{1}{\frac{8}{15} \frac{R_1}{\lambda_I} \ln \frac{R_2}{R_1}}} \quad (19)$$

which yields a value twice as large as the actual heat loss at low pressures. As one can learn from Knudsen's formula [Eq. (18)] the heat loss at low pressures is proportional to the difference between the gas temperature and the temperature of the solid wall. Grad's formulation lacks the "two-sided" angular effect, and always overestimates the temperature difference at the wall by a factor of two. (See next section.) The same factor is found when the Fourier relation is used in conjunction with the Maxwell-Smoluchowski temperature "jump" condition (Section I).

Numerous experiments have been performed using the heated fine wire to determine gaseous conductivity, or mostly thermal accommodation coefficients. Conductivity measurements are often made at

normal density with different temperatures, while the determinations of accommodation coefficients are usually done at low pressures. Unfortunately, data obtained in the past years are utterly inconsistent. Values of accommodation coefficient for a given pressure differing from each other by one or two orders of magnitude are not surprising at all. Hartnett¹⁶ in his survey report on accommodation coefficients attributes this discrepancy to three factors: (1) the properties of the solid surface which are usually unspecified greatly affect the result; (2) evaluation of the accommodation coefficient by Knudsen's formula [Eq. (18)] for free molecular flow is often unjustified, because the pressures are usually not low enough to insure the free molecular limit; (3) use of an excessive radiation correction. Besides the inconsistency of these experiments, most publications give only the final accommodation coefficients; a backward deduction to the heat loss is not only dangerous but also impossible owing to lack of knowledge of some physical constants employed in their computations.

The most recent measurement designed solely to study conductive heat transfer is done by Bomelburg¹⁷. He uses Wollaston wire of diameters 1.25μ , 5μ , 10μ , and bell jars of diameters 4 inches and 10 inches*. His results in the transition regime are reproduced in Figure 3, in which the three curves represent calculations according to Eq. (16). It is understandable that at low pressures when $\lambda_1 > 200 R_1$, radiation and end losses become dominant; thus conduction measurements at this range would be more difficult. But it has been clearly shown in Figure 3 that Bomelburg's experiment agrees

* Private communication through D. K. Ai.

with Eq. (16) fairly well.

Tracing back chronologically, we find the measurements by Schäfer, Rating, and Eucken in 1942². They use a platinum wire of $R_1 = 0.00208$ cm in a tube of inner radius $R_2 = 0.294$ cm. Tests are run at 3.5°C with pressures ranging from 1. to $1/3000$ atmosphere, so the ratio $2R_1/\lambda_1$ covers a wide region from 0.1 to 1000. Heat transfer results for Argon and CO_2 are plotted in Figure 4, in which the solid curve again represents Eq. (16). Points for Argon all fall along the predicted curve with a maximum deviation of 10 per cent at the lowest pressure point. The fact that the heat loss for CO_2 also obeys Eq. (16) is rather amazing, as the experiments of CO_2 went down to as low as $1/200$ atm. One would expect that the factor $4/15$ in Eq. (16) supposedly valid for monatomic gas only should be modified for a polyatomic gas. However, the general agreement is certainly not accidental.

Other experiments giving heat loss data have all been performed with diatomic gases. Gregory and Archer's measurement³ (1926) using air and hydrogen gave Q/Q_∞ values 20 - 30 per cent lower than that predicted by Eq. (16). Knudsen's classical experiment¹⁸ (1911) also using hydrogen at various pressure levels showed higher heat loss than expected. Fredlund¹² later correlated Knudsen's data with a formula exactly like Eq. (16). His correlation required a numerical factor approximately three times larger than $4/15$, which is qualitatively in the right direction for a polyatomic gas correction.

IV. B. Temperature Distribution

The expression for the mean gas temperature [Eq. (17)] is rewritten here

$$\frac{1 - \bar{T}}{1 - \bar{T}_I} = \delta \left[\frac{1}{2} + \frac{1}{\pi} \cos^{-1} \left(\frac{R_1}{R} \right) \right] + (1 - \delta) \frac{\ln \left(\frac{R}{R_1} \right)}{\ln \left(\frac{R_2}{R_1} \right)} \quad (20)$$

where

$$\delta = \left[1 + \frac{4}{15} \frac{R_1}{\lambda_I} \ln \left(\frac{R_2}{R_1} \right) \right]^{-1}$$

the significance of this parameter will be clear shortly. This expression shows that the temperature field is composed of two parts (See Figure 5): the first (part 1) is an angular part weighted by δ , the second part (part 2) is logarithmic, and it is in turn weighted by the quantity $(1 - \delta)$. Part 1 has the character of a free molecular temperature field, while the other part has the same character as the Fourier solution. One should note that $\cos^{-1} (R_1/R)$ becomes practically equal to $\pi/2$ at about ten diameters from the center of the inner cylinder. Thus, at fairly low pressures the physical presence of the wire has no influence on the temperature at a point several diameters away. As δ becomes smaller, the logarithmic part would penetrate deeper from R_2 towards R_1 , and it finally dominates the whole temperature field when $\delta \rightarrow 0$. A sketch of the temperature distribution for various values of $2\lambda_I/R_1$ is given in Figure 6.

From another point of view, the temperature distribution can be interpreted as the composition of an "outer" solution and an "inner" solution. The "outer" solution describes the temperature field

corresponding to the solution of the Fourier heat conduction problem with a temperature "jump" at the inner wire when $R_2/R_1 \gg 1$, which is the only case in which this "splitting" makes sense. This field is given by the expression

$$\left(\frac{1 - \bar{T}}{1 - \bar{T}_{II}} \right)_{OUTER} = \delta \left[1 + \frac{4}{15} \frac{R_1}{\lambda_I} \ln \frac{R_2}{R_1} \right]$$

The inner solution is of the form

$$C \left[\frac{1}{2} + \frac{1}{\pi} \cos^{-1} \left(\frac{R_1}{R} \right) \right]$$

where the quantity in brackets is exactly the free-molecule solution, and C is an undetermined constant. Now, if one matches the inner and outer solutions by requiring that

$$\lim_{\bar{R} \rightarrow \infty} \left(\frac{1 - \bar{T}}{1 - \bar{T}_{II}} \right)_{INNER} = \lim_{\bar{R} \rightarrow 1} \left(\frac{1 - \bar{T}}{1 - \bar{T}_{II}} \right)_{OUTER}$$

then $C = \delta$. Evidently Eq. (20) represents the full solution which is valid over the whole region.

Temperature jump phenomenon is solely accounted for by the angular part (part 1), which contributes to $(1 - \bar{T})/(1 - \bar{T}_{II})$ a difference of $\delta/2$ at the surface of the wire [Eq. (20)]. So the gas temperature at the free molecular limit equals the algebraic mean of T_I and T_{II} as one would expect in this linearized case. Grad's scheme employing only the logarithmic term gives a temperature profile

$$\frac{1-\bar{T}}{1-\bar{T}_{II}} = \delta + (1-\delta) \frac{\ln\left(\frac{R}{R_1}\right)}{\ln\left(\frac{R_2}{R_1}\right)} \quad * \quad (21)$$

from which one finds the "temperature jump" at the wire surface to be δ , which differs from the present result by a factor of two, thus over-estimating the heat loss by the same factor. Moreover, Eq. (21) yields a minimum (or maximum) somewhere in the annulus and is clearly physically unrealistic. The importance of the two-sided angular effect is fully shown here. On the other hand, at the wall of the outer cylinder the gas temperature there is practically the same as the wall temperature T_{II} for any value of R_1/λ_I if $R_2 > 20R_1$. In that case, as far as the outer cylinder is concerned, there is virtually no free molecular limit regardless how large the mean free path becomes.

At the surface of the hot wire there exists a thin region usually known as a Knudsen layer at small degrees of rarefaction where the angular part (part 1 ; Figure 5) effectively influences the temperature profile. This layer can be brought out by considering that

$$\text{at } \bar{R}_\ell = 1 + \Delta \quad \text{with } \Delta \ll 1 ,$$

$$\cos \alpha = 1 - (\alpha^2/2) + \dots = 1/\bar{R}_\ell = 1 - \Delta + \dots$$

$$\alpha = (2\Delta)^{\frac{1}{2}} = [2(\bar{R}_\ell - 1)]^{\frac{1}{2}}$$

and

$$\ln \bar{R}_\ell = \Delta = \bar{R}_\ell - 1$$

so

$$\frac{1}{\delta} \left(\frac{1-\bar{T}}{1-\bar{T}_{II}} \right) \approx \frac{1}{2} + \frac{1}{\pi} \sqrt{2(\bar{R}_\ell - 1)} + \frac{4}{15} \left(\frac{R_1}{\lambda_I} \right) (\bar{R}_\ell - 1) \quad (22)$$

* This expression though not given explicitly in Reference 23 can be deduced from it easily.

Figure 7 sketches the separate terms of Eq. (22). The layer is then defined by the region where the angular and logarithmic parts are of the same order of magnitude, namely,

$$\frac{1}{\pi} \sqrt{2(\bar{R}_l - 1)} \simeq \frac{4}{15} \left(\frac{R_1}{\lambda_I} \right) (\bar{R}_l - 1)$$

or,

$$\bar{R}_l - 1 \simeq 2.86 \left(\frac{\lambda_I}{R_1} \right)^2$$

when $(\lambda_I/R_1) \ll 1$.

Thus the thickness of this Knudsen layer is proportional to the square of the Knudsen number.

A comparison between predicted and experimental temperature distributions has not been possible, because up to the present time, the only temperature distribution measurements in rarefied gases were done by Lazareff¹⁹, Mandell, and West²⁰ between two parallel plates. Experiments designed to chart temperatures between two concentric cylinders have not yet been initiated.

IV. C. "Free Molecular" Criterion

The minimum size of the mean free path required to insure that free molecular conditions prevail in an experiment has always been a puzzling question. The choice between conditions like $\lambda_I \gg R_2 > R_1$ or $R_2 > \lambda_I \gg R_1$ is quite uncertain. The confusion can be totally avoided by considering the quantity δ . One realizes that δ is in fact the true criterion for free molecular flow; neither R_1/λ_I nor R_2/R_1 alone governs the situation; i. e., $\delta \rightarrow 1$ signifies the free

molecular limit, while $\delta \rightarrow 0$ represents the continuum regime. For instance, with an apparatus of given R_2/R_1 , $\delta \rightarrow 1$ can be reached by reducing the gas density; or at a given gas condition, one achieves free molecular flow by increasing the R_2/R_1 ratio.

Referring to the definition of δ , one can now safely impose numerically that

$$\frac{R_1}{\lambda_I} \ln\left(\frac{R_2}{R_1}\right) \leq \frac{1}{10}$$

or equivalently

$$\frac{\lambda_I}{R_2 - R_1} \geq \frac{10 \ln\left(\frac{R_2}{R_1}\right)}{\left(\frac{R_2}{R_1}\right) - 1}$$

as the domain of free molecular flow, where Knudsen's formula [Eq. (18)] is valid within about 3 per cent. On the other hand, the condition

$$\frac{4}{15} \frac{R_1}{\lambda_I} \ln\left(\frac{R_2}{R_1}\right) > 20. \text{ (say)}$$

or

$$\frac{\lambda_I}{R_2 - R_1} \leq \frac{1}{75} \cdot \frac{\ln\left(\frac{R_2}{R_1}\right)}{\left(\frac{R_2}{R_1}\right) - 1}$$

represents the continuum limit where the Fourier result will be correct within 5 per cent. Figure 8 shows these two domains as well as the transition region for different values of R_2/R_1 .

IV. D. Fourier-Maxwell-Smoluchowski Formulation

It has been generally accepted that the Fourier relation with the Maxwell-Smoluchowski temperature jump boundary condition would be fairly correct for gases of small degree of rarefaction. Its limit of validity for a problem involved curvatures has never been investigated. According to the relation

$$q_R = -k_c (dT/dR)$$

and the boundary conditions that

$$T_I - T(R_1) = -\frac{15}{8}\lambda_I \left(\frac{dT}{dR}\right)_{R=R_1}$$

and

$$T(R_2) - T_{II} = -\frac{15}{8}\lambda_I \left(\frac{dT}{dR}\right)_{R=R_2}$$

one would obtain an expression equivalent to Eq. (20) for the temperature distribution, namely,

$$\frac{1 - \bar{T}}{1 - \bar{T}_{II}} = \delta' + \left[1 - \left(1 + \frac{R_1}{R_2}\right)\delta'\right] \frac{\ln\left(\frac{R_1}{R_2}\right)}{\ln\left(\frac{R_2}{R_1}\right)} \quad (23)$$

with

$$\delta' = \left[\left(1 + \frac{R_1}{R_2}\right) + \frac{8}{15} \frac{R_1}{\lambda_I} \ln\left(\frac{R_2}{R_1}\right) \right]^{-1}$$

The ratio of heat transfer to the heat transfer in the limit $\lambda_I/R_1 \rightarrow 0$ is

$$\frac{Q}{Q_\infty} = \frac{q_R}{q_{R_\infty}} = \frac{1}{1 + \frac{(1 + R_1/R_2)}{\frac{8}{15} \frac{R_1}{\lambda_I} \ln\left(\frac{R_2}{R_1}\right)}} \quad (24)$$

In the case when $R_2 \simeq R_1$, namely, the gap between two cylinders is small in comparison with R_1 , the curvature effect then is not

important and Eqs. (23) and (24) would be quite correct even at low pressures. This situation is not surprising, as we have learned from the linearized case

$$\left[\frac{T_I - T_{II}}{T_I} \ll 1 \right]$$

of the plane Couette flow problem^{15, 24}. There the Fourier-Maxwell-Smoluchowski result can be valid even when λ_I is large, at least with the minimum number of moments. However, the present type of apparatus normally has a large R_2/R_1 ratio; therefore, the heat transfer predicted by the Smoluchowski method [Eq. (19)] overshoots by a factor of two when $\lambda_I > R_1$, exactly as Ai's result*. The present temperature profile [Eq. (23)] differs from Ai's [Eq. (21)] appreciably, because $\delta \neq \delta'$ in general. Now, one may confidently confirm a long time belief that, as far as gross quantities (like heat flux, total drag) are concerned, the Navier-Stokes-Fourier relations along with velocity-slip or temperature-jump boundary conditions would be fairly good for a linearized problem in which all curvature effects can be considered negligible, but details (like velocity or temperature profile) so obtained would be open to doubt.

The domain of validity of the Fourier-Maxwell-Smoluchowski formulation for this "hot-wire" instrument now can be estimated from Eqs. (23) and (24) as

* Ai in his study has imposed a boundary condition $T(R_2) = T_{II}$ at all density levels, which would be true only if $R_2 > 20 R_1$ [see Section IV. B.], so his solution contains an implicit assumption of $R_2/R_1 \gg 1$.

$$\lambda_I/R_1 \ll (8/15) \ln(R_2/R_1) \quad (\text{if } (R_2/R_1) \gg 1)$$

or numerically (say)

$$\lambda_I/R_1 \leq 8/150 \ln(R_2/R_1) .$$

A sketch of the $q_R / -k_c(dT/dR)$ ratio [Figure 9] based on Eqs. (5) and (15) shows that Fourier's "law" is valid either far from the center wire at any density, or everywhere at normal density. One interesting note is that the ratio falls to zero at the wire surface for finite λ_I ; this behavior arises owing to the infinite temperature gradient resulting from differentiation of $\cos^{-1}(R_1/R)$. It is quite similar to the situation of having an infinite velocity gradient at the forward stagnation point of a cylinder in rarefied gas flow. The gradient becomes finite if the curvature becomes small and the cylinder is transformed to a flat disk²⁵.

REFERENCES

1. Weber, S., "Über den Einfluss des Akkommodations-koeffizienten auf die Wärmeleitung und Radiometerkraft in Gasen", D. Kgl. Danske Videnskabernes Selskal. Medd. 19:11, 1942.
2. Schäfer, K., W. Rating and A. Eucken, "Über den Einfluss des Gehemmten Austauschs der Translations - und Schwingungsenergie auf des Wärmeleitvermögen der Gase", Ann. Physik, Vol. 42, p. 176, 1942.
3. Gregory, H. and C. T. Archer, "Experimental Determination of Thermal Conductivities of Gases", Proc. Royal Soc. (London), Vol. A110, p. 91, 1926.
4. Dickins, B. G., "The Effect of Accommodation on Heat Conduction through Gases", Proc. Royal Soc. (London), Vol. A143, p. 517, 1934.
5. Smoluchowski, M. v., "Über den Temperatursprung bei Wärmeleitung in Gasen", Akad. Wiss. Wien., Vol. 107, p. 304, 1889, Vol. 108, p. 5, 1899.
6. Gregory, H. S., "The Determination of the Coefficient of Accommodation from Aspects of the Temperature Drop Effect", Phil. Mag., Vol. 22, p. 257, 1936.
7. Zener, C., "The Exchange of Energy between Monatomic Gases and Solid Surfaces", Phy. Rev., Vol. 40, p. 335, 1932.
8. Devonshire, A. F., "The Introduction of Atoms and Molecules into Solid Surface -- VIII. The Exchange of Energy between a Gas and a Solid", Proc. Royal Soc. (London), Vol. A158, p. 269, 1937.
9. Welander, P., "Heat Conduction in a Rarefied Gas: The Cylindrically Symmetrical Case", Arkiv for Fysik, Vol. 7, pp. 555, 1954.
10. Welander, P., "On the Temperature Jump in a Rarefied Gas", Arkiv for Fysik, Vol. 7, p. 507, 1954.
11. Schleiermacher, A., "Ueber die Wärmeleitung der Gase", Ann. Physik und Chemie, Vol. 34, p. 623, 1888.
12. Fredlund, E., "Über die Wärmeleitung in verdünnten Gasen", Ann Physik, Vol. 28, p. 319, 1937.
13. Lees, L., "A Kinetic Theory Description of Rarefied Gas Flows", GALCIT Hypersonic Research Project, Memorandum No. 51, 1959.
14. Maxwell, J. C., "On the Dynamical Theory of Gases", Phil. Trans. Royal Soc., Vol. 157, p. 49, 1867. "Scientific Papers", Vol. 2, pp. 26-78, Dover Publications, New York, N. Y.

15. Lees, L. and C. Y. Liu, "Kinetic Theory Description of Plane, Compressible Couette Flow", GALCIT Hypersonic Research Project, Memorandum No. 58, 1960. Also, Proceedings of Second International Symposium on Rarefied Gas Dynamics, p. 391, Academic Press, New York, N. Y.
16. Hartnett, J. P., "A Survey of Thermal Accommodation Coefficients", RAND Research Memorandum, RM-2585, RAND Corporation, Santa Monica, California, 1960. Also, Proceedings of Second International Symposium on Rarefied Gas Dynamics, p. 1, Academic Press, New York, N. Y.
17. Bomelburg, H. J., "Heat Loss from Very Thin Heated Wires in Rarefied Gases", Physics of Fluids, Vol. 2, No. 6, p. 717, 1959.
18. Knudsen, M., "Die Molekulare Wärmeleitung den Gase und der Akkommodationskoeffizient", Ann. Physik, Vol. 34, p. 593, 1911.
19. Lazareff, P., "Über den Temperatursprung an der Grenze zwischen Metall und Gas", Ann. Physik, Vol. 37, No. 2, p. 233, 1912.
20. Mandell, W. and J. West, "On the Temperature Gradient in Gases at Various Pressures", Proc. Phys. Soc., Vol. 37, p. 20, 1925.
21. Kennard, E. H., "Kinetic Theory of Gases", pp. 311-327, 1st. ed., McGraw-Hill Book Co., New York, N. Y.
22. Mann, W. B., "The Exchange of Energy Between a Platinum Surface and Gas Molecules", Proc. Royal Soc. (London), Vol. A146, p. 776, 1934.
23. Ai, D. K., "Cylindrical Couette Flow in a Rarefied Gas According to Grad's Equations", GALCIT Hypersonic Research Project, Memorandum No. 56, 1960.
24. Yang, H. T. and L. Lees, "Plane Couette Flow at Low Mach Number According to the Kinetic Theory of Gases", GALCIT Hypersonic Research Project, Memorandum No. 36, 1957. Also, Proceedings of 5th Midwestern Conference on Fluid Mechanics, 1957.
25. Oguchi, H., "Density Distributions along Stagnation Line in Rarefied Gas Flows", Paper presented at American Rocket Society International Hypersonic Conference held at Massachusetts Institute of Technology, August, 1961.
26. Knudsen, M., "Kinetic Theory of Gases", Methuen, London, 1934.
27. Bhatnager, P. L., E. P. Gross, and M. Krook, "A Model for Collision Processes in Gases. I. Small Amplitude Processes in Charged and Neutral One-Component Systems", Physical Review, Vol. 94, No. 3, p. 511, 1954.

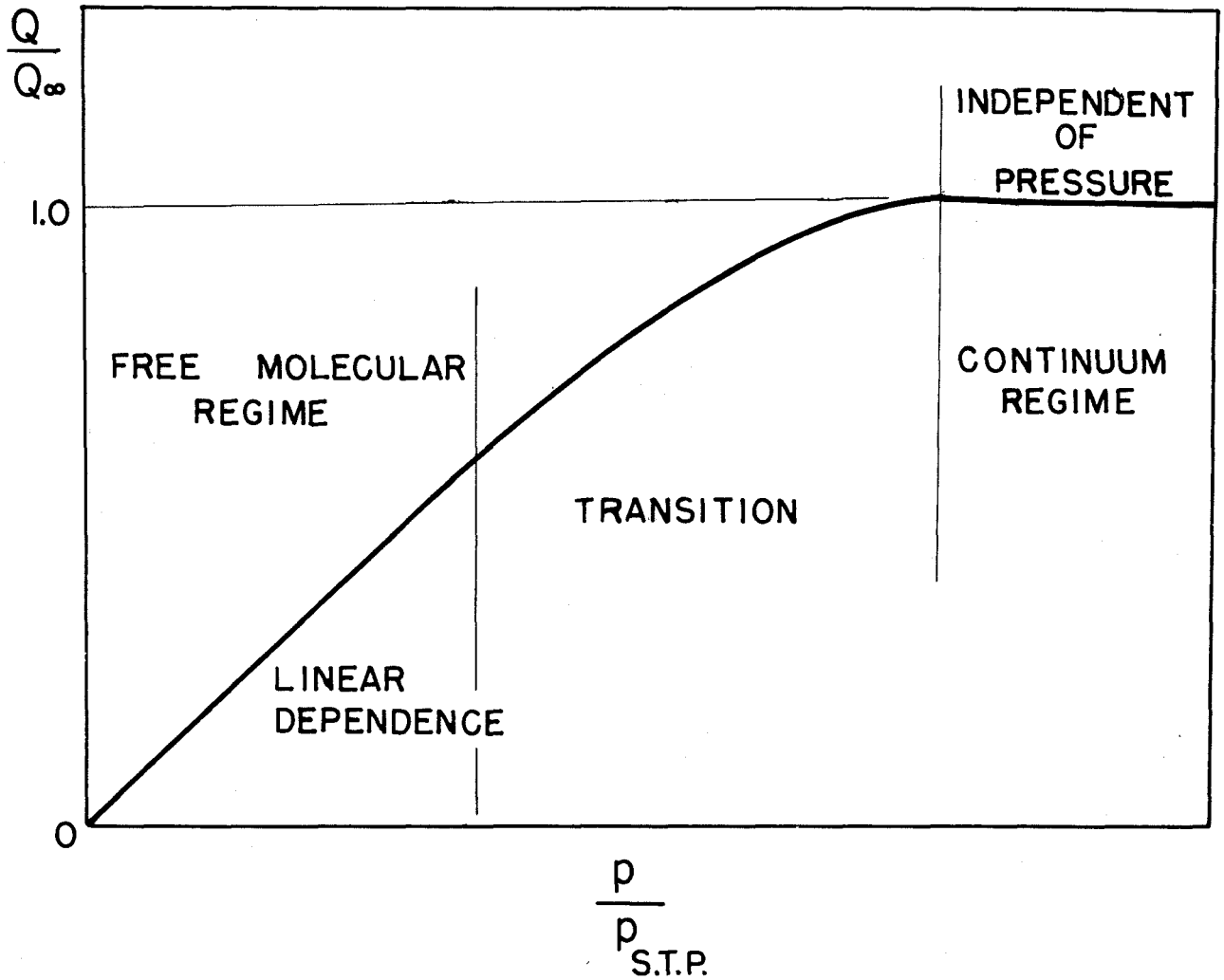


FIG. 1
VARIATION OF HEAT TRANSFER WITH GAS PRESSURE

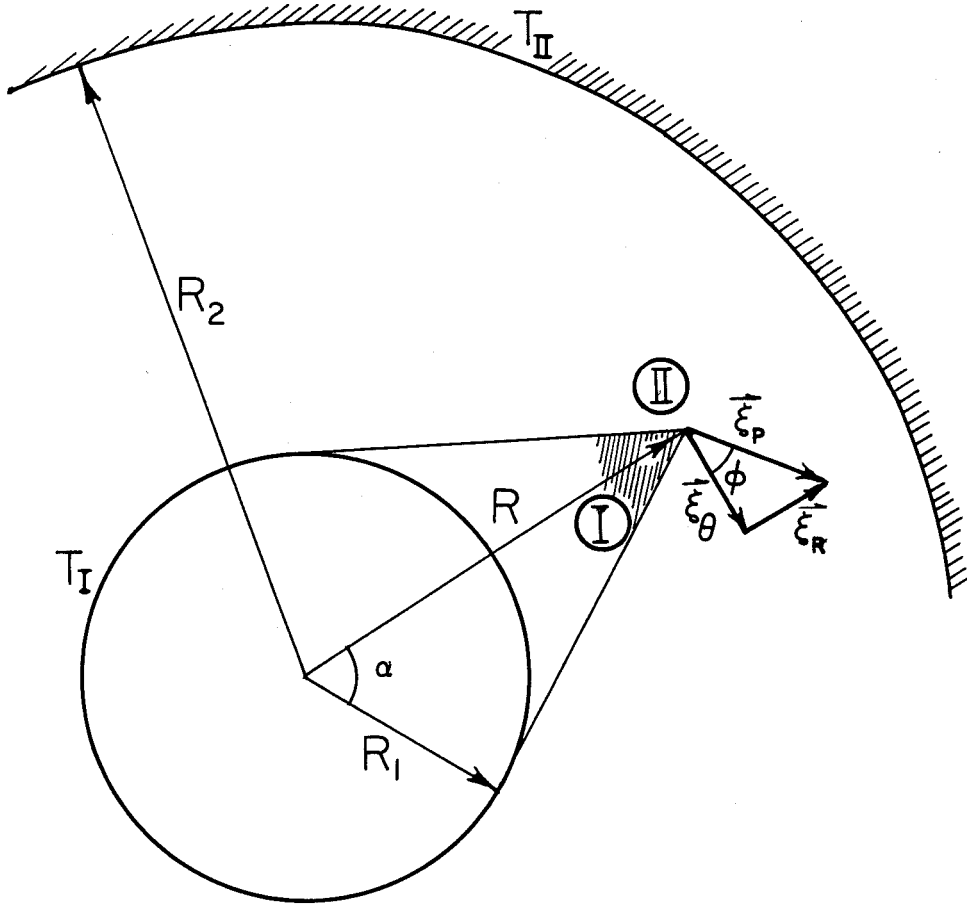


FIG. 2 CONFIGURATION IN CYLINDRICAL COORDINATES

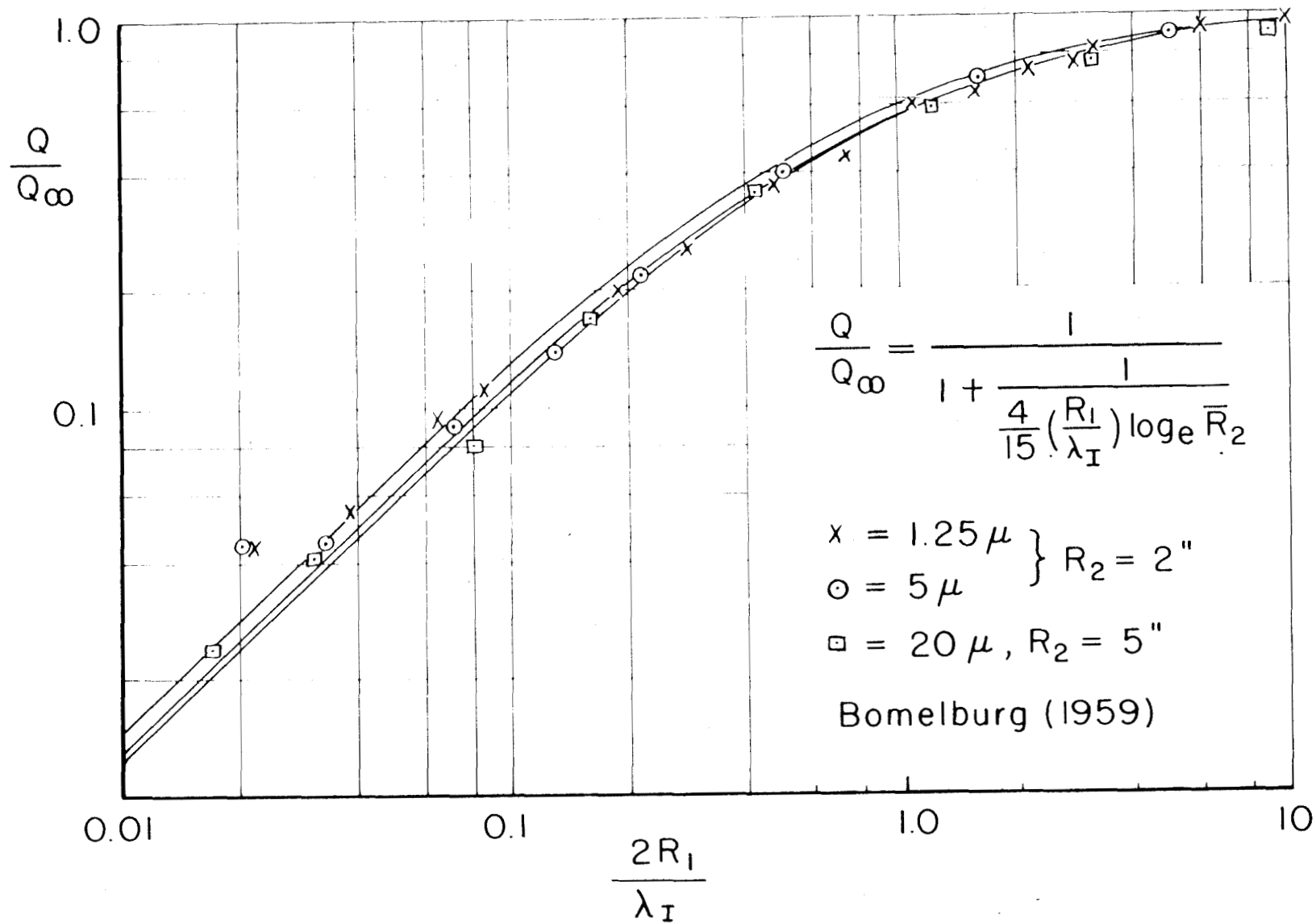


FIG. 3 COMPARISON WITH EXPERIMENT (REF. 17)

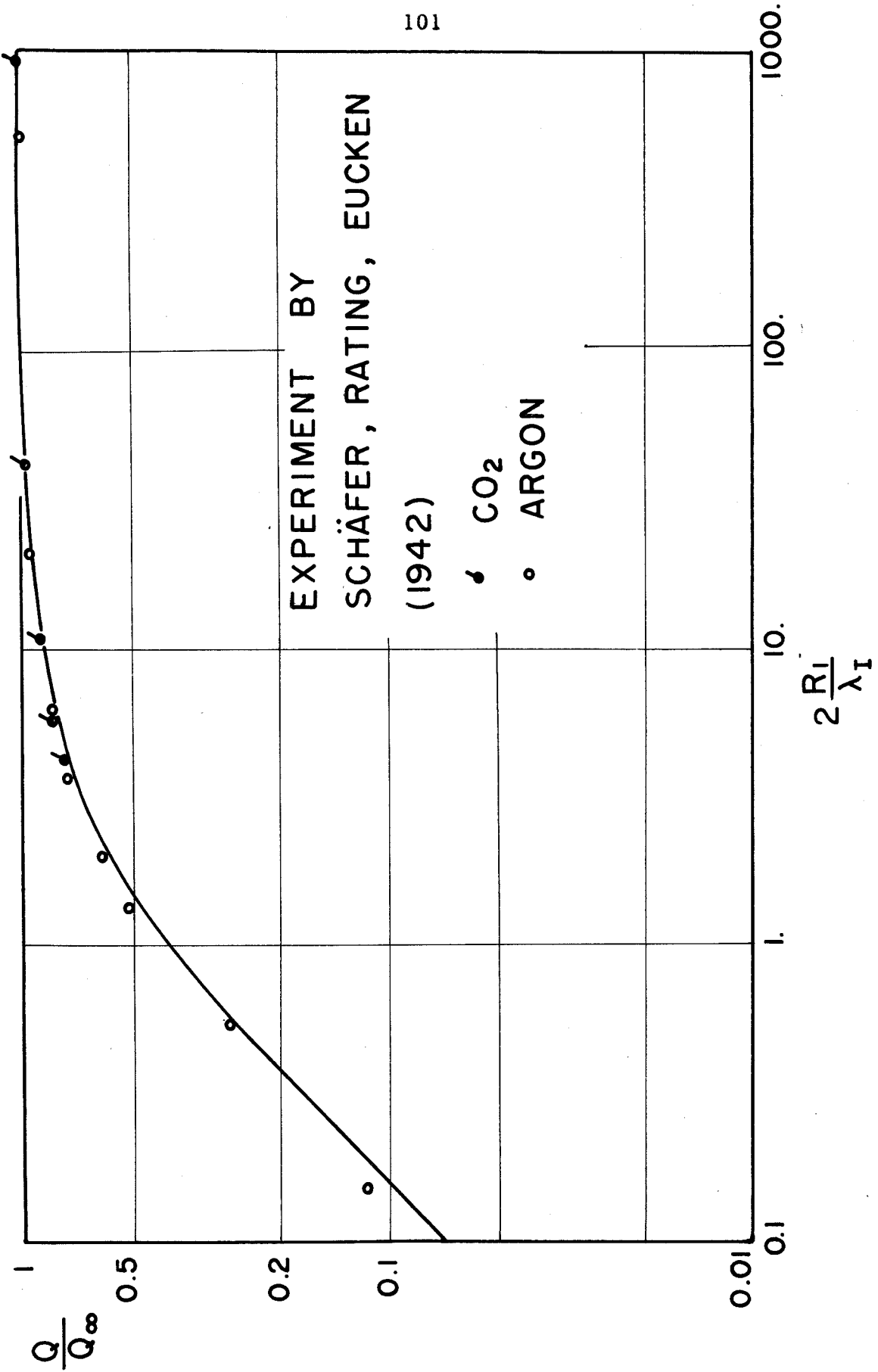


FIG. 4. COMPARISON WITH EXPERIMENT (REF. 2)

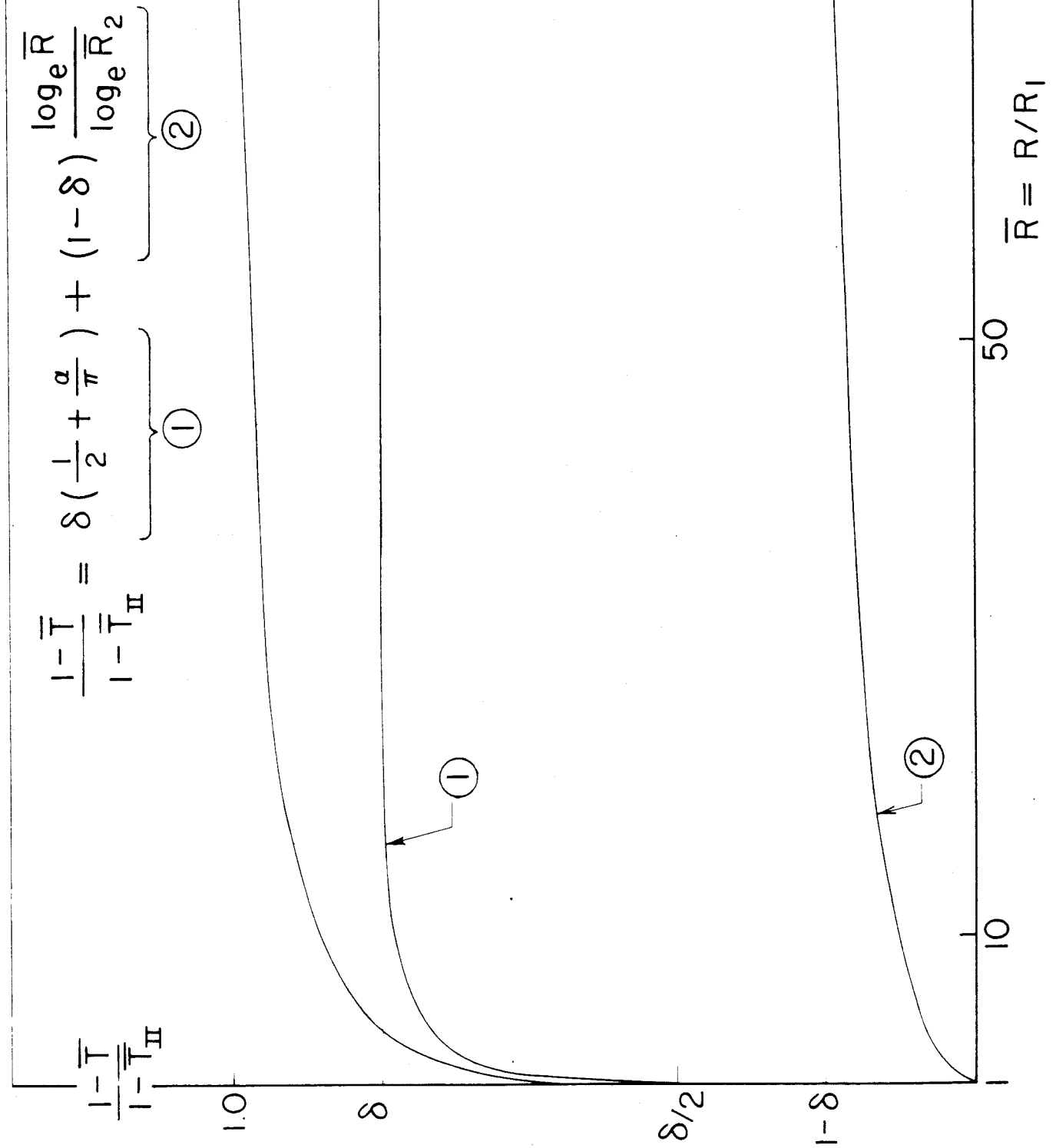


FIG 5 TEMPERATURE DISTRIBUTION BETWEEN TWO CYLINDERS

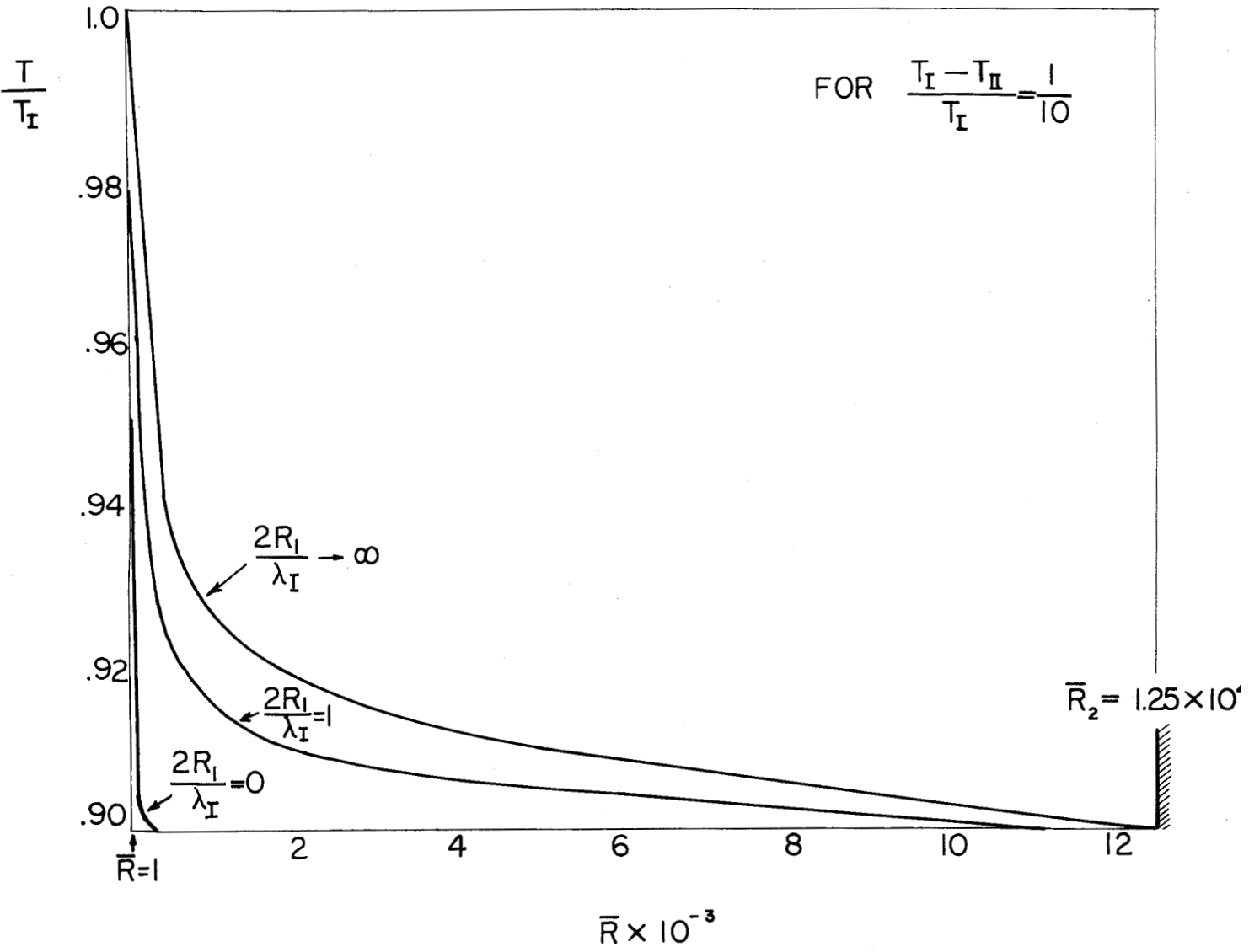


FIG. 6

TEMPERATURE DISTRIBUTION FOR VARIOUS
VALUES OF $2R_I/\lambda_I$

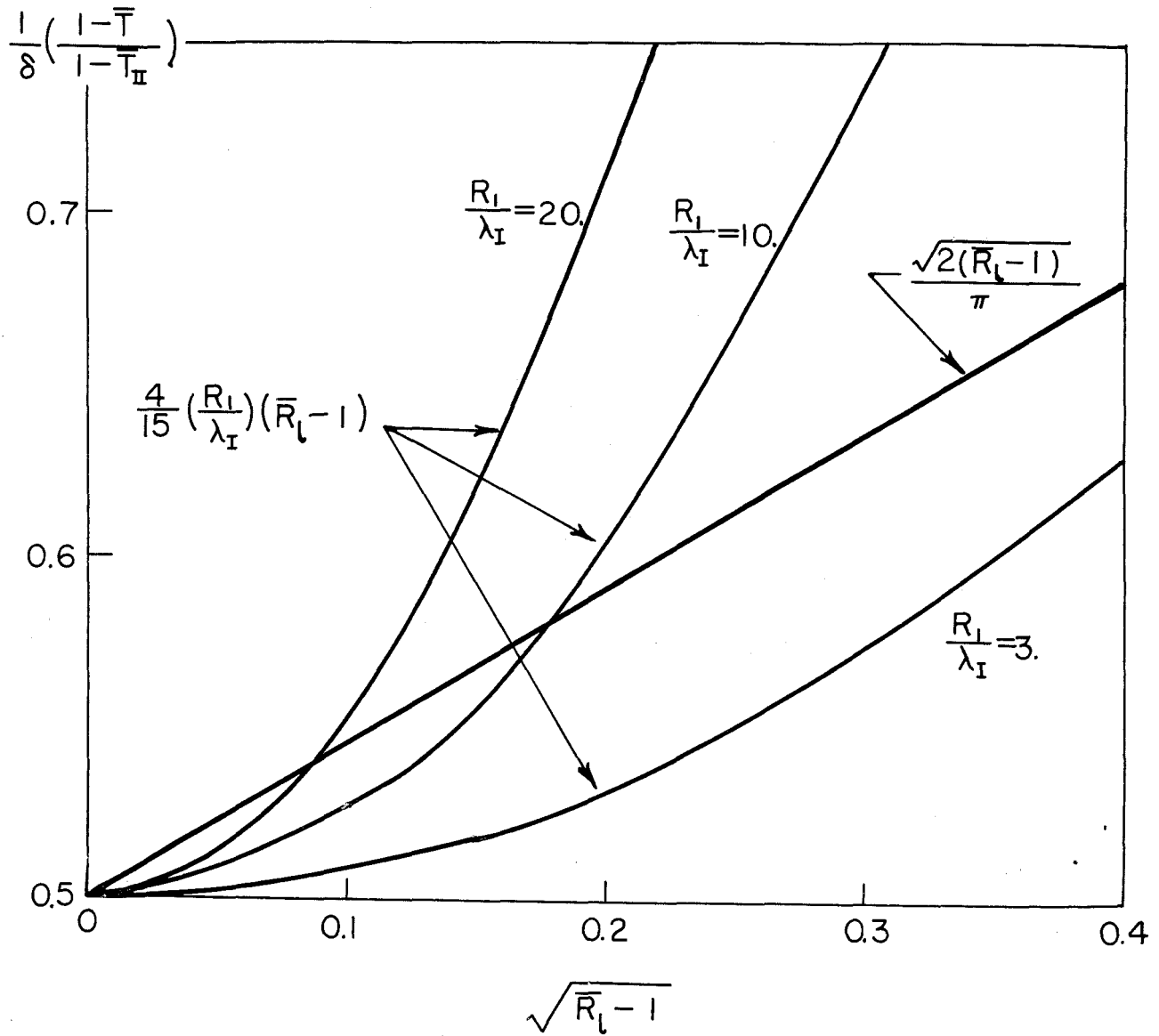


FIG. 7

THICKNESS OF KNUDSEN LAYER

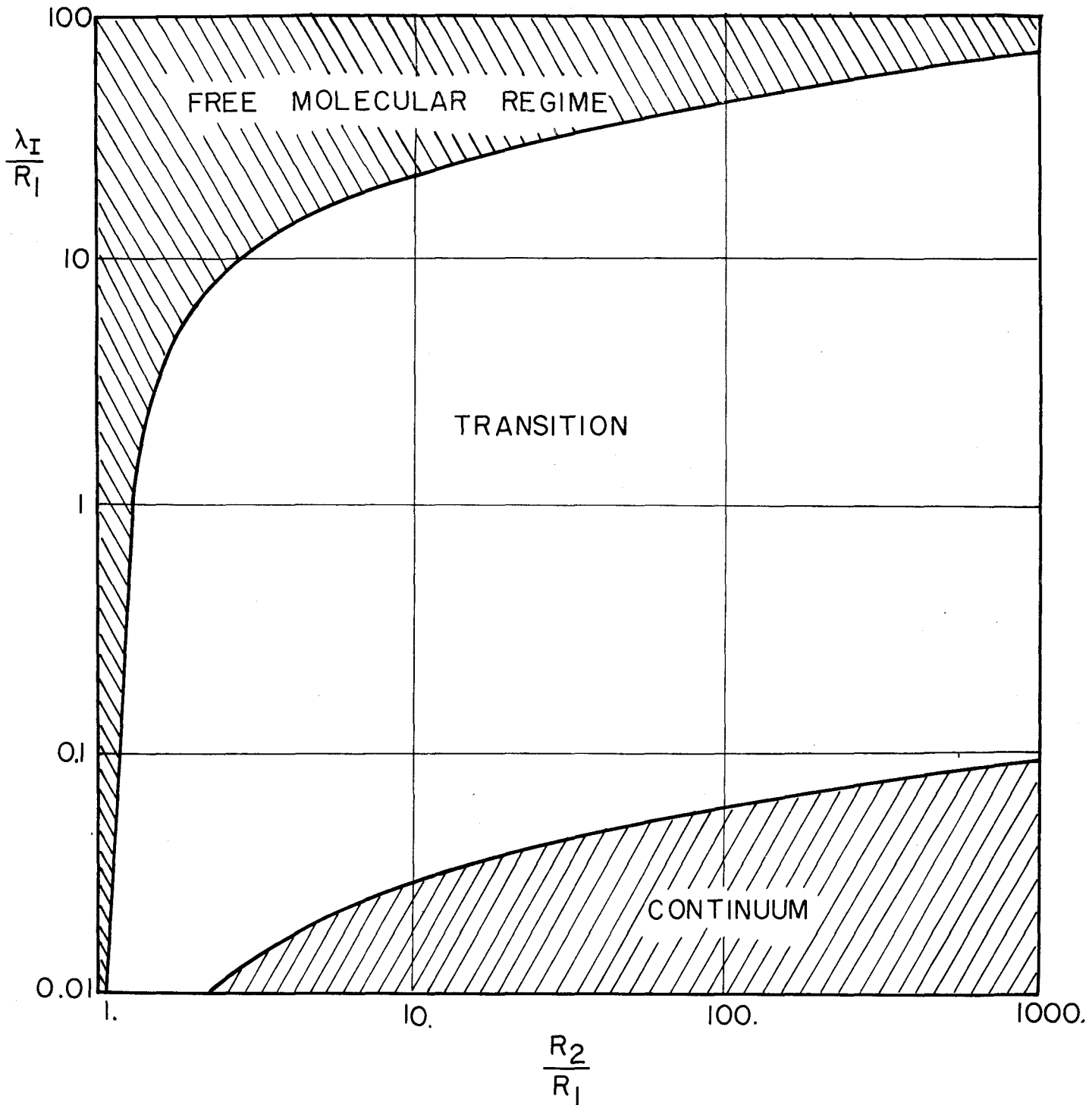


FIG. 8
CLASSIFICATION OF DENSITY REGIMES

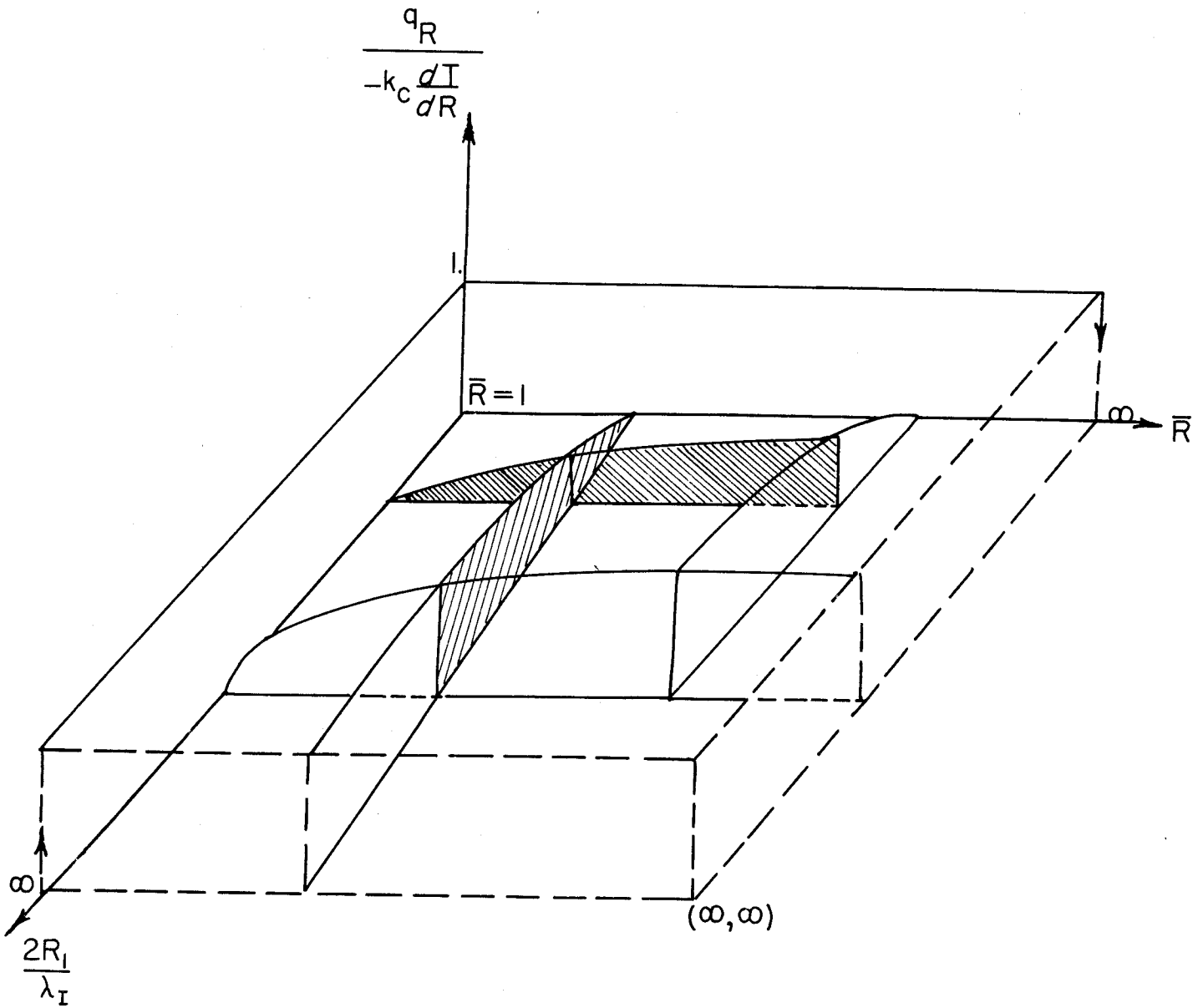


FIG. 9 DEPARTURE FROM FOURIER'S RELATION